Université catholique de Louvain
Faculty of Medicine
Institut de Recherche Expérimentale et Clinique (IREC)
Laboratory of Paediatric Hepatology and Cell Therapy

Adult derived human liver stem/progenitor cells for the treatment of Crigler Najjar syndrome type 1: A functionality study of long-term transplantation in the Gunn rat

Cédric Maerckx

Promoter: Professor E. Sokal
Co-Promoter: M. Najimi

Thesis for doctoral degree (PhD) in Medical Sciences
Orientation: Stem cell therapy and Hepatology
March 2014

Université catholique de Louvain
Faculty of Medicine
Institut de Recherche Expérimentale et Clinique (IREC)
Laboratory of Paediatric Hepatology and Cell Therapy

Adult derived human liver stem/progenitor cells for the treatment of Crigler Najjar syndrome type 1: A functionality study of long-term transplantation in the Gunn rat

Cédric Maerckx

Promoter: Professor E. Sokal
Co-Promoter: M. Najimi

Thesis for doctoral degree (PhD) in Medical Sciences
Orientation: Stem cell therapy and Hepatology
March 2014

This work was supported by a research FRIA grant n°FC79864

Université catholique de Louvain
Faculty of Medicine

Members of the jury:

President:	Professor Isabelle Leclercq Université catholique de Louvain
Promoter:	Professor Etienne Sokal Université catholique de Louvain
Co-promoter:	Doctor Mustapha Najimi Université catholique de Louvain
Members:	Professor Marie-Françoise Vincent Université catholique de Louvain
	Professor Pedro Buc Calderon Université catholique de Louvain
	Professor Denis Dufrane Université catholique de Louvain
Invited member:	Professor Maurizio Muraca Ospedale Pediatrico Bambin Gesù, Italy

A Lidia,

A Raphael et Teresa

A mes proches et amis

« Un chercheur universitaire est une personne

qui en sait toujours plus sur un sujet toujours plus restreint

si bien qu'il finit par savoir tout de rien »

« Un chercheur est celui qui risque sa vérité

et qui accepte de se casser la figure. »

Michel Serres

Remerciements – Acknowledgments

Je remercie l'Université Catholique de Louvain et plus particulièrement le recteur Monsieur Bruno Delvaux pour la formation que j'ai pu acquérir au sein de l'Université.

Je remercie le Fonds National de la Recherche Scientifique et notamment Madame Véronique Halloin, secrétaire générale du FNRS de m'avoir accordé la bourse FRIA qui m'a permis de réaliser ce travail.

Je témoigne toute ma gratitude à la présidente, Madame Isabelle Leclercq ainsi qu'aux membres de mon comité d'encadrement et de jury de thèse, Messieurs Denis Dufrane, Perdro Buc Calderon et Madame Marie-Françoise Vincent pour leur soutien, leur disponibilité, leurs encouragements et les conseils promulgués tout au long de mon parcours.

Vi sono riconoscente e onorato della vostra presenza Sign. Maurizio Muraca - Professore presso IRCCS Ospedale Pediatrico Bambin Gesù, Roma - membro straniero della giuria e specialista di biologia cellulare del fegato e della terapia epatica.

Je remercie particulièrement mon promoteur, le Professeur Etienne Sokal, responsable du département de pédiatrie des Cliniques Universitaires Saint Luc et responsable du laboratoire d'hépatologie pédiatrique et de thérapie cellulaire. Je lui suis reconnaissant de m'avoir accordé sa confiance en m'ouvrant les portes de son laboratoire. Je le remercie pour la supervision de ce travail ainsi que pour ses conseils et son apport scientifique éclairé.

Je tiens également à remercier mon co-promoteur, Monsieur Mustapha Najimi, pour son suivi quotidien, pour ses conseils avisés, pour son implication dans la vie et la gestion du labo ainsi que pour sa disponibilité.

J'adresse mes plus profonds remerciements aux docteurs David Campard et Tatiana Tondreau pour leur implication dans ce projet, pour leur soutien dans les moments difficiles, pour les discussions et conseils scientifiques fournis.

Merci a tout les membres du Laboratoire d'Hépatologie Pédiatrique et de Thérapie cellulaire : A Guy Souris, Ridwan Bakkali, Céline Cailliau, Floriane André, Nawal Jazouli, Stéphanie Evrard, Valérie Rosseels, Joachim Ravau, Jonathan Evraerts pour leur travail et leur implication en tant que techniciens ou licenciés au sein du laboratoire.

Aux docteurs Olivier Vosters, Carole Monterrat, Philippe Lysy, Xavier Stéphenne, Françoise Smets pour leur engagement au sein du laboratoire et leurs judicieux conseils.

Au docteur Catherine Lombard, pour sa relecture minutieuse de mes travaux et sa disponibilité à toute épreuve.

Au docteur Gisèle Deblandre pour ses conseils et son écoute.

A Isabelle Scheers, Gwenaelle Sana, Dung Ngoc Khuu, Silvia Berardis, Ivone Malla, Emmanuelle Nicastro et Massimiliano Paganelli, doctorants et collègues au quotidien. Merci pour votre soutien et pour nos échanges fructueux.

A Ilse Van Elewijck, pour sa gentillesse, sa disponibilité à toute épreuve et son anticipation permanente.

Je souhaite exprimer mes sincères remerciements à toutes les personnes et les laboratoires qui ont apporté, d'une façon ou d'une autre, leur concours ou leur expérience à l'édifice du présent travail.

Au Professeur Pierre Wallemacq et aux membres du laboratoire de toxicologie clinique et médico-légale ainsi qu'à Madame Catherine Fillée et à toute l'équipe du laboratoire de biochimie médicale des Cliniques Universitaires Saint-Luc pour aide tant technique qu'intellectuelle.

Au Professeur Devuyst et à Sébastien Druart (NEFR) pour leur aide matérielle.

Wij danken hartelijk de Heer Professor Jos van Pelt en de Heer Marcel Zegers voor hun vriendelijkheid, hun beschikbaarheid, de kwaliteit van hun talrijke adviezen en hun welwillende wetenschappelijke samenwerking.

A tous les membres du laboratoire CHEX et plus particulièrement au Professeur Pierre Gianello et à Eric Legrand d'avoir permis la réalisation des chirurgies et l'hébergement de certains animaux.

A tous les membres du laboratoire de gastroentérologie et nutrition (GAEN) et en particulier au Professeur Isabelle Leclercq et à Jorge Abarca Quinones pour leur aide tant matérielle qu'intellectuelle et le partage de leur expérience *in vivo*.

Au Professeur Jean-Paul Dehoux pour ses conseils vétérinaires et les discussions amicales.

A tous les membres du laboratoire de gynécologie pour leur aide et nos nombreux échanges.

A Madame Sandrine Wollanders pour sa patience, sa gentillesse et le suivi administratif des étudiants en doctorat.

A Madame Catherine Rasse (SMCS) pour son aide et ses précieux conseils dans le domaine statistique.

Merci au Professeur René Rezsohazy, aux docteurs Sophie Remacle et Barbara Lambert avec qui j'ai eu l'occasion de réaliser mon mémoire et qui m'ont transmis leur curiosité, leur passion pour la recherche et le gout de l'excellence.

A toutes les personnes qui ne sont pas reprises ici et auxquelles je témoigne toute ma reconnaissance.

Enfin je dédie ce travail à mes proches qui m'ont toujours soutenu.

Gracias a ti Lidia por tu amor indefectible, por tu paciencia, tu confianza y tu apoyo incondicional durante estos años. Gracias por nuestros tesoros Raphael y Teresa.

A mes parents, pour toutes les valeurs que vous m'avez transmis et qui font de moi ce que je suis aujourd'hui. Merci pour l'affection permanente que vous me témoignez.

A mes amis et ma famille pour la confiance qu'ils m'accordent et pour leur soutien.

Merci pour tout.

Table of contents

Abbreviations

ADHLSC	Human adult derived liver stem cell
Alb	Albumin
$APPCCl_{2p}$	Adenosine 5'-(β, γ-dichloromethylene) triphosphate
ASMA	alpha smooth musle actin
ATP	Adenosine-5'-triphosphate
AxLT	Auxiliary liver transplantation
BM	Bone marrow
cAMP	Cyclic adenosine monophosphate
CCl_4	Carbon tetrachloride
CK	Cytokeratin
cMOAT	Canalicular multispecific organic anion transporter 1
CN	Crigler-Najjar
CsA	Cyclosporine A
Cx	Connexin
CYP	Cytochrome P450
DNA	Deoxyribonucleic acid
EBV	Epstein–Barr virus
EDTA	Ethylenediaminetetraacetic acid
ESC	Embryonic stem cells
FISH	Fluorescence in situ hybridization
G6P	Glucose-6-phosphate
G6Pase	Glucose-6-phosphatase
GFP	Green fluorescent protein
GMP	Good Manufacturing Product
GST	Glutathione S-transferases
GT	Glucuronosyltransferase

hHep	Human hepatocyte
HLA	Human leukocyte antigen
HLSC	Human liver stem cell
HNF	Hepatic nuclear factor
HPLC	High-performance liquid chromatography
HSC	Hematopoietic stem cell
HSL	Hepatic stem like cell
IHC	Immunohistochemistry
IP	Intraperitoneal
LCT	Liver cell transplantation
LDL	Lactate Dehydrogenase
LDPC	Liver-derived progenitor cells
LPC	Liver progenitor cells
MHC	Major histocompatibility complex
MOAT	Canalicular multispecific organic anion transporter 1
mRNA	Messenger RNA
MRP	Multidrug resistance-associated protein
MSC	Mesenchymal stem cell
NAC	N-acetylcysteine
NADH	Nicotinamide adenine dinucleotide
NADPH	Nicotinamide adenine dinucleotide phosphate
OLT	Orthotopic liver transplantation
OV	Ovalbumin
PBS	Phosphate buffered saline
PCNA	Proliferating cell nuclear antigen
PCR	Polymerase chain reaction
PO	Per Os

rFLDC	Rat fibroblastic-like liver derived cell
RNA	Ribonucleic acid
RT	Room temperature
RTPCR	Reverse transcription PCR
SCID	Severe combined immunodeficiency
SD	Standard deviation
SNP	Single-nucleotide polymorphism
STR	Short tandem repeat
TAT	Tyrosine aminotransferase
TDO	Tryptophan 2,3-dioxygenase
TRP	Transplantation
UCB	Unconjugated bilirubin
UDP	Uridine diphosphate
UGT	Uridine diphosphoglucuronate glucuronosyltransferase
UGT1A1	Uridine diphosphate glucuronosyltransferase 1A1
uPA	Urokinase-type plasminogen activator
WB	Western blot
WT	Wild type
αFP	Alpha fetoprotein

Introduction

1. Bilirubin metabolism

Bilirubin is a yellow pigment derived from the degradation of heme proteins. In humans, 250 to 400 mg of bilirubin is formed daily consequently to the breakdown of hemoglobin, others hemoproteins and free heme [1]. Approximatively 80% of bilirubin is derived from the hemoglobin of senescent erythrocytes [2].

In the circulation, bilirubin is tightly but reversibly bound to albumin, which keep it in soluble form during its transfer from the production to the excretion site, the liver (Figure 1). In healthy subjects, normal albumin concentrations (500-700 µM) exceed that of bilirubin (<17µM). However, in patients with Crigler-Najjar syndrome, a pathology characterized by hyperbilirubinemia, the molar ratio of unconjugated bilirubin to albumin can exceed 1. In this context bilirubin can also bind to a second, third and a fourth site of albumin. However, such binding is weaker, so that the unbound fraction of bilirubin increases sharply.

Tightly bound to albumin, bilirubin is rapidly removed from circulation by the liver. Bilirubin dissociates from albumin before entering the hepatocytes. Because its water solubility is very low at physiologic pH, unconjugated bilirubin is kept in solution bound to a cytosolic protein, the ligandin (Figure 1) [3, 4].

Bilirubin remain stored within hepatocytes before excretion into bile [5], this step is efficiently performed, across the bile canaliculus, after its conversion to polar conjugates by esterification with a glucuronic acid. Bilirubin conjugation is catalyzed by a specific isoform of uridine diphosphoglucuronate glucuronosyltransferase (UGT). UGT enzymes are present in the endoplasmic reticulum and nuclear envelope of hepatocytes [6] and are integral membrane proteins [7, 8].

Biliary excretion of bilirubin conjugates (mono- and diglucuronides) is carried out thanks to an ATP-dependent canalicular non-bile acid organic anion transporter (also called cMOAT). Maximal bilirubin secretion capacity depends on bile flow which is increased by infusion of bile acids [9] or after phenobarbital treatment.

Bilirubin reaches the intestinal tract mainly under conjugated form and is not substantially absorbed, it is degraded by bacteria into a series of urobilinogen and related products (Figure 1) [10] but a portion of unconjugated bilirubin excreted in bile may be reabsorbed in the small intestine.

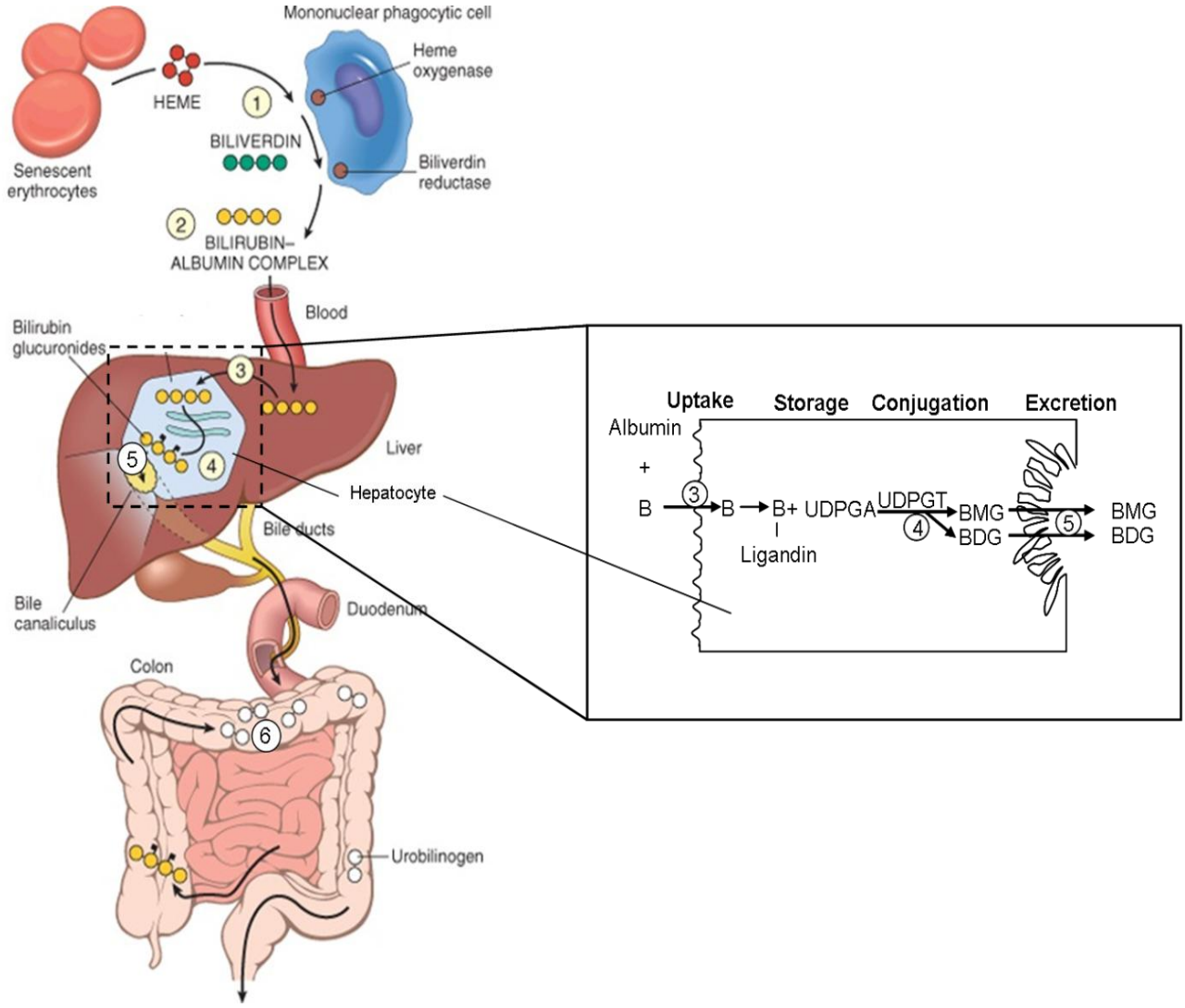

Figure 1: Bilirubin formation, hepatic metabolism and excretion.
Bilirubin derives (B) from the degradation of heme proteins (1). In the circulation, bilirubin is tightly bound to albumin (2) which kept it in solution form the excretion site, the liver. The bilirubin-albumin complex dissociates in the liver sinusoïds and bilirubin then enters the hepatocyte (3). Within the hepatocyte bilirubin binds to a group of cytosolic proteins termed ligandins; this inhibits the efflux of bilirubin from the cell. UDP-glucuronosyltransferase (UDPGT) (4), an endoplasmic reticulum enzyme, catalyzes the transfer of glucuronic acid from UDP-glucuronate (UDPGA) to bilirubin, forming bilirubin monoglucuronide (BMG) and diglucuronide (BDG). Mono- and diglucuronides are excreted to the bile thanks to an ATP-dependent canalicular non-bile acid organic anion transporter (called cMOAT) (5). Bilirubin reaches the intestinal tract and is degraded by bacteria into a series of urobilinogen and related products (6). Modified from www.studentconsult.com and Chowdhury et *al*. [11]

2. Crigler-Najjar syndrome

The Crigler-Najjar syndrome is an autosomal recessive disease characterized by unconjugated hyperbilirubinemia due to a hepatic deficit of bilirubin glucuronosyltransferase (GT) activity. So far, the disease is divided in two types: type I and type II. It remains rare hepatic disorders with a prevalence estimated at 1/1000000 birth [12]. Absence or bare detection of bilirubin-UGT enzyme activity distinguishes both diseases.

a. Crigler-Najjar syndrome type I

Crigler-Najjar syndrome type I is characterized by severe unconjugated hyperbilirubinemia due to a complete absence of hepatic bilirubin glucuronosyltransferase activity. This metabolic disorder was firstly described by Crigler and Najjar in 1952 in six infants of three families [13]. Five of the six infants died of bilirubin encephalopathy (kernicterus) by the age of 15 months. The single surviving was free of neurologic disease until 15 years of age, when kerincterus suddenly developed and he died 6 months later [14]. Crigler-Najjar syndrome type I occurs in all races, is transmitted as an autosomal-recessive trait and could be associated with consanguinity in some cases [14-17].

Hepatic parameters related to Crigler-Najjar syndrome type I are normal except for the serum bilirubin level, which is usually up to 20-25 mg/dl, but may be as high as 50 mg/dl [14-16, 18]. In healthy patients, the serum bilirubin level is around 0.1-1.2mg/dl. High plasma concentrations of bilirubin increase the risk of bilirubin encephalopathy (kernicterus) which leads to long term sequelae including delay in motor development, chorioathetosis, dental dysplasia, cognitive dysfunction and

mental retardation. The histological analyze of Crigler-Najjar patient liver biopsy reveal normal biliary tract and vascular structures.

b. Crigler-Najjar syndrome type II

Crigler-Najjar syndrome type II was first described by Arias in 1962 in a study of chronic unconjugated hyperbilirubinemia in eight patients [19]. Crigler-Najjar syndrome type II is characterized by unconjugated hyperbilirubinemia due to reduced and inducible activity of hepatic bilirubin glucuronosyltransferase but is phenotypically similar to Crigler Najjar syndrome type I, except that the serum bilirubin concentration is usually below 20 mg/dl but may be as high as 40mg/dl during fasting [20] or intercurrent illness [21].

c. Molecular defects in Crigler-Najjar syndrome

Numerous mutations in the *UGT1A1* gene (2q37) are linked to both Crigler-Najjar syndrome types and result in absent or reduced bilirubin GT activity, with marked impairment of bilirubin conjugation. UGT isoforms are expressed from multiple loci (Figure 2). The C-terminal domain of UGT isoforms has a high degree of homology and is responsible for binding of the common donor substrate, UDP-glucuronic acid [22] whereas the N-terminal domains are more heterogenous and account for the aglycone substrate specificity of individual isoforms [23]. Only one isoform is specific for bilirubin glucuronidation[23]; other isoforms are specific to other substrates (such as phenolic substrates, steroids, drugs,…) as illustrated in Table 1. The locus that expresses bilirubin-UGT is termed UGT1A1.

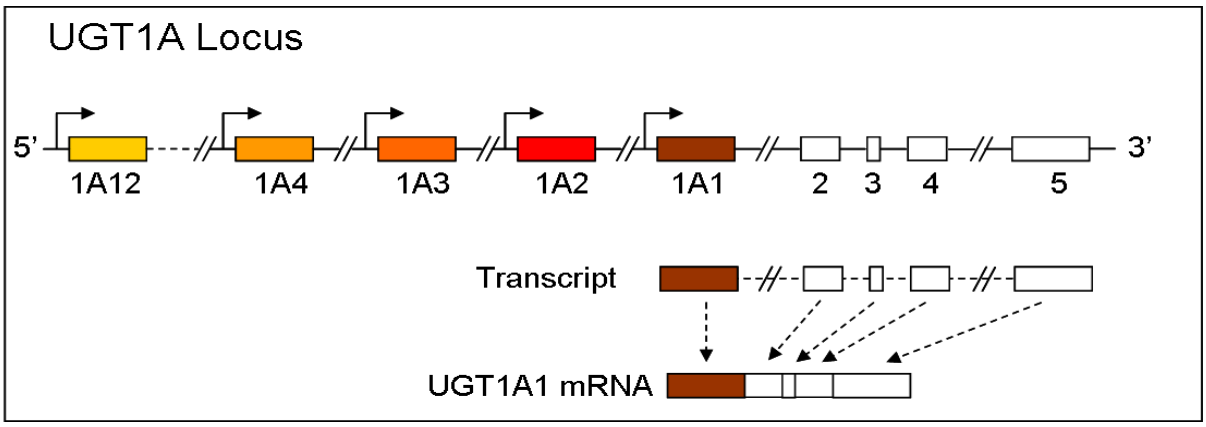

Figure 2 : Schematic representation of the *UGT1A* locus.
This locus contains multiple genes that express UGT1A isoforms. Exon 2,3,4 and 5, located at the 3' end of UGT1A, encode the identical C-terminal domains of all UGT isoforms expressed from this locus. Upstream to these common regions exons are a series of unique sequences (exons 1A1 through 1A12), each of which encodes the variable N-terminal domain of a different UGT isoform expressed from this locus. Each unique region exon is preceded by a separate promoter region (arrows), permitting independent regulation of gene expression. Transcription can start from any of the promoters, producing transcripts of varying length. The unique exon located at the 5' end of the transcript is spliced to the 3' end of exon 2 and other unique region exons present in the transcript are spliced out. Thus, based on differential promotor usage, several mRNAs, each encoding a different member of the UGT1A subfamily are generated. Genes belonging to this locus are named according to unique exon used in the expressed mRNA. When the transcription starts 5' to exon 1A1, the mRNA encoding bilirubin UGT is generated. This gene which consists of exon 1A1 plus the common region exons 2 to 5 is termed *UGT1A1* and the expressed enzyme is termed UGT1A1. Modified from Chowdhury et *al*. [11]

Genetic lesions in the exons constituting the *UGT1A1* gene that cause Crigler-Najjar syndrome type I were first described in 1992 [23-27]. Genetic lesions can be deletions, insertions, missense mutations or premature stop codons and can be located in any of the five exons comprising the UGT1A1 mRNA (Figure 2) [26]. When the genetic lesion is located in exon 1, only UGT1A1 activity is abnormal, whereas when the mutation affects one of the common region exons (exons 2 to 5), all UGT isoforms expressed from UGT1A locus are expected to be abnormal. Crigler-Najjar syndrome type II is caused by mutations of one of the five exons that encode *UGT1A1* [28]. This mutation consists of point mutations and results in marked reduction, but not a total loss of bilirubin-UGT activity.

Enzyme	Substrate
UGT1A1	Bilirubin, morphine, irinotecan and oestrogen
UGT1A2	Oestrogen (rat and mouse)
UGT1A3	Estrone and 2-hydroxyestrone
UGT1A4	Sapogenins, tamoxifen and arylamine
UGT1A5	Not expressed
UGT1A6	Aspirin, acetaminophen, irinotecan and antioxidant genes inductor
UGT1A7	Moderate glucuronidase activity with phenols
UGT1A8	Coumarins, phenols, anthraquinones, flavones, opioids, oestrogen and tamoxifen
UGT1A9	Irinotecan, arylamine, nicotine and estrogen
UGT1A10	Mycophenolic acid, coumarins, quinolines, irinotecan and oestrogen
UGT1A11	Not expressed
UGT1A12	Not expressed

Table 1: Substrates for the different UGT1A enzymes
The C-terminal domain of UGT isoforms is responsible for binding of glucuronic acid whereas the N-terminal domains are substrate specific. For example UGT1A1 is involved in bilirubin, morphine, irriontecan and oestrogen pathway glucuronidation.

3. Animal models for Crigler-Najjar syndrome type 1

a. Gunn rat

Animals presenting nonhemolytic unconjugated hyperbilirubinemia were first described in 1938 by Gunn [29] in Wistar strain. Jaundice in these animals is inherited as an autosomal recessive trait [30]. Heterozygous rats are anicteric and exhibit conjugated bilirubin levels ranging between 0.2-0.6 mg/dl whereas homozygous Gunn rats have bilirubin levels that range from 3 to 20 mg/dl. Homozygous rats have a light yellow bile due to the excretion of small amounts of unconjugated bilirubin [30] and similarly as in the human liver, histology is normal [31].

The rat *UGT1A1* locus closely resembles its human counterpart in exon organization. The genetic lesion in Gunn rats consists of the deletion of a single guanosine residue in the common region exon (exon 4), which creates a frameshift and deletes a large segment of the C-terminal domain of all UGT isoforms that are expressed from this locus [32, 33]. Consequently, not only bilirubin glucuronidation is absent in this strain, other UGT isoforms expressed from *UGT1A* locus are also truncated and non functional [34].

Homozygous Gunn rats frequently develop kernicterus [18]. Cytoplasmic neuronal changes develop in these rats on the third day of life and, after 2 weeks, degeneration of Purkinje cells and other neurons occurs. The degenerative changes begin by enlargement of mitochondria and formation of membranous cytoplasmic bodies. Moreover bilirubin inhibits RNA synthesis, protein synthesis and carbohydrate metabolism in brain and inhibits protein synthesis in liver [35]. Bilirubin also decreases respiration activity of isolated brain mitochondria,

uncouples oxidative phosphorylation, inhibits ATPase activity and inducs brain oedeme [36]. Bilirubin has been shown to inhibit protein kinase-mediated phosphorylation of neural proteins [37, 38]. All these effects can lead to induced brain dysfunction, also known as kernicterus.

Furthermore, Gunn rats cannot concentrate urine and do not tolerate water deprivation [39] because the renal medullary bilirubin concentration is high which interferes with sodium and water transport. Occasionally renal papillary necrosis can also occur [40].

b. UGT1 knock-out mice

UGT1 knock-out mouse was generated into C57BL/6 background by the elimination of mouse UGT1 activity from the germ line by interrupting exon 4 into ES cells. This interruption of the reading frame leads to a complete absence of UGT1A RNA [41]. Within 8 h following $UGT1^{-/-}$ mouse birth the visible appearance of jaundice is evident by the orange skin color of the neonates. The normal levels of UCB in 5-day-old UGT1+/+ mice ranges from 0.1 to 0.3 mg/dl in comparison to 7–10 mg/dl in the $UGT1^{-/-}$mice. Longevity studies show that all of the $UGT1^{-/-}$neonatal mice die within the first 2 weeks following birth and exhibit intense yellow staining in the brain resulting from UCB deposits due to high level of UCB [42].

c. UGT1 knock-in mice

In 2011, Bortolussi et *al*. generated a C57BL/6 Ugt1 knock-in mouse [43]. A single base deletion was introduced by gene targeting in exon 4, this mutation, similar to the one present in the hyperbilirubinemic Gunn rat model leads to a frameshift generating a stop codon immediately downstream. Mutant mice were characterized by Ugt1 truncated protein, lacking the transmembrane domain.

Enzymatic assays using UCB as a substrate demonstrated that liver microsomes from 5 days old mutant mice had no Ugt1a1 glucuronidation activity.

Mutant mice developed jaundice as early as 36 h after birth, evidenced by the yellowish-orange color of the skin. Within a few days after birth, jaundice progressed to a severe hyperbilirubinemic condition, reaching UCB levels 42 times higher than in control littermates (wild type: 0.29±0.17 mg/dl and mutant: 12.22±1.49 mg/dl). 50% of mice died within 5 days after birth with no survivors after 11 days.

Neonatal mutant mice (d3–d6) displayed many of the clinical symptoms of kernicterus, including severe motor impairment characterized by a marked improper posture of the rear limbs, poor and slow movement, and decreased feeding. The cerebellum of mutant mice was less developed compared with that of wild-type littermates. A closer examination revealed that mutant mice had an abnormal stratification of the cerebellar layers explained by a reduction of Purkinje cells. A detailed observation of histological preparations showed that, in mutant mice, the Purkinje cell layer architecture was disorganized, and the dendritic arbor was underdeveloped.

4. Treatments of Crigler-Najjar syndrome

Advantages and disadvantages of Crigler-Najjar treatments are summarized in table 4 at the end of chapter 5.

a. Phototherapy

Phototherapy can be used to treat both CN syndrome type I and II. Bilirubin exhibits a ZZ conformation and is virtually insoluble in water. Exposure of circulating bilirubin to light changes the configuration to an E or cis-configuration

(Figure 3). The resulting ZE, EZ or EE isomers are more polar than ZZ bilirubin and can be excreted in the bile without conjugation.

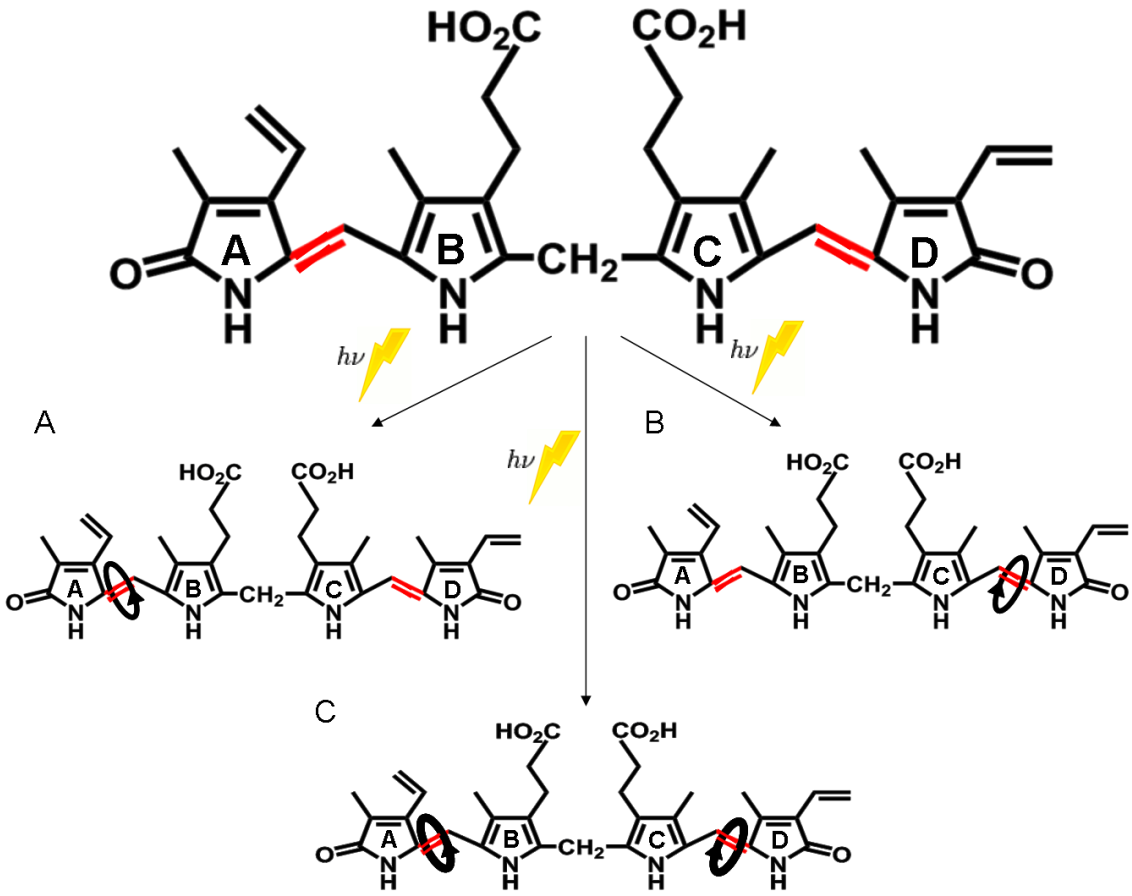

Figure 3: Bilirubin isomerization
Bond between pyrrolenone rings A and B or C and D can change into an E (cis) configuration resulting in the EZ (A), ZE (B) or EE (C) isomers. E configuration of the bond between the pyrrolenone rings interferes with hydrogen bonding and renders the molecule relatively polar. Modified from http://www.atarnotes.com

Phototherapy is the first line treatment for icteric newborns whose serum bilirubin concentrations place them at risk for kernicterus [18, 44, 45]. Later in life, such a therapeutic approach deeply impairs the patient quality of life of CN patients who require phototherapy for up to 12 hours daily. More over about the time of puberty, phototherapy becomes relatively less effective because of thickening of the skin, increased skin pigmentation and decreased surface in relation to body mass [18]. Like in healthy patients, a portion of unconjugated bilirubin excreted in bile may be reabsorbed in the small intestine. Oral administration of agar, cholestyramine, or calcium salts [45] improves the effect of phototherapy, by inhibiting the reabsorption of unconjugated bilirubin.

b. Plasmapheresis

Plasmapheresis is the most efficient method to rapidly reduce serum bilirubin concentration. This method is particularly used in crisis phase [15, 18, 46]. It consists in the removal, treatment, and return of (components of) blood plasma from blood circulation. This procedure takes advantage of the fact that bilirubin is tightly bound to serum albumin and removal of albumin results in the removal of equimolar amounts of bilirubin. Sellier et *al*. reported a case of a 6 year old Crigler-Najjar type I patient who had previously developed kernicterus in the neonatal period [47]. In spite of intensification of phototherapy, the patient developed severe hyperbilirubinemia (up to 48.5 mg/dl, with bilirubin/albumin ratio at 1.2). With two plasmapheresis procedures, bilirubin serum concentration finally decreased to 24.6 mg/dl and bilirubin/albumin ratio to 0.55. Following the acute episode of very severe unconjugated hyperbilirubinemia, the child recovered.

c. Phenobarbital treatment

This treatment can exclusively be used to treat CN syndrome type II. The reduced levels of hepatic bilirubin-UGT activity in type II suggested that an inducer of microsomal enzymes could ameliorate hyperbilirubinemia [19]. Studies revealed that serum bilirubin concentrations are reduced significantly (greater than 25 percent) following treatment with phenobarbital. Phenobarbital activates the transcription of *UGT1A1* linking a 290-bp sequence phenobarbital responsive enhancer module located from -3483 to -3194pb of the *UGT1A1* gene [48].

d. Liver transplantation

Orthotopic or auxiliary liver transplantation rapidly normalizes serum bilirubin levels.

i. Orthotopic liver transplantation

Orthotopic liver transplantation (OLT) is up to now considered as the only definitive treatment for Crigler-Najjar syndrome type I [15, 45, 46, 49, 50] but this procedure seems disproportionate to correct one single missing enzymatic function in an otherwise normal liver. Indeed, up to 15% of OLT patients require re-transplantation, and progressive fibrosis of the graft is a subject of concern at long term [51]. Moreover, transplanted patients must follow a life long immunosuppressive treatment.

ii. Auxiliary liver transplantation

Auxiliary liver transplantation (AxLT) uses a partial left or right lobe from the donor which acts as support for the recipient's liver, which remains in place. The partial graft is placed below the native liver (heterotopic auxiliary transplantation)

or replaces the resected right or left native lobe (auxiliary partial liver transplantation).

This technique is also an invasive surgical procedure and remains difficult mainly because of perilous anastomosis that can hamper the venous in-or outflow and can lead to graft atrophy / ischemia or vascular thrombosis. Another complication is the small-for-size liver syndrome, defined as liver impairment, following inadequate liver mass replacement [52].

5. The potential role of cell therapy in liver metabolic diseases

a. Mature liver cell transplantation

Alternatives to orthotopic and auxiliary liver transplantation, considered as expensive and risky procedures, are being sought. In this context, liver cell therapy (LCT) appeared as a new alternative treatment. Isolated hepatocytes can be safely infused in the diseased liver and are expected to bring sufficient enzyme activity to restore bilirubin metabolism, setting the patients within safer metabolic limits and improving its quality of life. Hepatocyte infusion has been shown to restore metabolic function not only in CN patients [53], but also in disorders of ammonium metabolism [54] glucose metabolism [55], clotting factor deficiencies [56],... However these studies have shown that the metabolic control remains partial and the durability of the results is limited in time, less than one year in most cases. The first demonstration of LCT efficacy was provided in 1998 by Fox et *al.* [57]. In this case, 7.5 billion viable liver cells were infused to a 10-year-old Crigler-Najjar type I patient with a subsequent significant decrease of bilirubin levels for up to 11 months. Glucuronoconjugates were found in bile confirming the functional integration of transplanted healthy hepatocytes. As evidenced in table 2

several groups obtained a significant (from 25 to 60%) decrease in bilirubin levels after LCT [58-63] and review [64].

Using the Short tandem repeat (STR) analysis, the authors confirm the engraftment of donor hepatocytes into the recipient liver. Our team performed LCT in two CN pediatric cases [62]. The first patient was a 9-year old girl. Pre-transplant bilirubin values attained 17.5±0.49 mg/dl (mean ± SD) and dropped after LCT to the lowest value of 11.4 mg/dl (mean ± SD: 13.6±0.42 mg/dl). After a period of 6 months, bilirubin values increased suddenly without concomitant event and the patient was scheduled for OLT. The second patient, a 1-year old girl, presented bilirubin preLCT levels of 17.6±3.5 mg/dl (mean ± SD), the serum bilirubin dramatically decreased to values of 13.3±2.4 mg/dl (mean ± SD) with the lowest value at 6 mg/dl (Figure 4). Skin jaundice reduced rapidly and the daily phototherapy schedule was alleviated from 10 to 8 hours without any influence on the bilirubin levels. After 4 months of progressive decrease of serum bilirubin, the values increased suddenly following an intercurrent Epstein-Barr virus infection. The girl underwent OLT. More recently, Ribes-Koninckx published a case of a 7 months patient who exhibited a drastic bilirubin decrease of 50% for more than 17 months [63].

Despite these encouraging results, LCT is confronted to several limitations as for instance metabolism recovery durability, donor organ shortage and the inability of hepatocytes to proliferate *in vitro*. In addition, Stephenne et *al*. demonstrated that cryopreservation of hepatocytes induced functional alteration of the mitochondrial respiratory chain complex 1 and structural modifications due to ice crystal formation during cryopreservation [65].

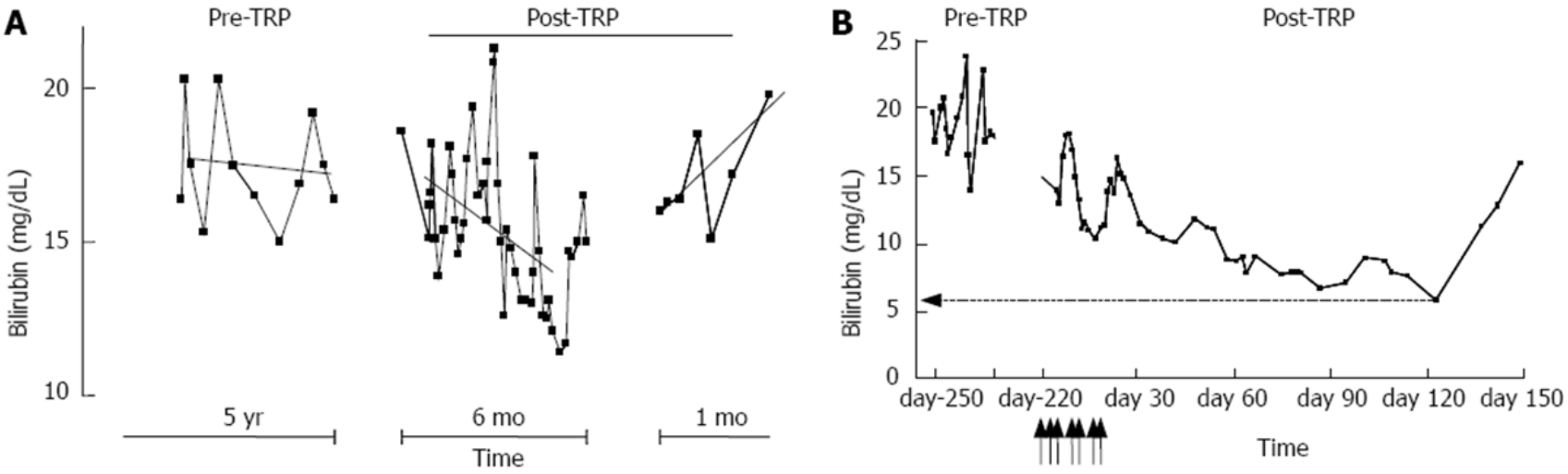

Figure 4: Evolution of serum bilirubin before and after LCT in two Crigler-Najjar patients transplanted in Brussels' center

A: After fluctuating over a period of five years, serum bilirubin of patient 1 decreased significantly to the lesser value of 11.4mg/dl in 6 months. Subsequently, increasing values were observed and patient was listed for OLT. **B**: For patient 2, after cell infusions, the serum bilirubin dramatically decreased to the value of 6mg/dl in 4 months. At this time, concomitantly to an EBV (Epstein–Barr virus) infection, higher values were observed and the patient underwent OLT. Arrows indicate the timing of cell infusions. TRP: transplantation. From Lysy et *al*. [62]

Case	Age at LCT (months)	Injected viable cells (10^9)	% of fresh cells	Follow-up	Outcome	Reference
1	120	7.5	100	60% bilirubin decrease, conjugates into the bile and demonstration of UGT1A1 enzyme activity on biopsy	Persistence up to 11 months	Fox 1998 [57]
2	96	6	32	40% bilirubin decrease for 4 months	OLT after 20 months	Darwish 2004 [59]
3	108	7.5	100	50% bilirubin decrease for a few weeks, donor hepatocytes engraftment not evidenced by STR analysis 40d post injection	OLT	Ambrosino 2005 [58]
4	18			50% bilirubin decrease for7 months, conjugates into the bile, donor hepatocytes engraftment evidenced by STR analysis	OLT after 8 months	Dhawan 2006 [60]
5	36			30% bilirubin decrease	Under follow-up	Dhawan 2006 [60]
6	9	2.2	18	50% bilirubin decrease for 5 months	Lost on follow-up	Smets 2008 [64]
7	108	4.88		35% bilirubin decrease for 6 months	OLT after 6 months	Lysy 2008 [62]
8	12	2.16		25% bilirubin decrease	OLT after 4 months	Lysy 2008 [62]
9	7	6.7		50% bilirubin decrease for 17 months	Under follow-up	Ribes-Koninckx 2012 [63]

Table 2: Liver cell transplantation in Crigler-Najjar patients

OLT: orthotopic liver transplantation, STR: short tandem repeat analysis.

b. Alternative cell sources

In liver cell therapy field, stem cells are considered as potential candidates thanks to their proliferation and differentiation potential as well as to their immuno-modulatory properties [66, 67]. Indeed, stem cells are defined by three important characteristics that distinguish them from other cell types. First, stem cells are undifferentiated cells and can renew themselves extensively, which allows having large yield available. Second, under certain physiological or experimental conditions, stem cells can be induced to differentiate into multiple specialized cell types, a property that can be kept even after cryopreservation/thawing [68-71]. Stem cells can be classified according to their potency: pluripotent (for which differentiation potential is extended to any of the three germ layers: endoderm, mesoderm or ectoderm), multipotent (which have the gene activation potential to differentiate into multiple, but limited cell types), oligopotent (with an ability to differentiate into a few cell types), unipotent or precursor cells (illustrate the concept that one stem cell has the capacity to differentiate into only one cell type) and finally specialized cells. Third, stem cells have the ability to functionally and robustly reconstitute a given tissue, when transplanted in a (damaged) recipient. In this context, stem cells would be an interesting alternative source for LCT after their plasticity had been illustrated [72, 73]. Different populations of stem cells have been widely studied and characterized for their potential use as alternative therapeutic tools in liver regenerative medicine.

i. Embryonic stem cells

Embryonic stem cells (ESCs) are pluripotent cells derived from the inner cell mass of the blastocyst (Figure 5); due to their immature status, constitute a good model for studying hepatocyte differentiation [74]. Hepatogenic differentiated hESCs were able to highly express CYP1A1, CYP1A2 and UGT1A1 mRNA following omeprazol stimulation [75]. hESCs were confronted to ethical [76, 77] and safety [78] concerns which limit their use in clinical settings.

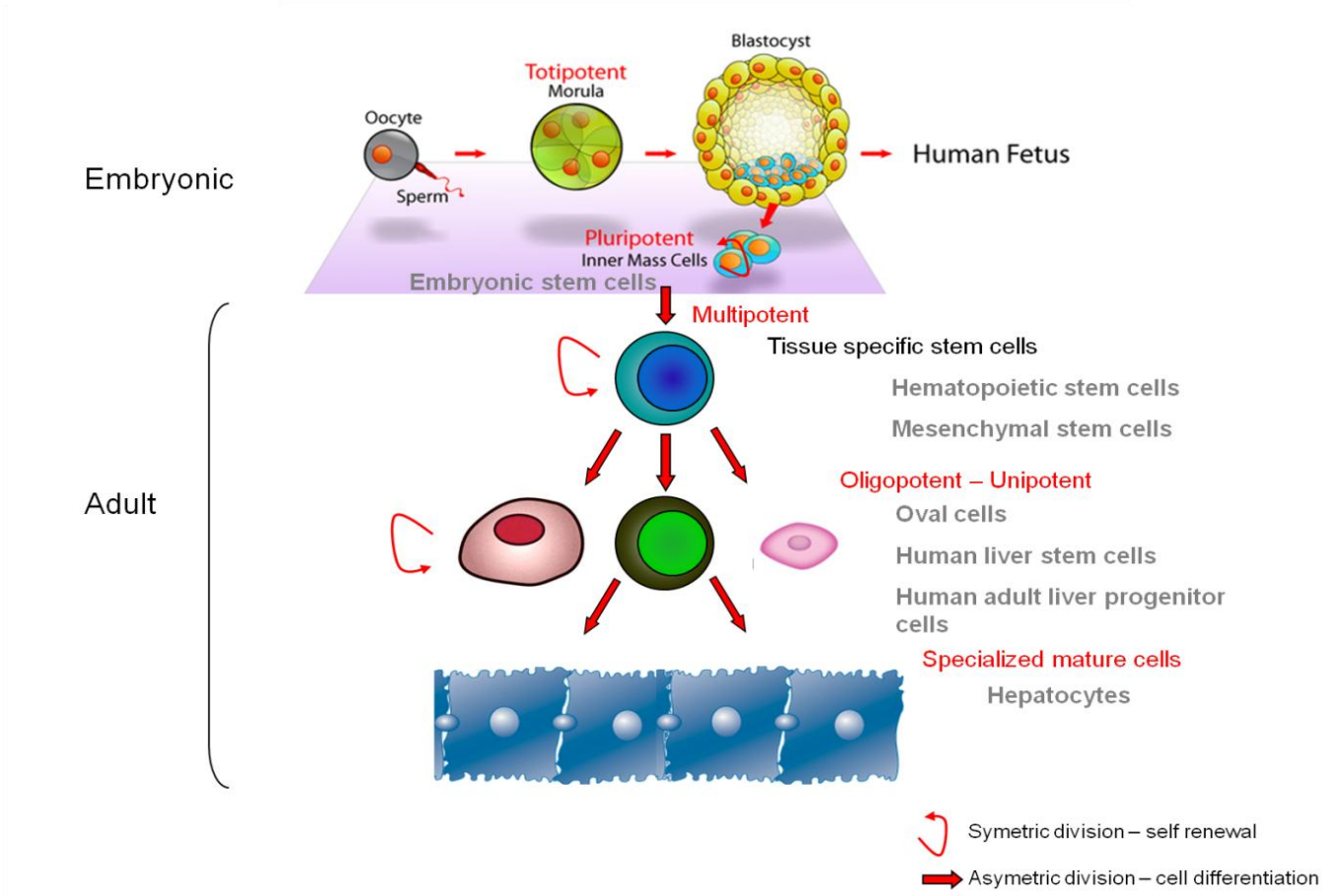

Figure 5: stem/progenitor cells origin
Image adapted from http://wikipedia.org/stem cells diagram. and Scheers I. [79]

ii. Adult stem cells

1. Hematopoietic stem cells

Hematopoietic stem cells (HSCs) are multipotent cells that can be isolated from bone marrow (BM), umbilical cord blood or peripheral blood [80]. Cell identity and phenotype are mainly determined by selection procedure whose criteria remain debated [81]. HSC showed hepatocyte differentiation potential but this potential is discussed [82-86] and lack of precision concerning identification of cell population involved in differentiation process make these cells less considerable for clinical use [87, 88].

2. Extra-hepatic Mesenchymal stem cells

Mesenchymal stem cells (MSCs) are multipotent cells and are serious candidates for liver tissue engineering. MSC can be obtained from many adult tissues [89] as various as bone marrow, adipose, cord blood or umbilical cord. These cells show extensive proliferation ability and are resistant to cryopreservation process. Moreover MSCs are well characterized: they present a spindle-shaped morphology, are adherent to plastic, and express CD73, CD90 and CD105 mesenchymal markers. MSCs are multipotent cells: they are able to differentiate into mesodermal but also endodermal and ectodermal lineage [90]. MSC have the particularity to lack expression of human leukocyte antigen (HLA) major histocompatibility complex (MHC) class II (HLA-DR) and present moderate expression of MHC class I antigen (MHC-ABC). These cells can support *in vitro* differentiation [91] and generate hepatocyte-like cells which could display advanced hepatocytic features like albumin and urea secretion as well as expression of phase I drug metabolism enzymes[92].

As regards their potential therapeutic benefit in hepatic diseases, human albumin immunostaining has been demonstrated in most preclinical studies that have transplanted human MSCs into immunocompromised rodents [92-95]. However albumin-positive immunohistology alone may hardly be considered as sufficient to claim hepatic functionality of MSC-derived engrafted cells. Rare studies have provided additional evidence through the detection of additional hepatocytic lineage markers or secretion of human albumin in rodent blood [96, 97].

3. Hepatic stem/progenitor cells

a. Oval cells

Oval cells, historically discovered in rodents [98] and found subsequently in humans, are bipotent progenitors cells located at the canals of Hering in the portal zone. They are small cells (approximately 10 μm) with a high nucleus/cytoplasm ratio and an oval-shaped nucleus. These progenitors express markers in common with bile duct cells, fetal and adult hepatocytes [99]. In response to severe or chronic injury and particularly when the proliferative response of hepatocytes is impaired [100], oval cells proliferate extensively and, depending on the injury site, either migrate to the liver parenchyma and adopt the hepatocyte cell fate or differentiate into cholangiocytes [101]. Attempts to isolate oval cells and culture them *in vitro* have delivered various cell populations characterized by different cell surface expression profiles (Table 3). The concept of oval cell response is preferred over the label of oval cell, which would suggest that these cells constitute a unique and homogenous cell population [102].

b. Hepato-mesenchymal cell types

Hepato-mesenchymal cell types are oligo/unipotent cells emerged from the parenchymal fraction of human post-natal livers after collagenase digestion [103]. Herrera et *al*. isolated Human liver stem cells (HLSC) characterized by expression of mesenchymal stem cell markers CD29, CD73, CD44, and CD90 but not hematopoietic stem cell markers[103]. They also express hepatic markers like albumin, α-fetoprotein, a small percentage of cells express CK8 and CK18 (table 3). After specific differentiation protocol, HLSC presented functional cytochrome P450, albumin, and urea production and downregulated α-fetoprotein and expressed cytokeratin-8 and cytokeratin 18.

In 2007, Najimi et *al*. described oligo/unipotent cells called human adult-derived liver progenitor cells (ADHLSCs). ADHLSC were obtained following enzymatic liver desegregation and primary culture of isolated liver cells [104]. ADHLSC expressed CD90, CD73, CD29, and CD44, documented markers for mesenchymal lineage and negative for hematopoietic markers such as CD45 and CD117. In addition, the mesenchymal phenotype of ADHLSC was confirmed by positive immune-staining for vimentin and ASMA and negative for biliary and hepatic cytokines 7, 8, 18 and 19. ADHLSC also express hepatic markers such as albumin, α-fetoprotein, AAT, CYP3A4, hepatic nuclear factor4 (HNF4) and UGT1A1 (table 3). These results suggest that ADHLSC are different from differentiated and dedifferentiated hepatocytes. Hepatic differentiation of ADHLSC was displayed in both the morphological, gene expression pattern and glycogen storage, a specific function related to mature hepatocytes. In vivo, ADHLSC were also able to engraft into uPA$^{+/+}$-SCID liver parenchyma. More recently, Khuu et *al.* [105], also

demonstrated under specific hepatogenic protocol of differentiation, ADHLSC displayed ammonia detoxification capacity and urea secretion. Using conventional RT-PCR they showed that mRNA levels of the analyzed cytochrome isoforms CYP1A1, CYP2A6, CYP2D6, CYP2C8 and CYP3A4 were increased in differentiated ADHLSC.

Hepatic progenitor cells	Most representative markers
Oval cells	α-fetoprotein
	Albumin
	CK7
	CK8
	CK18
	CK19
	OV6
Human liver stem cells	α-fetoprotein
	Albumin
	CK8
	CK18
Human adult liver progenitor cells	α-fetoprotein
	Albumin
	CYP3A4
	HNF4
	UGT1A1

Table 3: markers expressed by liver progenitor cells
Oval cells are characterized by albumin, α-fetoprotein, cytokeratin (CK) 7, 8, 18, 19 and ovalbumin (OV) 6 expression. Human liver stem cells express albumin, α-fetoprotein, cytokeratin (CK) 8, 18 but not OV6. Human adult liver progenitor cells express albumin, α-fetoprotein, cytochrome P450 (CYP) 3A4, Hepatic nuclear factor (HNF) 4, UDP-glucuronosyltransferase (UGT) 1A1

Treatment	Advantages	Disadvantages
Phototherapy	• Decrease serum bilirubin concentration	• Impairs quality of life • Less effective with age
Plamsapheresis	• Rapid decrease serum bilirubin concentration	• Punctual (during crisis phase)
Phenobarbital	• Decrease serum bilirubin concentration in Crigler-Najjar type II	• Not effective in Crigler-Najjar type I
OLT/AxLT	• Only curative treatment	• Invasive • Risky • Expensive • Life long immunosuppression • Organ shortage
Mature liver cell transplantation (experimental)	• Easier than OLT/AxLT	• Efficiency limited in time • Life long immunosuppression • Organ shortage • Inability of hepatocyte to proliferate in vitro • Poor cryopreservation resistance
Embryonic stem cell transplantation (experimental)	• Easy obtaining cell protocol • Self renewal capacity	• Ethical problems • Safety problems **To be tested/ameliorated** • Hepatic differentiation ability in vitro • Engraftment • Metabolic effect
Adult stem/progenitor cell transplantation (experimental)	• Easy obtaining cell protocol • In-vitro proliferation	• Cell population/phenotype identification **To be tested/ameliorated** • Hepatic differentiation ability in vitro • Engraftment • Metabolic effect

Table 4: advantages and disadvantages of well established and experimental treatments for Crigler-Najjar syndrome
OLT: Orthotopic liver transplantation, AxLT: auxiliary liver transplantation

Aims of the study

Liver stem/progenitor cells offer a promising therapeutic alternative for the treatment of hepatic diseases. This study is part of a larger translational research project that aims to treat inherited metabolic diseases with stem cell therapy. Ideally, stem/progenitor cells should maintain a sufficient repopulation capacity after injection into a recipient and display the desired metabolic function to recover the deficient enzymatic activity.

Adult derived human liver stem/progenitor cells (ADHLSCs) isolated from healthy adult human liver parenchymal fraction, have demonstrated their ability to be expanded *in vitro* and to display a hepato-mesenchymal profile. Under appropriate culture conditions with specific cytokines and growth factors, ADHLSC acquire a typical polygonal hepatic morphology as well as hepatocyte metabolic hepatic functions such as gluconeogenesis, urea production and xenobiotic detoxification. Khuu et *al*. [106] also demonstrated that ADHLSC are able to engraft into the SCID mouse liver and remained stable up to 60 days post-transplantation.

Next step of this research project was to prove the efficiency of ADHLSC to restore a liver deficient metabolic activity in an animal model and more specifically bilirubin conjugation deficiency in the Gunn rat model. In these conditions obtaining homologous cells in animal would be very useful to perform pre-clinical studies using syngeneic cells, instead of the current xenotransplantation not fully controlled models.

Accordingly, *our first aim* was to evaluate the possibility to obtain homologous stem/progenitor cells from the healthy adult rat liver which would display the same advanced hepatogenic profile as that obtained in human (in green on figure 6) (see

Part III chapter 1 “Hepato-biliary profile of potential candidate liver progenitor cells from healthy rat liver”).

Our second aim, described in Part III chapter 2, was to assay the ability of ADHLSC to specifically conjugate bilirubin (in blue on figure 6) before injecting directly in an animal model of liver deficient metabolic activity (bilirubin conjugation deficiency). After determining the optimal immunosuppressive treatment that will reduce human cell rejection, ADHLSC were transplanted into Gunn rat in order to correct UGT1A1 deficiency (animal model of human hyperbilirubinemic Crigler-Najjar syndrome type I).

Finally our third aim, thanks to their labeling using Indium-111 oxine, ADHLSC biodistribution following intraportal transplantation was monitored in catheterized rats as described in Part III chapter 3 “*In vivo* biodistribution of Adult Human Liver Stem/Progenitor Cells following intraportal transplantation in catheterized rats” (in purple on figure 6).

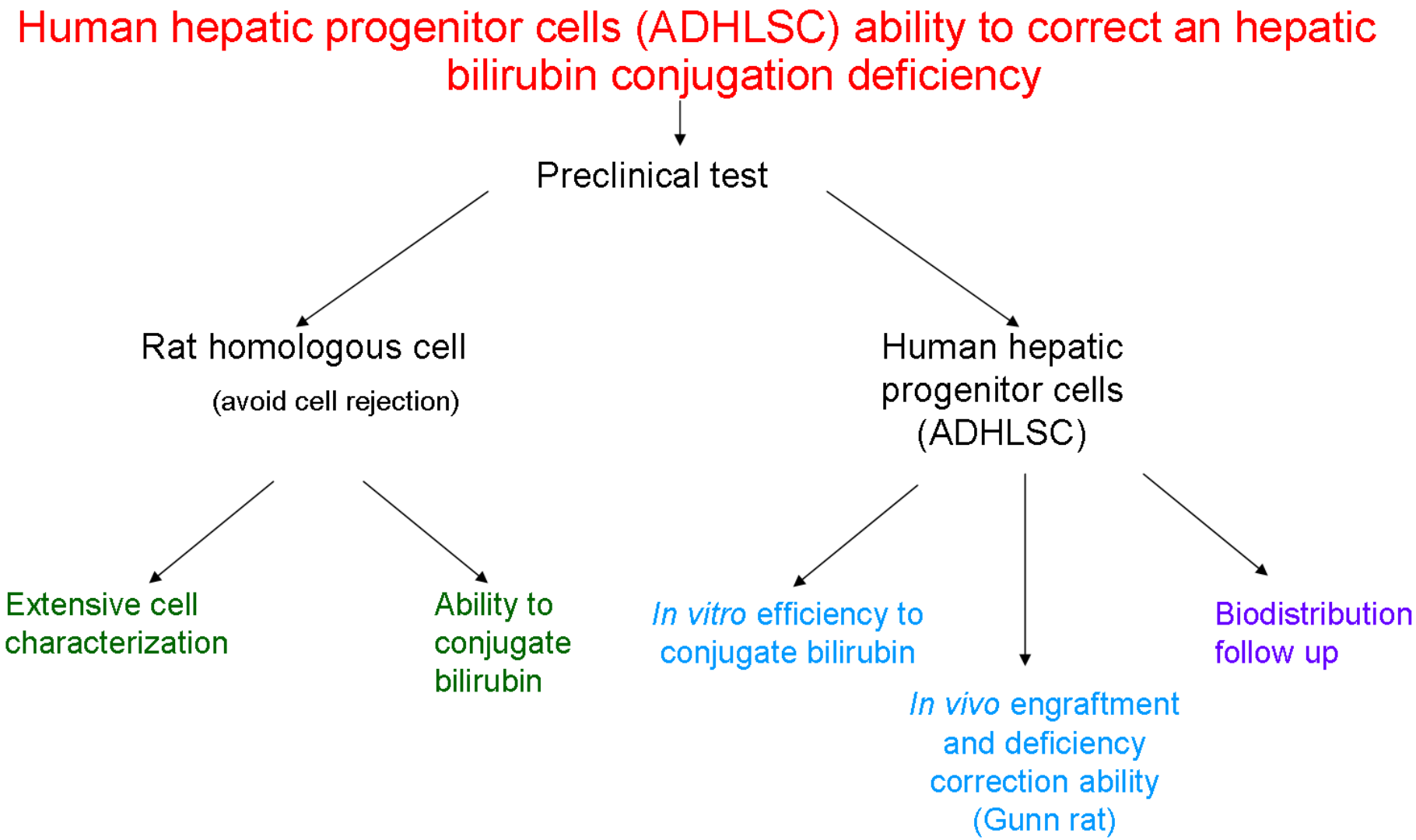

Figure 6: Experimental design of the thesis study

Results

1. **Hepato-biliary profile of potential candidate liver progenitor cells from healthy rat liver**

(Maerckx et al, World J Gastroenterol. 2012;18(27):3511-3519)

Adult derived human liver stem/progenitor cells (ADHLSCs) obtained from the parenchymal fraction can be expanded *in vitro*, displayed a hepato-mesenchymal profile and exhibited the potential to differentiate into hepatocyte-like cells both in vitro and in vivo in immunodeficient mice [104-106].

In the preclinical context, a mandatory test was to prove the efficiency of ADHLSC to restore a liver deficient metabolic activity in an animal model and more specifically bilirubin conjugation deficiency in the immuno-competent Gunn rat model. In these conditions, using homologous rat stem/progenitor cells would be very useful to perform pre-clinical studies using syngeneic cells, instead of the current xenotransplantation not fully controlled models.

In this first part, we evaluated the possibility to obtain homologous stem/progenitor cells from the healthy adult rat liver which would display the same advanced hepatogenic profile as those obtained in human. After adopting the same isolation procedure than in human as well as the identical culture conditions, we obtained a fibroblastic-like cell population (rFLDC) from the parenchymal fraction that we deeply characterized in vitro. Our data reveal that advanced hepatic features observed in human liver progenitor cells could not be demonstrated in rFLDC. However, we demonstrated the presence of a novel type of liver progenitor cell population with both hepatic and biliary phenotype.

World Journal of Gastroenterology

Online Submissions: http://www.wjgnet.com/1007-9327office
wjg@wjgnet.com
doi:10.3748/wjg.v18.i27.3511

World J Gastroenterol 2012 July21;18(27):11-3519
ISSN 1007-9327(print)ISSN 2219-2840 (online)

ORIGINAL ARTICLE

Hepato-biliary profile of potential candidate liver progenitor cells from healthy rat liver

Cédric Maerckx, Isabelle Scheers, Tatiana Tondreau, David Campard, Omar Nyabi, Mustapha Najimi, Etienne Sokal

Cédric Maerckx. , Isabelle Scheers, Tatiana Tondreau, David Campard, Omar Nyabi, Mustapha Najimi, Etienne Sokal, Laboratory of Pediatric Hepatology and Cell Therapy, Université Catholique de Louvain, 1200 Brussels, Belgium
Author contributions: Maerckx C and Scheers I performed the majority of experiments and wrote the manuscript; Campard D and Najimi M designed the study; Tondreau T, Nyabi O and Sokal E coordinated the study and were also involved in editing the manuscript.

Supported by Fonds pour la formation à la recherche dans l' industrie et dans l'agriculture (FRIA)
Correspondence to: Etienne Sokal, MD, Professor of Medicine Laboratory of Pediatric Hepatology and Cell Therapy, Université Catholique de Louvain, Cliniques Universitaires Saint Luc, 52, Avenue Mounier, Tour Vésale +3, 1200 Brussels, Belgium. etienne.sokal@uclouvain.be
Telephone: +32-2-7641387 Fax: +32-2-7648909
Received: February 8, 2011 Revised: October 15, 2011
Accepted: May 12, 2012
Published online: July 21, 2012

Abstract

AIM: To evaluate the presence of progenitor cells in healthy adult rat liver displaying the equivalent advanced hepatogenic profile as that obtained in human.

METHODS: Rat fibroblastic-like liver derived cells (rFLDC) were obtained from collagenase-isolated liver cell suspensions and characterized and their phenotype profile determined using flow cytometry, immunocytochemistry, reverse transcription polymerase chain reaction and functional assays.

RESULTS: rFLDC exhibit fibroblastoid morphology, express mesenchymal (CD73, CD90, vimentin, α-smooth muscle actin), hepatocyte (UGT1A1, CK8) and biliary (CK19) markers. Moreover, these cells are able to store glycogen, and have glucose 6 phosphatase activity, but not UGT1A1 activity. Under the hepatogenic differentiation protocol, rFLDC display an up-regulation of hepatocyte markers expression (albumin, tryptophan 2,3-dioxygenase, G6Pase) correlated to a down-regulation of the expression of the biliary marker CK19.

CONCLUSION: Advanced hepatic features observed in human liver progenitor cells could not be demonstrated in rFLDC. However, we demonstrated the presence of an original rodent hepato-biliary cell type.

Key words: Hepato biliary profile; Hepatogenic differentiation; Liver; Progenitor cell; Rat

Peer reviewer: Dr. Abdel-Majid Khatib, PhD, INSERM, UMRS 940, Equipe Avenir, Cibles Thérapeutiques, IGM 27 rue Juliette Dodu, 75010 Paris, France

Maerckx C, Scheers I, Tondreau T, Campard D, Nyabi O, Najimi M, Sokal E. Hepato-biliary profile of potential candidate liver progenitor cells from healthy rat liver. World J Gastroenterol 2012; 18(27): 3511-3519 Available from: URL: http://www.wjgnet.com/1007-9327/full/v18/i27/3511.htm DOI: http://dx.doi.org/10.3748/wjg.v18.i27.3511

INTRODUCTION

Liver transplantation is considered to be the standard treatment for end-stage liver diseases. Unfortunately, clinical applications are restricted by the scarcity of organs and uncertainty about the very long-term success of the procedure.

In recent years, liver cell transplantation using hepatocytes was successfully performed in patients with inborn errors of metabolism as an alternative, or at least as a bridge to orthotopic liver transplantation[1-5]. However, the success of such a therapeutic approach remains limited by the quality of transplanted cells. In fact, cryopreservation procedures induce significant alterations at morphological

and functional levels of the thawed hepatocytes[6,7].

To overcome these problems, several approaches to isolate and propagate liver stem or progenitor cells have been developed. In our laboratory, Najimi et al[8] isolated adult derived human liver stem/progenitor cells (ADHLSC) with hepato-mesenchymal profile. Under specific hepatogenic conditions, these cells exhibit hepato-specific functions like glycogen storage, gluconeogenesis, urea synthesis, glucuronoconjugation, and pharmacologic properties such as activity of phase I and II enzymes[9]. These cells are also able to specifically engraft and differentiate into mature human hepatocytes in mouse liver parenchyma[8].

Preclinical studies using homologous animal models of human liver metabolic diseases are attractive. It is therefore a prerequisite to obtain homologous cells from syngenic animals to perform such studies. The relevance of using human progenitor cells in immunosuppressed animal models is indeed questionable.

In this context, we evaluated the presence of a liver progenitor cell in adult rat liver that would express the same specifications as the previously reported human progenitor cell, referred to as ADHLSC.

In the current study we isolated and characterized rat fibroblastic-like liver derived cells (rFLDC) from healthy adult rats. Characterization included proliferation rate, phenotype, genotype and hepatic-specific functional assays.

MATERIALS AND METHODS

Rat fibroblastic-like liver derived cells

Five male Wistar rats weighing ± 200 g were purchased from UCL Animalerie Centrale (Brussels, Belgium) and treated in accordance with the internal Animal Ethic and Welfare Committees (UCL/MD/2009/003).

We isolated rat liver parenchymal cells in a two-step collagenase A (1100 units/L) (Roche, Mannheim, Germany) perfusion procedure according to the Seglen method[10]. We then obtained a hepatocyte enriched cell fraction following low-speed centrifugation (160 r/min for 3 min).

Viable hepatocytes, 1.5 million (> 75%, trypan blue exclusion), were seeded onto rat tail collagen I-coated plates (Greiner, Wemmel, Belgium) in Williams' E medium (Invitrogen, Merelbeke, Belgium) supplemented with 10% fetal bovine serum (FBS) (AE Scientific, Marcq, Belgium), 25 μg/L human epidermal growth factor (EGF) (Peprotech, London, United Kingdom), 10 mg/L human insulin (Lilly, Brussels, Belgium), 1 μmol/L dexamethasone (Sigma, Bronem, Belgium), and 1% penicillin/streptomycin (P/S) (Invitrogen) at 37°C in a fully humidified atmosphere containing 5% CO2. After 24 h we changed the medium in order to eliminate the non-adherent cells and thereafter we renewed it every 3 d. On days 7-12, hepatocytes died and small colonies of spindle-shaped fibroblastic cells emerged and proliferated. At this time, we switched the culture medium to Dulbecco's modified Eagle's medium (DMEM medium) [DMEM high glucose (Invitrogen) supplemented with 10% FBS and 1% P/S] in order to accelerate the proliferation of emerging cells. When cell cultures reached 90% confluence, we trypsinized them with 0.05% trypsin-1 mmol EDTA solution (Invitrogen) and replated them on a collagen-coated plate at a density of 10^4 cells/cm^2. The medium was refreshed every 3 d.

Population doubling (PD) was evaluated after each passage using the following equation: [log (harvested cells)/log (seeded cells)]/log 2. Cumulative population doubling (CPD) was calculated with the sum of PD at all passages.

At passages 2, 4 and 8, cells were analyzed using reverse transcription polymerase chain reaction (RT-PCR), immunocytochemistry and flow cytometry.

Bone marrow mesenchymal stem cells

We obtained bone marrow from Wistar rats by flushing the femur and tibia with ice cold phosphate-buffered saline (PBS) (Lonza, Verviers, Belgium) and isolated the cell fraction using Ficoll (GE Healthcare, Uppsala, Sweden) density gradient centrifugation at 340 r/min for 30 min.

Cells were then resuspended in α-MEM (Invitrogen) supplemented with 10% FBS (Perbio, Erembodegem, Belgium) and 1% P/S (Invitrogen) and seeded in 75 cm^2 culture flasks. We removed non-adherent cells after 1 d and then refreshed the medium every 3-4 d. When cultures had reached 80%-90% confluence, we harvested the cells with 0.05% trypsin-1 mmol EDTA solution and replated them at a density of 7 x 10^3 cells/cm^2. These cells were used as the internal control in mesodermal differentiation studies.

Characterization of rFLDC

Flow cytometry: Cells from the initial parenchymal fraction or after passaging were suspended at a concentration of 1000 cells/μL in PBS and 0.5% bovine serum albumin (BSA, Sigma) and then incubated for 25 min at room temperature with the following antibodies: CD29-PE (rabbit monoclonal, 1/70), CD44-FITC (mouse monoclonal, 1/20), CD45-FITC (mouse monoclonal, 1/20) (Abcam, Belgium), CD73-FITC (mouse monoclonal, 1/20), CD90-PE (mouse monoclonal, 1/20) (BD, Erembodegem, Belgium). Unspecific binding of antibodies, was evaluated using mouse IgG1 FITC and the PE isotypes control (BD).

We then washed and fixed them in cytofix/cytoperm (BD) until analysis with a FACSCantoII flow cytometer (BD).

Immunocytochemistry: We fixed rFLDC cultured on 24 well rat collagen type-1 coated plates with 3.5 % formaldehyde (v/v, VWR, Leuven, Belgium) for 15 min at room temperature. After rinsing in PBS, we permeabilized cells with 1% Triton x100 (w/v Roche) in PBS for 10 min. Before incubation with specific rat antibodies, endogenous peroxidase activity was inhibited with PBS supplemented with 3% H2O2 (VWR) solution for 3 min. Non-specific immunostaining was prevented by incubation with 3% BSA solution (Sigma) for 1 h. Cells were

then incubated for 1 h with 0.3% BSA containing the following antibodies: fibronectin (rabbit polyclonal, 1/50) (Dako, Heverlee, Belgium), vimentin (mouse monoclonal, 1/100), and α-smooth muscle actin (ASMA) (rabbit polyclonal, 1/100) (BD). After rinsing with PBS, cells were finally incubated for 30 min with Envision®, a secondary antibody against mouse or rabbit (Dako). Immunostaining results were evidenced by the addition of diaminobenzidine and urea reagents (Sigma) and counterstained with Mayer hematoxylin solution.

RT-PCR analysis: We extracted total RNA from expanded or differentiated rFLDC using the TriPure isolation reagent (Roche) and carried out cDNA with the Thermoscript RT-PCR system (Invitrogen) using 1 μg total RNA, according to the manufacturer's instructions. Rat specific primers used for gene amplification are listed in Table 1. We thereafter electrophoresed amplified cDNA on a 1% agarose gel (Invitrogen) followed by 0.01% ethidium bromide (Sigma) staining.

Plasticity assessment

Hepatogenic differentiation: rFLDC from passage four were seeded at a density of $10^4/cm^2$ into 6 wells and 24 wells rat tail type I collagen-coated plates in the presence of expansion medium. When cell cultures reached 90% confluence, we switched the medium to Iscove's modified Dulbecco's medium (IMDM, Invitrogen) supplemented with 20 μg/L human EGF (Peprotech, London, United Kingdom) and 10 μg/L human basic fibroblast growth factor-2 (FGF2) (Peprotech) for 2 d. Thereafter, we subjected cells to differentiation induction for 10 d with IMDM containing 20 μg/L human hepatocyte growth factor (HGF) (Peprotech), 10 μg/L FGF2, nicotinamide 0.61 g/L (Sigma), and 1% insulin-transferrin-selenium (ITS) (Invitrogen). An intermediate step of differentiation/maturation in IMDM containing 20 μg/L HGF, 20 μg/L human oncostatin M (Peprotech), nicotinamide 0.61 g/L and 1% ITS was performed over 10 d. The subsequent maturation step consisted of treatment with IMDM containing 20 mg/L oncostatin M, 1 μmol/L dexamethasone (Sigma), and 1% ITS premix for 10 d. For each step, we changed the medium every 3-4 d.

Mesodermal differentiation: At passages 0, 2 4 and 8, rFLDC were plated at 1.5 x 10^4 cells/cm^2 on six-well rat tail collagen I-coated plates. At confluency, we performed osteogenic differentiation with complete DMEM medium containing 0.1 μm dexamethasone, 0.1 mmol/L ascorbate and 10 mmol/L β-glycerophosphate (Sigma). After 4 wk, calcium deposition was evidenced using alizarin red staining. For adipogenic differentiation, we incubated cells with expansion medium complete DMEM containing 1 μm dexamethasone, 0.5 mmol/L isobutylmethylxanthine, 0.2 mmol/L indomethacin (Sigma) and 10 μg/mL insulin (Lilly). Medium change was carried out twice a week. After 4 wk, oil red O staining revealed the presence of lipid vesicles. As a control of mesodermal differentiation capacity, the differentiation procedure was validated with rat bone marrow mesenchymal stem cells using α-MEM complete medium.

Table 1 Primers used for reverse transcription polymerase chain reaction

Gene	Amplicon size (bp)	Primers
Vim	241	F: AAGCAGGAGTCAAACGAATA
		R: GAGCCATCTTTACATTGAGC
Fn	392	F: ACCGTGGAGTATGTGGTTAG
		R: GGTGACACCTGAGTGAACTT
ASMA	385	F: ATGCTTCTGGACGTACAACT
		R: GACTCCATTCCAATGAAAGA
CK8	378	F: TGGAGAATGAGTTTGTCCTC
		R: TGATGTTACGGTTCATCTCA
CK19	287	F: GCCAGTACTTCAAGACCATC
		R: ACTAATTTCCTCCTCGTGGT
HNF4	332	F: CGGATGTGTGTGAGTCTATG
		R: AAAGAAGATGATGGCTTTGA
TAT	275	F: CTGGACAAAACATCCTCATT
		R: GATCTCGTCAGCTAAGATGG
TDO	366	F: CTCCTGGTACAGCAGTTCTC
		R: CTTTTTCGCCTGAATCTTTA
aFP	289	F: AACGTAGCTACCATTGTCGT
		R: CAGTTTCTGGAAAGTGGAAG
Alb	365	F: TTTACGAGAAGCTTGGAGAG
		R: TGTGCAGATATCAGAGTGGA
UGT1A1	369	F: CCATGTTGCTTTTATTAGGG
		R: ACAAAACATGAGCACAGTGA
G6Pase	386	F: GAAGATGTTTCCCTGATGAA
		R: AGTCACCATTACCATTCAGG
GAPDH	315	F: CCACTCAGAAGACTGTGGAT
		R: TGTTGAAGTCACAGGAGACA
CD29	321	F: TTCAATGAACTTGTTGGTCA
		R: AGTGACTGCAAAAATCGTCT
CD44	383	F: AGGATTTCCCCAGAACTTAG
		R: ACAGGTCAAGATGGAAGATG
CD45	321	F: TGAACATACGGATTGTGAAA
		R: TTTGTTCGGACTGTAAGGTT
CD73	341	F: ATAGTCACCTCTGACGATGG
		R: ATTTCATCTGGGTGTCTGAG
CD90	380	F: AAGGAGAAACAGGAAACCTC
		R: ACAGACACAGTCCAACTTCC
CD105	386	F: TACCTCCAAGACACAGATCC
		R: TCTGCATATTGTGGTTGGTA

Fn:Fibronectin;Vim:Vimentin;ASMA:α-smooth muscle actin;CK:Cytokeratin;HNF4:Hepatocyte nuclear factor 4;TAT:Tyrosine aminotransferase;TDO:Tryptophan 2,3-dioxygenase;αFP:α-fetoprotein;Alb:Albumin;UGT1A1:UDP-glucuronosyltransferase 1A1;G6Pase:Glucose-6-phosphatase;GAPDH:Glyceraldehyde-3-phosphate dehydrogenase.

Functional hepatic tests

Glycogen storage: Undifferentiated and differentiated rFLDC fixed with 3.5% formaldehyde (Sigma) were incubated for 10 min in 1% periodic acid (Sigma). After washing with distilled water, the cells were incubated with Schiff 's reagent (Sigma) for 15 min. The preparations were then washed and mounted.

Glucose-6-phosphatase activity: We investigated glucose-6-phosphatase (G6Pase) activity in undifferentiated and differentiated rFLDC. After washing with PBS, cells were incubated for 4 h at 37 °C in 1.5 mL 50 mmol/L Tris (Sigma) and 50 mmol/L maleate (Sigma) buffer (pH

6.7) solution containing 5 mmol/L glucose-6-phosphate (G6Pate, Sigma) and 0.03 g lead nitrate (Acros, Geel, Belgium). We obtained brownish precipitates of lead sulfate following incubation of cells in a solution containing 0.1% ammonium sulfide (Sigma)[11]. Cells were then mounted and viewed by light microscopy (Leica DM IL, Groot-Bijgaarden, Belgium).

Bilirubin conjugation assay

Undifferentiated and differentiated rFLDC were incubated in William's medium and 1% FBS containing unconjugated bilirubin (Sigma) for 24 h and 48 h. Afterwards, we harvested the supernatant and added 2 μg/mL xantobilirubinic acid (use as internal standard: IS). We then submitted the product obtained in this reaction to an alkaline methanolysis followed by nitrogen evaporation as described by Muraca et al[12]. Precipitates were resuspended with 10 μL chloroform (Sigma) and 100 μL dimethyl sulfoxide (Sigma). We then injected ten microliters of this solution into the liquid chromatograph (Waters 515 HPLC pump) and eluted it with a C18 column (Macherey-Nagel, Düren, Germany). Elutriation flow started at 1 mL/min with methanol/water/tetrabutylammonium (solvent A) and ended after 11 min with methanol/ethanol/water/tetrabutylammonium (solvent B). Elution was continued for 6 min with solvent B, and the column was re-equilibrated with solvent A. The absorbance of the eluted pigments was monitored at 436 nm using a 996 photodiode array detector (Waters, Zellik, Belgium) and the area under peak was integrated electronically (Millennium software, Waters). We calculated the concentration, in micromoles per liter, of each bilirubin fraction in samples using the following equation: $(Area_{pigment}/area_{IS})$ x (IS/IV) x RF.

In which IS corresponds to micrograms of internal standard added to the sample, SV to the volume of sample (mL), and RF to the response factor.

Conjugation rate (CR) was evaluated using the equation: (Conjugated bilirubin concentration)/(total bilirubin concentration) x 100.

In which total bilirubin concentration was the sum of unconjugated and conjugated bilirubin.

RESULTS

Isolation and expansion of rFLDC

An enriched population of hepatocytes obtained after collagenase A digestion and low speed centrifugation was plated on type I collagen-coated 6-well plates.

During the first step of culture, mature hepatic cells present in the culture died due to their inability to proliferate (Figure 1). After 7 to 12 d, cells with a fibroblastic-like shape emerged and proliferated (Figure 1B and C). These cells demonstrated a high proliferative potential with a CPD of 294.55 ± 20.91 after 50 passages (Figure 2).

rFLDCs were reproducibly isolated from at least five different liver cell suspensions.

Characterization of rFLDC

All isolated rFLDC were analyzed and characterized after passages 2, 4 and 8 using FACS analysis and RT-PCR. Furthermore, a stable expression profile was observed up to P50 (data not shown).

Representative flow cytometry data at passage 4 demonstrated that the most described mesenchymal markers, CD73 and CD90 constituted 44% ± 36% and 71% ± 43% of the cell population, respectively (Figure 3), whereas the expression of CD29 protein was only detected in 2.4% ± 1.1%. The hematopoietic marker, CD45 (1.1% ± 0.6%) was almost undetectable.

To further characterize our cell population, we performed immunocytochemistry (ICC) for vimentin, fibronectin and ASMA proteins and compared the findings with rat bone marrow-derived mesenchymal stem cells (rBM-MSC) (Figure 4). The results indicated positive staining for ASMA, vimentin and fibronectin as observed with rBM-MSC.

To confirm the phenotypic profile of isolated rFLDC we performed RT-PCR analysis using specific mesodermal, hepatocyte and cholangiocyte markers at passage 4 (Figure 5).

The mesenchymal expression profile was confirmed by the detection of vimentin, fibronectin, ASMA, integrin β-1 (CD29), hyaluronic acid receptor (CD44), ecto 5'-nucléotidase (CD73), Thy-1 (CD90) and endoglin (CD105) mRNAs. RT-PCR also confirmed the absence of CD45 expression (Figure 5).

Because of their liver origin, rFLDC were also studied for their expression of hepatocyte and cholangiocyte markers. mRNA analysis revealed the expression of UDP-glucuronosyl transferase 1A1 (UGT1A1), cytokeratin 8 (CK8) and G6Pase (Figure 5). However, tyrosine aminotransferase (TAT), tryptophan 2,3-dioxygenase (TDO), albumin (Alb), α-fetoprotein (αFP) and hepatocyte nuclear factor 4 (HNF4) transcripts were not detected, all expressed by fully differentiated hepatocytes. mRNA analysis also revealed the expression of cytokeratin 19, a biliary marker.

In-vitro differentiation

First, we checked the ability of rFLDC to differentiate into adipocytes in the presence of specific media supplemented with dexamethasone, isobutyl-methylxanthine, indomethacin and insulin (Figure 6). We noticed that at early passages (P0-P2) two out of five rat fibroblastic-like liver derived cell cultures demonstrated a weak localized adipocytic differentiation. This ability was lost in further passages. Under osteogenic induction, no calcium deposit was noted (Figure 6).

In order to demonstrate their potential to differentiate into mature hepatocytes we seeded 10^4 cells/cm^2 from passage 4 in serum free-medium in the presence of several "hepatogenic" factors, as described in the Materials and Methods section. After 32 d, cells showed a slight morphology change and few cells adopted a polygonal shape (Figure 7). Using RT-PCR, we compared the expression of immature and mature hepatocytic/biliary mRNA on undifferentiated and differentiated rFLDC (Figure 5). Despite a variation in serum concentration (10% vs 2%) between the expansion medium and hepatogenic control medium, respectively, no differences in mRNA expression

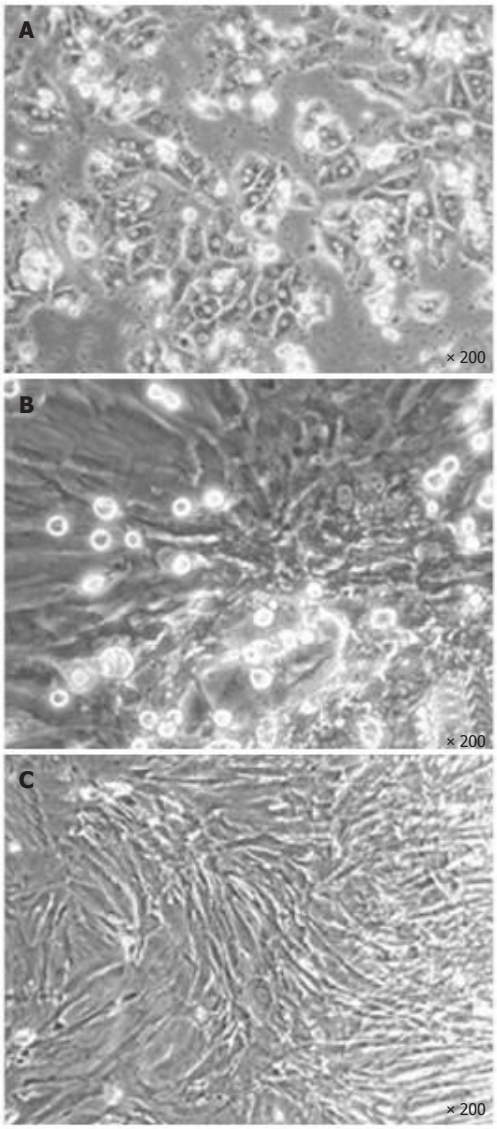

Figure 1 Rat fibroblastic-like liver derived cell obtention from adult liver parenchymal fraction. A: Cell suspension 24 h after liver parenchyma collagenase A digestion; B: 21 d culture: Rat fibroblastic-like liver derived cells (rFLDC) emergence and hepatocyte death; C: Culture purification due to rFLDC proliferation.

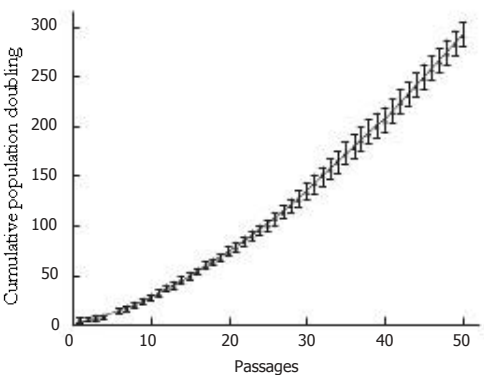

Figure 2 Proliferative capacity of rat fibroblastic-like liver derived cells. Average of cumulative population doubling of rat fibroblastic-like liver derived cells for passage 0 to passage 50.

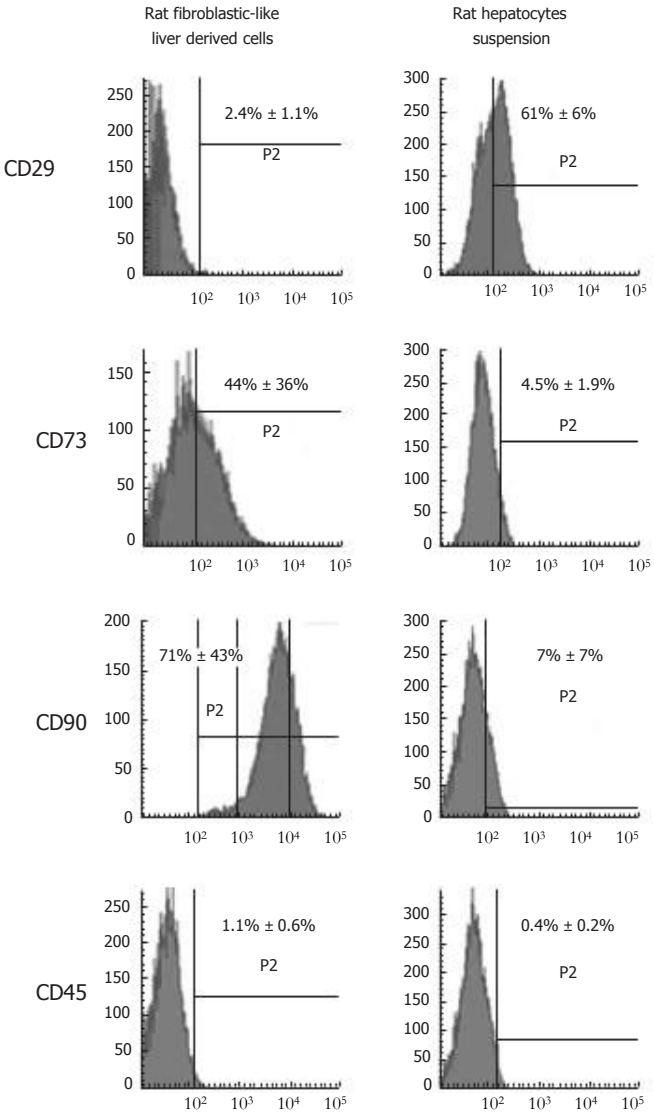

Figure 3 Representative surface markers expression analysis by flow cytometry. Results are mean ± SE of positive cells for 5 independent experiments.

were noted (data not shown). Interestingly, differentiated rFLDC lost the expression of CK19, a biliary marker. Moreover, differentiated rFLDC acquired the expression of mature hepatocyte lineage markers including TDO and albumin.

To test their liver metabolic activity, we explored their ability to store glycogen and to perform glucogenesis (G6Pase activity) and their potential to conjugate bilirubin.

Glycogen storage, evidenced by periodic-acid shift staining, showed that, like rat hepatocytes (Figure 8A), undifferentiated and differentiated cells can store glycogen (Figure 8B and C).

As shown at Figure 8D-F, rat hepatocytes and rFLDC cells also revealed a basal G6Pase activity. These results were corroborated by the expression of G6Pase at the mRNA level.

In addition to glycogen storage and G6Pase activity we assessed the ability of differentiated and undifferenti-

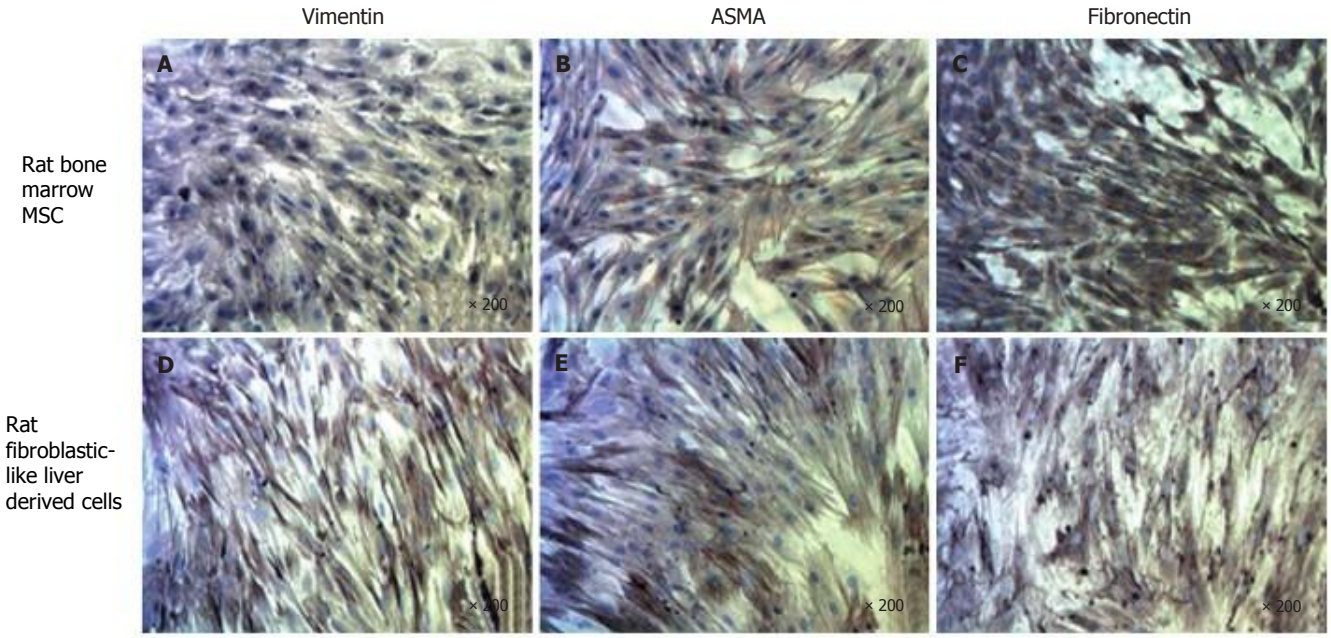

Figure 4 Rat fibroblastic-like liver derived cells mesenchymal characterization by immunocytochemistry. A-C: Rat bone marrow mesenchymal stem cells (MSC); D-F: Rat fibroblastic-like liver derived cells. ASMA: α-smooth muscle actin.

ated rFLDC to conjugate bilirubin. Therefore, we incubated 10^4 cells/cm^2 with William's medium-1% serum containing unconjugated bilirubin. After 24 h and 48 h, no bilirubin conjugate was observed in the culture medium in comparison with freshly isolated hepatocytes used as positive controls. For this late population the bilirubin CR reached 11% and 33% after 24 h and 48 h, respectively (Figure 9).

DISCUSSION

Because preclinical studies use animal models mimicking human diseases, we tried to isolate from rodent liver a liver progenitor cell that would display characteristics reported for ADHLSC. The use of human derived cells in animal models is considered irrelevant, as they may not engraft and function similarly in a xenogenic rodent environment.

Like human cells, rFLDC were isolated and emerged in vitro after culture of liver cell suspension following enzymatic-mediated disaggregation of liver. However, many differences were observed: rFLDC demonstrated a higher proliferative potential and did not reach senescence after at least 50 passages in contrast to human cells which stopped proliferating after 10-12 passages[13]. rFLDC were able, at early passages, to differentiate into adipocytes, in contrast to ADHLSC.

Like human cells, rFLDC displayed a mesenchymal profile as evidenced by the expression of CD44, CD73, CD90 and CD105. The cell population was not contaminated by hematopoietic stem cells as evidenced by the absence of CD45 expression. These results confirmed the presence of a new enriched cell population different from the freshly isolated hepatic cells. RT-PCR also revealed expression of CK8, UGT1A1 and G6P under-

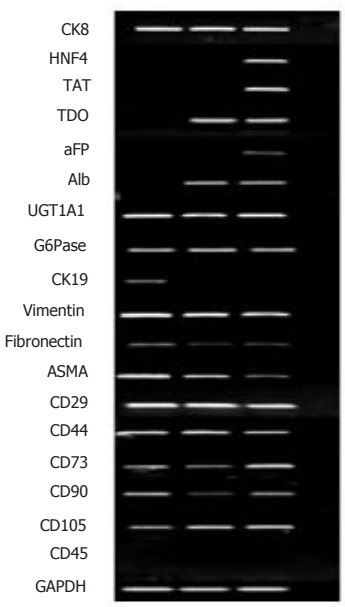

Figure 5 Representative reverse transcription-polymerase chain reaction characterization of undifferentiated and differentiated rat fibroblastic-like liver derived cells in comparison with rat hepatocyte suspension. Hepatic markers: Cytokeratin 8 (CK8), hepatic nuclear factor 4 (HNF4), tyrosine aminotransferase (TAT), tryptophan 2,3-dioxygenase (TDO), α-fetoprotein (αFP), albumin (Alb), UDP glucuronosyltransferase 1A1 (UGT1A1), glucose-6-phosphatase (G6Pase); Biliary marker: CK19; Mesenchymal markers: Vimentin (Vim), fibronectin (Fn), α-smooth muscle actin (ASMA); Cell surface markers: Integrin β-1 (CD29), hyaluronic acid receptor (CD44), tyrosine phosphatase (CD45), ecto-5'-nucleotidase (CD73), Thy-1 (CD90), endoglin (CD105); Housekeeping gene: Glyceraldehyde-3-phosphate dehydrogenase (GAPDH).

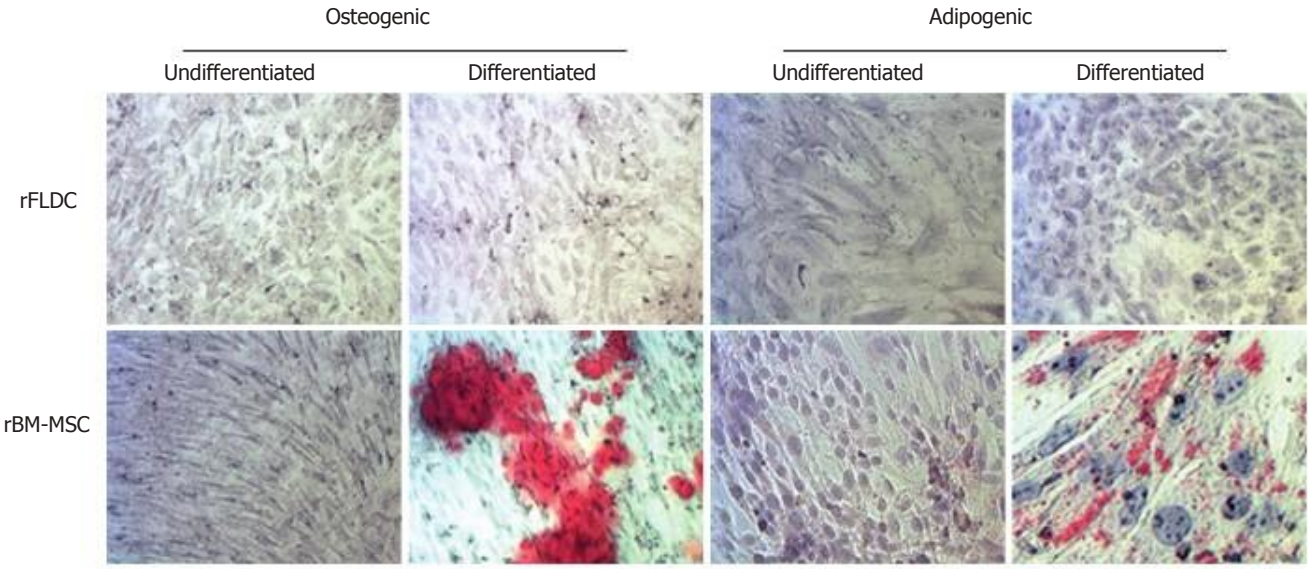

Figure 6 Evaluation of osteogenic and adipogenic differentiation potential of rat fibroblastic-like liver derived cells (alizarin red and red oil O coloration). rFLDC: Rat fibroblastic-like liver derived cells; rBM-MSC: Rat bone marrow-derived mesenchymal stromal cells.

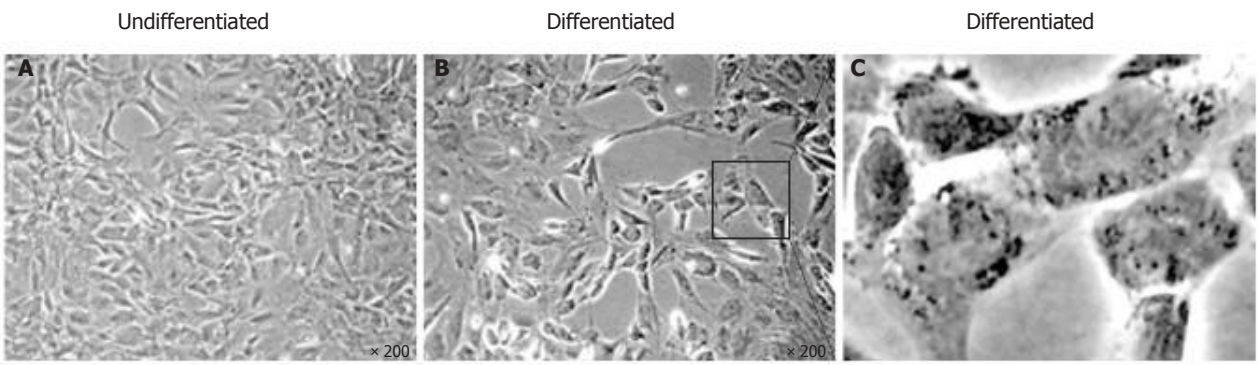

Figure 7 Rat fibroblastic-like liver derived cells hepatogenic differentiation. A: Undifferentiated; B, C: Differentiated.

lining their hepatic-like profile. Undifferentiated rFLDCs have the capacity to store glycogen and show G6Pase activity as mature hepatocytes.

In a hepatogenic differentiation medium, low numbers of rFLDC display the polygonal morphology of mature hepatocytes. Differentiated rFLDC express both albumin and TDO. However, we did not observe the expression of more specific hepatic markers such as HNF4 or TAT.

Candidate progenitor cells reported in this study were isolated from healthy rat livers, in contrast to other progenitor liver cells described elsewhere, such as oval cells, obtained after submitting animals to carcinogenic agents or toxic injuries[14-19]]. Stellate cells[20]] and rFLDC share common features like the expression of vimentin, ASMA, CK19, and CD90, although no expression of αFP was detected in rFLDC.

Differentiated rFLDC do not express CK19 or αFP, and differ therefore from small hepatocytes and epithelial cells also recovered from normal livers[17-19]].

Recently, Sahin et al[19], using a 2-step collagenase protocol, reported a cell population derived from adult rat liver and called them LDPCs (liver-derived progenitor cells). Regarding their oval morphology and expression of HNF3β, CD45, CD34 and CD90, these cells seem to be closely related to oval cells despite the absence of CK7, CK8 and CK19 expression.

In conclusion our results showed that rodent progenitor cells homologous to ADHLSC can not easily be obtained even when the same isolation and culture protocolwas applied using a rat model. However, this protocol allowed the isolation of a novel type of liver progenitor cell population with both hepatic and biliary phenotype including G6Pase activity, glycogen storage, CK8, UGT1A1 and CK19 expression.

In the presence of a hepatogenic differentiation medium, rFLDC lose the CK19 biliary marker, but do not acquire a more mature hepatic status possibly due to the use of human cytokines and growth factors, which may not be appropriate for rodent precursors, stressing again the difficulty in generating homologous models.

Further characterization and in vitro hepatogenic differentiation improvement are required before their relevant use in preclinical studies.

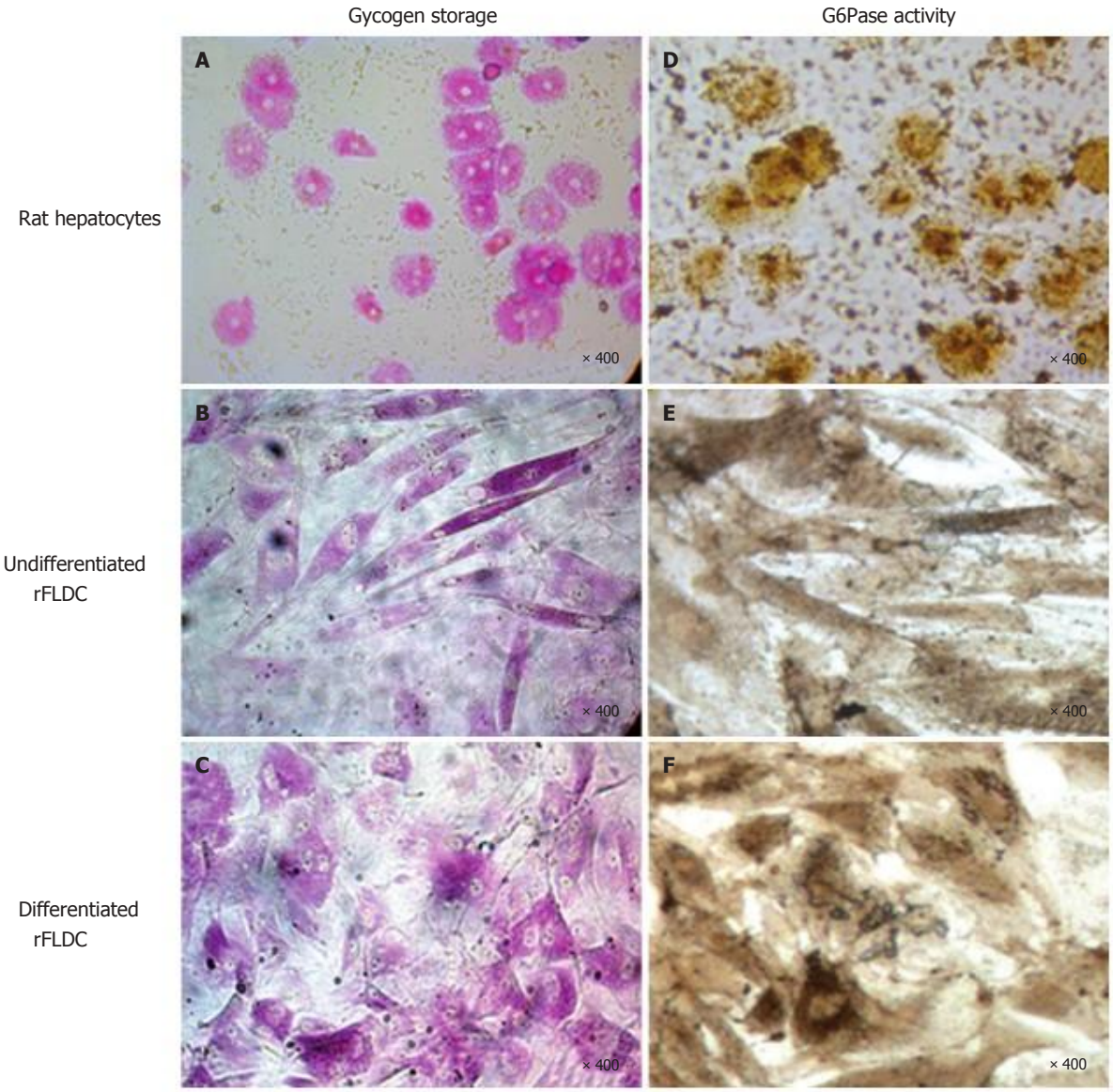

Figure 8 Hepatic functions. A-C: Glycogen storage ability assessed by periodic acid schiff reaction; D-F: Glucose-6-phosphatase (G6Pase) activity after incubation with glucose-6-phosphate and lead nitrate. rFLDC: Rat fibroblastic-like liver derived cells.

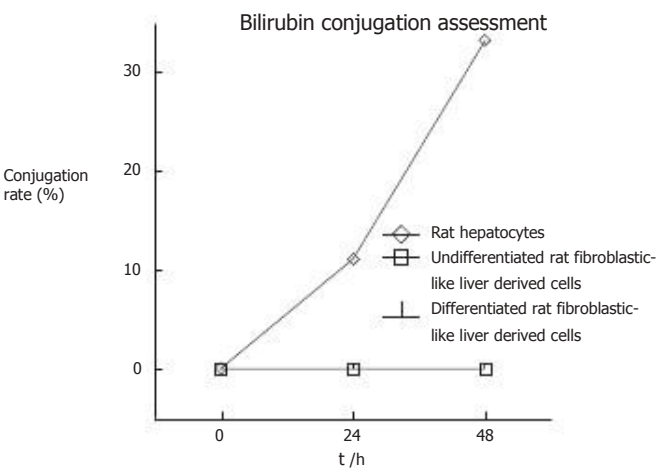

Figure 9 Bilirubin conjugation assay. Comparison between rat hepatocytes, undifferentiated and differentiated rat fibroblastic-like liver derived cells.

COMMENTS

Background

Liver cell transplantation using hepatocytes was successfully performed in patients with inborn errors of metabolism. However, the success of such a therapeutic approach remains limited by the quality of transplanted cells. To overcome these problems several approaches to isolate and propagate liver stem or progenitor cells have been developed. The capacity of those cells to restore a liver metabolic function must be demonstrated.

Research frontiers

Preclinical studies using homologous animal models of human liver metabolic diseases are attractive. It is therefore a prerequisite to isolate and propagate human homologous liver stem or progenitor cells from syngenic animals to perform such studies. In this study, the authors showed that rodent progenitor cells homologous to human adult-derived liver stem/progenitor cells can not easily be obtained even when the same protocol was applied.

Innovations and breakthroughs

In this study, the authors reported the isolation of novel potential candidate liver progenitor cells isolated from healthy rat liver called rat fibroblastic-like liver derived cells (rFLDC). These cells express both hepatic and biliary phenotype and

are able to acquire some hepatic characteristics in the presence of hepatogenic differentiation medium.

Applications

Isolation and characterization of progenitor/stem cells would be very useful to assay the in-vivo efficacy of liver mesenchymal progenitor cells in syngeneic animal models of liver metabolic diseases, particularly in the Gunn rat, a model of hyperbilirubinemia.

Peer review

This study shows that the advanced hepatic features of human liver progenitor cells have not been demonstrated in rFLDC. Although it strengthens the unique specificity of these human liver progenitor cells, it also shows that homologous models for cell therapy can not easily be developed even when the same isolation and culture protocols are applied. The authors should make a comparison of their cells with human established liver cells.

REFERENCES

1 **Muraca M**,Gerunda G,Neri D,Vilei MT,Granato A,Feltracco P,Meroni M,Giron G,Burlina AB. Hepatocyte transplantation as a treatment for glycogen storage disease type 1a. *Lancet* 2002;**359**:317-318

2 **Najimi M**,SokalE. Update on liver celltransplantation. *J Pediatr Gastroenterol Nutr* 2004;**39**:311-319

3 **Najimi M**,SokalE. Liver celltransplantation. *Minerva Pediatr* 2005;**57**:243-257

4 **Sokal EM**,Smets F,Bourgois A,Van Maldergem L,Buts JP,Reding R,Bernard Otte J,Evrard V,Latinne D,Vincent MF,Moser A,Soriano HE. Hepatocyte transplantation in a 4-year-old girlwith peroxisomalbiogenesis disease:technique,safety,and metabolic follow-up. *Transplantation* 2003;**76**:735-738

5 **Strom SC**,Fisher RA,Thompson MT,SanyalAJ,Cole PE,Ham JM,Posner MP. Hepatocyte transplantation as a bridge to orthotopic liver transplantation in terminalliver failure. *Transplantation* 1997;**63**:559-569

6 **Stéphenne X**,Najimi M,SokalEM. Hepatocyte cryopreservation:is it time to change the strategy? *World J Gastroenterol* 2010;**16**:1-14

7 **Stéphenne X**,Najimi M,Ngoc DK,Smets F,Hue L,Guigas B,SokalEM. Cryopreservation of human hepatocytes alters the mitochondrialrespiratorychain complex 1. *Cell Transplant* 2007;**16**:409-419

8 **Najimi M**,KhuuDN,LysyPA,Jazouli N,Abarca J,Sempoux C,SokalEM. Adult-derived human liver mesenchymal-like cells as a potentialprogenitor reservoir of hepatocytes? *Cell Transplant* 2007;**16**:717-728

9 **Khuu DN**,Scheers I,Ehnert S,Jazouli N,Nyabi O,Buc-Calderon P,Meulemans A,Nussler A,SokalE,Najimi M. In vitro differentiated adult human liver progenitor cells displaymature hepatic metabolic functions:a potentialtoolfor in vitro pharmacotoxicologicaltesting. *Cell Transplant* 2011;**20**:287-302

10 **Seglen PO**. Preparation of isolated rat liver cells. *Methods Cell Biol* 1976;**13**:29-83

11 **Sokal EM**,Trivedi P,Portmann B,Mowat AP. Developmentalchanges in the intra-acinar distribution of succinate dehydrogenase,glutamate dehydrogenase,glucose-6-phosphatase,and NADPH dehydrogenase in the rat liver. *J Pediatr Gastroenterol Nutr* 1989;**8**:522-527

12 **Muraca M**,Blanckaert N. Liquid-chromatographic assayand identification of mono- and diester conjugates of bilirubin in normalserum. *Clin Chem* 1983;**29**:1767-1771

13 **Scheers I**,Maerckx C,KhuuN,Marcelle M,Decottignies A,Najimi M,SokalE. Human liver progenitor cells in long term culture maintain appropriate gatekeepers mechanisms against transformation. In press

14 **Qin AL**,ZhouXQ,Zhang W,YuH,Xie Q. Characterization and enrichment of hepatic progenitor cells in adult rat liver. *World J Gastroenterol* 2004;**10**:1480-1486

15 **Yin L**,Sun M,Ilic Z,Leffert HL,SellS. Derivation,characterization,and phenotypic variation of hepatic progenitor celllines isolated from adult rats. *Hepatology* 2002;**35**:315-324

16 **Yovchev MI**,Grozdanov PN,ZhouH,Racherla H,Guha C,Dabeva MD. Identification of adult hepatic progenitor cells capable of repopulating injured rat liver. *Hepatology* 2008;**47**:636-647

17 **Nagai H**,Terada K,Watanabe G,Ueno Y,Aiba N,Shibuya T,Kawagoe M,Kameda T,Sato M,Senoo H,Sugiyama T. Differentiation of liver epithelial(stem-like)cells into hepatocytes induced bycoculture with hepatic stellate cells. *Biochem Biophys Res Commun* 2002;**293**:1420-1425

18 **Tateno C**,Yoshizato K. Growth and differentiation in culture of clonogenic hepatocytes that express both phenotypes of hepatocytes and biliaryepithelialcells. *Am J Pathol* 1996;**149**:1593-1605

19 **Sahin MB**,Schwartz RE,BuckleySM,Heremans Y,Chase L,HuWS,Verfaillie CM. Isolation and characterization of a novelpopulation of progenitor cells from unmanipulated rat liver. *Liver Transpl* 2008;**14**:333-345

20 **Geerts A**,Niki T,Hellemans K,De Craemer D,Van Den Berg K,LazouJM,Stange G,Van De WinkelM,De Bleser P. Purification of rat hepatic stellate cells byside scatter-activated cellsorting. *Hepatology* 1998;**27**:590-598

S- Editor Cheng JX L- Editor Webster JR E- Editor Zheng XM

2. Adult Derived Human Liver stem/progenitor cells from large scale cultures decrease serum bilirubin in hyperbilirubinemic Gunn Rats

As described in the previous part, notably differences exist between human and rat cell types which make rat fibroblastic like liver derived cells not suitable for their use in syngenic models of liver metabolic diseases. We therefore evaluate the efficiency of adult-derived human liver stem/progenitor cells (ADHLSC) to restore bilirubin conjugation deficiency in the Gunn rat model under immunosuppression regimen.

In that study, we demonstrated that i) ADHLSC can maintain their initial characteristics after large scale culture conditions and ii) intraportal transplantation of ADHLSC can reverse hyperbilirubinemic symptoms in a Gunn rat model up to 26 weeks post-transplantation.

Name of journal: World Journal of Gastroenterology
ESPS Manuscript NO: 8067
Columns: Pre-Clinical Trials Study

Title: Human Liver stem/progenitor cells decrease serum bilirubin in hyperbilirubinemic Gunn rat

Runing title: Large scale culture progenitor cells correct bilirubin

Cédric Maerckx, Tatiana Tondreau, Silvia Berardis, Jos van Pelt, Mustapha Najimi, Etienne Sokal

Cédric Maerckx, Tatiana Tondreau, Sylvia Berardis, Mustapha Najimi, Etienne Sokal: Université Catholique de Louvain, Institut de Recherche Clinique et Expérimentale (IREC), Laboratory of Pediatric Hepatology and Cell Therapy, 1200 Brussels, Belgium
Jos van Pelt: Katholieke Universiteit Leuven, Hepatologie, 3000 Leuven, Belgium

Author contributions: Maerckx C performed the majority of experiments and wrote the manuscript, Jos van Pelt contributed reagents/analytic tools and analyzed the data, Tondreau T. and Najimi M. designed the study; Tondreau T, Najimi M and Sokal E coordinated the study and were also involved in editing the manuscript.

Supported by Fonds pour la formation à la recherche dans l'industrie et dans l'agriculture.

Correspondence to Sokal Etienne, MD, Professor of Medicine, Université Catholique de Louvain – Cliniques Universitaires Saint Luc, Laboratory of Pediatric Hepatology and Cell Therapy, 52, Avenue Mounier – Tour Vésale +3, 1200 Brussels, Belgium. etienne.sokal@uclouvain.be

Telephone +32 2 764 13 87 Fax: +32 2 764 89 09

Abstract:

AIM: test the ability of ADHLSC from large scale cultures to conjugate bilirubin in vitro and in bilirubin conjugation deficient rat.

MATERIALS AND METHODS: adult-derived human liver stem/progenitor cells (ADHLSC) from large scale cultures were tested for their phenotype and for their capacity to conjugate bilirubin in vitro after hepatogenic differentiation. In vivo, Gunn rats (UGT1A1 deficient animal) were injected with ADHLSC and cryopreserved hepatocytes (positive control). Two, 4, 13 and 27 weeks post-transplantation, transplanted Gunn rat bilirubin serum levels were determined by High performance liquid chromatography (HLPC). . Human cell engraftment of transplanted cells was assessed 27 weeks post-transplantation using immunohistochemistry and RTqPCR.

RESULTS: large scale culture conditions do not modified ADHLSC phenotype, ADHLSC were able to specifically conjugate bilirubin. ADHLSC were intraportally injected into Gunn rats and blood UCB was measured at different times post-transplantation, infused-Gunn rats exhibited a metabolic effect 3 months post-transplantation and maintained over a 6 months period. ADHLSC engraftment into Gunn rat's liver was demonstrated by RTqPCR and immunohistochemistry against albumin and UGT1A1.

CONCLUSION: ADHLSC from large scale cultures are efficient in conjugating bilirubin in vitro and in restoring a deficient metabolic function (reducing bilirubin level) in hyperbilirubinemic rats.

Key words: Liver Stem/progenitor cells, Gunn rat, Hepatocyte, in vitro and in situ differentiation, UGT1A1

Core tip:

In this study we demonstrated the ability of adult-derived human liver stem/progenitor cells (ADHLSC) to specifically conjugate bilirubin after intraportal injection into Gunn rats a model presenting a deficient bilirubin conjugation function (homologous to human Crigler-Najjar type I syndrome). Infused-Gunn rats exhibited a metabolic effect 3 months post-transplantation and maintained over a 6 months period. ADHLSC engraftment into Gunn rat's liver was demonstrated by immunohistochemistry and RTqPCR. These results suggest the potential of ADHLSC to restore a deficient metabolic function in-situ.

Introduction:

Bilirubin is a toxic derivative of the protoporphyrin moiety of haem proteins such as haemoglobin. For its clearance from serum, bilirubin is conjugated in hepatocytes with glucuronic acid thanks to uridine diphosphate-glucuronosyltransferase 1A1 (UGT1A1) activity.

Genetic variations in the gene encoding UGT1A1 lead to complete or partial inactivation of the bilirubin glucuronidation, which causes unconjugated bilirubin accumulation in the serum. This can result in hyperbilirubinemic conditions such as the human Crigler–Najjar syndrome type I and II.

Gunn rat, derived from Wistar parent strain, has constantly elevated concentrations of serum bilirubin which causes unconjugated hyperbilirubinaemia. Gunn rat inherently lacks all glucuronidation activities catalysed by the UGT1 isoforms and is therefore used as animal model for Crigler–Najjar syndrome type I[1-2].

Clinically, Crigler–Najjar syndrome type I is associated with progressive damage of the central nervous system leading to bilirubin encephalopathy (kerincterus)[3-5]. The current treatment induces biliary clearance of bilirubin by photoactivation under light exposure [6]. Unfortunately the treatment becomes inefficient due to progressive skin thickening and hence is insufficient to prevent brain damage. So far, orthotopic or auxiliary liver transplantation remains the only cure [7,8]. However, donor shortage, life-long immunosuppression to prevent rejection and risks related to surgery constitute major hurdles to an extensive use of this treatment [9].

As a mean to circumvent complications associated with organ transplantation, liver cell transplantation (LCT) has emerged as a new strategy to treat patients with chronic and acute liver disease and to restore metabolic liver functions in inherited

liver disorders [10-16]. Hepatocyte transplantation has namely been used for the treatment of Crigler-Najjar syndrome type I. The first demonstration of its efficacy in Crigler-Najjar type I patient was provided by Fox et al. [15]; the effect was a significant decrease of bilirubin levels for up to 11 months. We and others [16] reported four additional patients in which the reduction of serum bilirubin reached up to 50% over a follow-up of 7 months. LCT is confronted to limited availability of human hepatocytes, their incapacity to proliferate *in vitro* and their poor resistance to cryopreservation which prevent their wide use in the clinic [17,18]. In addition, mature hepatocytes do not provide long term support as these mature cells have lost their repopulation capacity.

Therefore researchers have turned towards adult stem/progenitor cells as alternative cell sources more suitable for regenerative medicine and more likely to integrate the regenerative niche and provide long term allogeneic cell renewal. Adult stem or progenitor cells which are resident in mature organs and tissues are rather tissue specific and lineage restricted. They have either the self-renewal capacity to proliferate indefinitely (stem cells) or display a limited proliferation potential as their daughter cells spontaneously differentiate into mature cells (progenitor cells) but altogether have advantages to proliferate *in vitro* and to resist to cryopreservation.

Our group [19] has isolated adult stem/progenitor cells from adult human liver (ADHLSC). These cells express mesenchymal (CD29, CD73, CD90, α-smooth muscle actin, Vimentin) and hepatic markers (albumin, Multidrug resistance-associated protein 2 (MRP2), Hepatocyte Nuclear Factor 4 (HNF4), cytochrome P450 (CYP)1B1 and CYP3A4) but no biliary markers [20]. Moreover, these cells have the capacity to

differentiate in hepatocyte-like cells under selective culture conditions and are not only able to engraft into the liver of immunodeficient mice and remained stable up to 60 days post-transplantation but to differentiated in situ and participate to liver regeneration after hepatectomy stimuli [21].

This study demonstrates that ADHLSC can be cultivated in large scale conditions without phenotype alterations and provides the proof of concept that ADHLSC transplantation can reverse hyperbilirubinemic symptoms in a relevant animal model of Crigler-Najjar disease. We demonstrate here the ability of ADHLSC to engraft in recipient rat livers where they participate in restoration of liver function by a significant reduction of the serum bilirubin levels. Our findings support ADHLSC as a promising candidate for liver cell-based therapy developments.

Materials and Methods

Study design:

All experiments using human material in the present study were done under the approval of the Institution Ethical committee and donor informed consent.

Human Adult Liver progenitor cells isolation and large scale culture

Hepatocytes were recovered post mortem (cerebral hemorrhage) from a healthy 11 years old male donor after 2 steps collagenase perfusion as described by Seglen [22]. The procedure was performed within the tissue bank of the hospital. Cells were tested negative for microbiological, viral and mycoplasma contaminations. Viable isolated hepatocytes, 20 millions, (79%, trypan blue exclusion), were seeded onto Cell Bind 175cm² flasks (Corning, Lasne, Belgium) in Williams'E medium (Invitrogen, Merelbeke, Belgium) supplemented with 10% fetal bovine serum (FBS) (AE scientific, Marcq, Belgium), 10 µg/ml human insulin (Lilly, Brussels, Belgium), 1 µM dexamethasone (Sigma, Bronem, Belgium), and 1% penicillin/streptomycin (P/S) (Invitrogen) at 37°C in a fully humidified atmosphere containing 5% CO_2 according to Najimi et *al.*[104] with some modifications. On days 7-12 hepatocytes died and small colonies emerged and proliferated. At this time, culture medium was switched to complete DMEM medium (DMEM high glucose with 10% FBS and 1% P/S) in order to accelerate the emerging cells proliferation. When cell cultures reached 90% confluence, cells were trypsinized with 0.05% trypsin-1 mM EDTA solution (Invitrogen) and replated on Cell Bind flasks at a density of $5x10^3$ cells/cm². Large scale culture using Cell Stack 10 (6360cm²) (Corning) was carried out in clean-room facility.

According to Najimi et *al*. [19], hepato-mesenchymal character was analyzed by FACS and immunocytochemistry using CD29, CD44, CD73, CD90, Vimentin, α-smooth muscle actin (ASMA), Albumin and Pan-CK antibodies (BD, Erembodegem, Belgium). In order to assess the homogeneity and to exclude hematopoietic contamination CD45 marker was also controlled as well as stem cell markers CD117 and CD133. Karyotype analysis as described by Scheers et *al*. [23] showed no structural or numerical chromosomal aberrations.

Hepatogenic differentiation protocol

Hepatic differentiation has been performed on ADHLSC at different passages as described by Najimi et *al*. [19] with some modifications. Briefly, cells were seeded at 10^4 cells/cm^2 in 6-well plates in expansion medium for 48 hours. Differentiation consisted of 4 steps protocol lasting 32 days: Culture medium was replaced by IMDM (Invitrogen) containing 1% PS, 20ng/mL epithelial growth factor (Peprotech, London UK) and 10ng/mL basic fibroblast growth factor (bFGF; Peprotech) for 48 hours (1 step). During step2, cells were cultured in IMDM supplemented with 1% PS, 20ng/mL hepatocyte growth factor (Peprotech), 10 ng/mL bFGF, 0.61 g/L nicotinamide (Sigma) and 1% insulin-transferrin-selenium premix (ITS; Invitrogen) for 10 days. In 3rd step, bFGF was replaced by 20 ng/mL oncostatin M (OSM; Peprotech) for 10 additional days. Maturation step was completed by changing the medium to IMDM containing 1% PS, 20ng/mL OSM, 1 µmol/L dexamethasone (Sigma) and 1% ITS for 10 days.

The undifferentiated cells (control) were kept during the whole process of differentiation in IMDM supplemented with 1%PS and 2% FBS. Medium was changed twice a week.

In vitro differentiation was controlled at morphological level, by CYP3A4 activity (Promega, Madison, Wisconsin) and by the ability to specifically conjugate bilirubin as described below.

Bilirubin assay

$6x10^5$ undifferentiated and differentiated ADHLSC were seeded per $10cm^2$ collagen coated well and incubated with William's medium, 1% FBS, containing 100µM (=5.84mg/dl) unconjugated bilirubin (UCB) (Sigma) for 24h and 48h. Supernatant was harvested at the end of incubation period and mixed with 2µg/ml Xantobilirubinic acid used as internal standard (IS). The reaction product was submitted to an alkaline methanolysis followed by nitrogen evaporation as described by Muraca et *al*. [25]. Precipitates were resuspended with chloroform and dimethyl sulfoxide (Sigma). The solution was injected into the liquid chromatograph (Waters 515 HPLC pump) for separation on C18 column (Macherey-Nagel, Düren, Germany). Elutriation flow started with methanol/water/tetrabutylammonium (solvent A) and ended after 11min with methanol/ethanol/water/tetrabutylammonium (solvent B). The absorbance was monitored at 436nm using a 996 photodiode array detector (Waters, Zellik, Belgium) and the area under peak was integrated electronically with Millennium software (Waters, Zellik, Belgium). The concentration, in micromoles per liter, of each bilirubin fraction in samples was calculated as follow: (area $_{pigment}$/area $_{IS}$) x (IS/SV) x RF, in which IS corresponds to micrograms of IS added to the sample, SV to the volume of sample (ml), and RF to the response factor. Conjugation rate (CR) was evaluated as follow: ((Conjugated bilirubin concentration)/(Total bilirubin concentration)) x100, in which total bilirubin concentration is the sum of unconjugated and conjugated bilirubin.

Gunn rat transplantation

Animal procedures were conducted according to the guidelines established by the Université Catholique de Louvain, in accordance with European Union Regulation and approval of the protocols by the local animal ethical and welfare committees (UCL/MD/2009/003). In order to confirm serum UCB level stability 11 naive Gunn rats were followed over 6 months. Non-differentiated ADHLSC cultured on Cell-Bind Corning plastic in clean-room facility were detached using 0.05 % trypsin-EDTA (Invitrogen) solution. ADHLSC used in this study were obtained from passages 4-6. After centrifugation cells were washed in PBS and recovered in PBS containing 4% N-acetylcystein (Lysomucyl, Zambon, Jette, Belgium). Cryopreserved hepatocytes, used as positive control were thawed in clean room, centrifuged, washed and also resuspended in PBS-4% N-acetylcystein suspension. $2{,}5x10^6$ millions ADHLSC (n=5 rats) or hepatocytes (n=3 rats) were injected into the portal vein of 9-11 week-old male Gunn rats. This corresponds, for a 200 gram rat, to an estimate of 0,25% of his total liver cell mass of 5 billion cells /kg body weight [26]. In order to limit cell rejection, rats were injected every 2 days with immunosuppressor medication: cyclosporine A (Sandimmum, Novartis, Vilvoorde, Belgium) at a dose of 5mg/kg of body weight [27]. Two, 4, 13 and 27 weeks post-transplantation, transplanted Gunn rat UCB serum levels were determined by High performance liquid chromatography (HLPC) as described above. Human cell engraftment of transplanted cells was assessed 27 weeks post-transplantation. Liver was then recovered, fixed in formaldehyde 3.5% (VWR International, Leuven, Belgium) and then embedded in paraffin for immunohistochemistry assessment of the engrafted cells.

Immuno-histochemistry analysis

Five µm liver sections were deparaffinized and rehydrated in xylene and graded alcohol series. Antigen retrieval was performed by incubating the sections in citric acid monohydrate solution (pH 6.0). Cells were permeabilized by incubating the sections into 0.1% triton X-100. Non-specific immunostaining was prevented by incubation in PBS buffer containing 1.5% normal goat serum at room temperature (RT). Sections were incubated overnight with anti-human Albumin (Calbiochem, UK) (1/1000) or anti-human UGT1A1 (Santa Cruz biotechnology, Heidelberg, Germany) (1/100), in 2% normal goat serum at 4°C. Staining detection was visualized with 1/500 AlexaFluor594 anti-rabbit antibody solution (Invitrogen) incubation at RT. The nuclei were counterstained using DAPI (1/500). Slices were scanned using a Mirax digital slide system (Zeiss, Zaventem, Belgium) and analyzed thanks to Mirax viewer version 1,12,22,0 (Zeiss). To determine cell repopulation, 10 000 nuclei were counted over two randomly chosen area per section. Repopulation ratio was obtained as follow: (marked cells/total cells) x100.

RNA extraction, cDNA synthesis and Real-time PCR

Cell culture

$6x10^5$ control and in vitro differentiated cells were lyzed in Tripure followed by phenol chloroform extraction. The aqueous phase was recovered after centrifugation (11500rpm) and total RNA precipitated with isopropanol (Sigma) and quantified using a nanodrop spectrophotometer (ThermoFisher, Erembodegem, Belgium). Two µg of total RNA was DNase–treated to eliminate genomic DNA and reverse transcribed using the Super Thermoscript kit (Invitrogen). Real time PCR was performed in 25µl reaction with TaqMan® Master mix containing Taq DNA

Polymerase (Applied Biosystems), 300nM concentration of forward and reverse primers (UGT1A and the house keeping gene: Cyclophilin A) and 5µl of cDNA samples. The PCR reaction was performed using StepOnePlus Real Time instrument (Applied Biosystems). Time and temperature profile of the PCR reaction consisted of the following steps: 2 minutes at 50°C, 10 minutes at 95°C, followed by 40 step cycles of 15 seconds of denaturation at 95°C followed by 1 minute of annealing/elongation at 60°C. For analysis, UGT1A Ct was normalized to Cyclophilin A (delta Ct) for both differentiated and undifferentiated status. The double delta Ct (ΔΔCt) is then calculated as the difference between delta Ct for differentiated and undifferentiated cells. Fold increase or relative quantification was obtained using the following formula: $RQ= 2^{-\Delta\Delta Ct}$

Rat liver analysis

Four mg liver tissue soaked in Tripure were disaggregated using tissue homogenizer (IKA Ultra-Turrax, Qlab, Vilvoorde, Belgium) and followed by phenol chloroform extraction. Total RNA was quantified using a nanodrop spectrophotometer. One µg of total RNA was DNase–treated and reverse transcribed using the Super ThermoscriptTM kit (Invitrogen). Real time PCR was performed in 25µl reaction with TaqMan® Master mix containing Taq DNA Polymerase (Applied Biosystems), 300nM concentration of forward and reverse primers (Human Albumin and Human GAPDH) and 5µl of cDNA samples.

PCR reaction was performed using StepOnePlus Real Time instrument as described above.

Statistical analysis

Analyses were done in the GraphPad Prism software program (GraphPad ,San Diego, California). Comparison for UCB mean between following times for a same group was analyzed using a paired T-test. Means statistical analyses was carried out using Student test. Statistical analyses are detailed on Annexe 2.

Results

Characterization of ADHLSC large scale cultures

The parenchymal cell suspension fraction obtained after human liver dissociation with a viability of 79% was plated on Corning CellBind surface flasks. After 2 weeks of culture in serum supplemented medium, ADHLSC with fibroblast-like morphology and prominent cytoplasm (figure 1A) started to emerge. From the second passage, cells were cultivated in large culture conditions (CellStack-10 corresponding to a surface area of 6360 cm^2) and phenotype of the growing cells was analyzed. Flow cytometry and immunocytochemistry confirmed that these cells shared the phenotype described previously for ADHLSC grown at smaller scale and on rat collagen([104]). At passage 2 already, cells were shown to be CD73, CD90, CD29 and CD44-positive. As expected the cells also expressed αSMA and vimentin, two additional markers of mesenchymal status, as demonstrated by immunocytochemistry (figure 1B). In addition immunocytochemistry confirmed their immuno-positivity for albumin as evidence of the hepatic-lineage commitment of ADHLSC. Hematopoietic stem cell contamination was excluded based on the lack of expression of CD45, CD117 and CD133. As illustrated in table 1, phenotypical characteristics were maintained at least until passage 6. These results confirmed that large scale culture provided cells displaying identical characteristics as the hepato-mesenchymal ADHLSC previously isolated and described.

In vitro differentiation of ADHLSC

We evaluated the capacity of ADHLSC large scale cultured to differentiate into tissue-specific cell types. To do so, cells were cultured for 32 days in hepatocyte

differentiation culture conditions as described by Najimi et *al*. [19] with some modifications. At the end of the protocol, differentiated cells adopted an hepatocyte-like morphology as shown in figure 2A in addition we noticed an 36 fold increase in CYP3A4 activity between undifferentiated and hepatogenic differentiated cells at passage 6 (data not shown).

In addition, we evaluated the ability of ADHLSC to express UGT1A mRNA and to conjugate bilirubin *in vitro*.

We assayed using QPCR technology, the expression of UGT1A mRNA constituted of the first 4 common exons of UGT1A family in total RNA extracts. Indeed, hepatogenic differentiation induced a 9.31 and 10.02 fold increase in UGT1A mRNA levels at passage 4 and 9 respectively (Figure2B). Expression of UGT1A mRNA was constant between passage 4 and 9 (no significant difference between UGT1A fold increase was noted).Thereafter, we assessed the ability of differentiated ADHLSC to conjugate bilirubin. For that we incubated both undifferentiated and differentiated ADHLSC with 100µM UCB for 24 and 48 hours after which supernatants were recovered to analyze the glucuronidation of bilirubin. We could determine that differentiated ADHLSC were able to specifically conjugate bilirubin as illustrated in figure 2C. Undifferentiated ADHLSC exhibited a low bilirubin conjugation potential *in vitro* after 24h (2.5 ± 0.4%) which increased with time reaching 7.4 ± 0.5% after 48h. Conjugation rate of differentiated ADHLSC reached 5.1 ± 1.8% and 9.0±1.1% after 24h and 48h respectively. Wild type hepatocytes used as positive control showed a conjugation percentage of 31.0 ± 6.6% and 45.0 ± 7.1% after 24h and 48h respectively. In contrast Crigler-Najjar hepatocytes, used as negative control were not able to

conjugate bilirubin indicating that the activity of either undifferentiated or differentiated ADHLSC is partial as compared to mature hepatocytes activity (16 to 20% of hepatocytes activity after 48 h incubation) but highly significant.

Transplantation of ADHLSC in the Gunn rats and functional integration in vivo

Building on the capacity of ADHLSC to conjugate bilirubin *in vitro*, we investigated their potential benefit after transplantation in providing UGT1A1 activity in the Crigler-Najjar animal model, the Gunn rat [28]. We performed transplantation of Gunn rats either by infusing 2.5 millions freshly trypsinized ADHLSC or cryopreserved and thawed hepatocytes into the portal vein of five and three rats respectively. Three additional control rats were subjected to surgery and received intraportal injection of vehicle only (4% NAC in PBS). Starting on day one after cell infusion, all rats received ciclosporine A via ip route once every two days. Rats were followed up for a total period of 27 weeks with weekly weighing. Body weight of transplanted rats during the experiment was comparable to weight evolution of normal Gunn rats used as controls (2weeks post transplantation: 229 ± 9g and 230 ± 6g for transplanted and control rats respectively, 27 weeks post transplantation: 399 ± 15g for transplanted rats and 400 ± 17g for control rats).

Blood drawings were used to measure serum UCB concentrations by a very sensitive high-performance liquid chromatography (HPLC) method. Beforehand we had demonstrated that serum UCB levels in 11 naive Gunn rats colony were stable over 6 months (figure 3A). In addition, to avoid any bias due to sublocalization of individual cages, one cage with two rats was moved to all parts of the room to measure a possible influence of light sources on serum UCB concentrations. As for the previous test, no significant modification in serum UCB were observed (data not

shown). Comparison of serum UCB levels measured 27 weeks after transplantation with levels measured 2 weeks post-transplantation revealed a 50% drop of UCB levels in rats transplanted with ADHLSC or hHepatocytes (Figure 3B). As illustrated in Figure 3C, when individual results were examined, it appeared that 4 of the 5 ADHLSC-transplanted rats showed a remarkable reduction of serum UCB levels after 3 months. UCB concentration reached 4.7 ± 0.5mg/dl in average for the four responsive rats instead of 7.0 ± 0.4mg/dl in average for the vehicle-infused Gunn rats. Further correction of UCB levels was achieved after 6 months when UCB levels reached 3.2 ± 0.5 mg/dl versus 6.1 ± 0.2mg/dl in the vehicle injected rats. One rat out of five transplanted with ADHLSC did not respond to the treatment. Paired T test analysis revealed a significant difference (p-val=0.003) between the serum UCB levels when compared at 2 and 27 weeks post-transplantation in the four responsive animals. Adding the fifth animal to the statistics caused the p-value to increase to 0,0625, just below statistical significance. Gunn rats transplanted with hHepatocytes also saw their serum UCB levels decrease with similar kinetics as the rats transplanted with ADHLSC from 6.3 ± 0.8mg/dl to 3.2 ± 0.2 mg/dl at 6 month post-transplantation (p-val=0.0658).

In order to confirm that metabolic improvement was due to ADHLSC engraftment, RTqPCR and immuno-fluorescence staining were performed on transplanted rat liver.

Engraftment of infused ADHLSC and hepatocytes was revealed by RTqPCR positive signal for human albumin and GAPDH (Figure 4D). ADHLSC injected rat livers revealed a positive signal for human albumin and human GAPDH after 37.68±0.11

and 34.98±0.38 cycles respectively whereas hepatocytes infused rat livers exhibit a positive signal after 36.77±0.42 and 35.62±0.17 cycles for human albumin and human GAPDH respectively.

In the four rats where UCB decrease after treatment, engraftment of infused ADHLSC was revealed by positive staining for human albumin (Figure 4A) using a specific antibody which does not cross-react with rat albumin as illustrated in PBS injected rat liver parenchyma (negative control). Since ADHLSC constitutively express albumin, human albumin positivity is not sufficient to infer about the differentiation status achieved by ADHLSC *in vivo*. Thus in addition to recognizing cells from human origin within the rat parenchyma, we also wanted to confirm that these cells expressed UGT1A1 *in vivo* and that improvement of hyperbilirubinemia observed in four rats could be correlated with implantation of functional cells. To do, we processed serial sections by immunofluorescence for human albumin detection as described above and for human UGT1A1 detection (Figure 4A). Such serial sections allowed us to demonstrate localisation of human albumin and UGT1A1 expression in the four rats where UCB decrease after treatment. As shown in figure 4A, 27 weeks post-transplantation, human cells not only appeared integrated into rat liver parenchyma but also exhibited a typical hepatocyte morphology which is consistent with their expression of UGT1A1, a marker of mature hepatocytes. Interestingly all human albumin- and UGT1A1-positive cells were for a majority found implanted in periportal zones.

We were also interested to evaluate the engraftment level of cells in a model of metabolic liver that was not subjected to any chemical or surgical insult as

regeneration stimulus since this is closest to the clinical setting for CN patients. A rough estimation was done by counting albumin-positive cells over two randomly chosen areas per section and per liver (see the schematic in Figure 4B). Total cells in these areas were counted based on nuclear DAPI staining. Areas corresponding to 10^4 total cells were counted visually on a scanned image of each section. Such quantification was used to provide a gross evaluation of engraftment levels 27 weeks post-transplantation. We found repopulation varies from 0 to 2.11% and from 0.58 to 1.31% for ADHLSC and hepatocytes respectively (Figure 4C); mean of repopulation ratio rates 1.3 ± 0.3% and 1.0 ± 0.2% for ADHLSC and hepatocytes respectively (Figure 4D).

Discussion

In the current study, we demonstrate that ADHLSCs from large scale cultures are able to engraft into the host liver parenchyma and to partially restore one important hepatic function (bilirubin conjugation) into the Crigler-Najjar animal model, the Gunn rat.

Hepatocyte transplantation experience in Crigler–Najjar disease patients had shown a significant reduction in bilirubin levels allowing to reduce the phototherapy requirement [24,26], but the clinical improvement remains limited in time as these mature cells have a limited self-renewal capacity [24,27]. In addition, human hepatocytes shortage, poor cryopreservation resistance [17,18] and absence of *in vitro* proliferation capacity constitute a major hurdle in large application of this mature liver cell therapy.

Therefore, other cell sources become mandatory. Stem/progenitor cells can be expanded *in vitro*, can engraft, proliferate and participate to host liver repopulation, and may modulate the host immune response [29,30]. In this study carried out in large scale culture conditions, we confirm the stable ADHLSC characteristics: expression of mesenchymal markers (CD73, CD90, CD29, CD44, vimentin and ASMA) and hepatic markers expression (albumin). Cells can also differentiate in tissue specific cell type when exposed to a specific hepatogenic culture medium as demonstrated by the i) acquisition of polygonal shape ii) increase in CYP3A4 activity (data not shown) iii) ability to increase the bilirubin conjugation activity (5.1 ± 1.8% and 9.0 ± 1.1% after 24h and 48h respectively) iv) increase in UGT1A mRNA (mRNA constituted of the 4 first common exons of UGT1A family).

Moreover, as demonstrated by HPLC and immunohistochemistry (IHC) our study provides long-term activity and engraftment of ADHLSC in xenogenic transplantation model for Crigler-Najjar metabolic liver disorder. HPLC results indicate that 3 months post-transplantation, 4 of the 5 ADHLSC intraportaly injected Gunn rat, exhibit a non significant decrease in unconjugated bilirubin (UCB) blood level: 4.7 ± 0.5mg/dl in transplanted rats instead of 7.0 ± 0.4mg/dl for the vehicle infused Gunn rats (negative control group). 27 weeks after transplantation the four responsive injected Gunn rat, exhibit a higher decrease in UCB blood level: 3.2 ± 0.5 mg/dl versus 6.1 ± 0.2mg/dl in the negative control group. A similar decrease was also observed in the positive control group (rats injected with hHepatocytes).

RTqPCR results indicated the presence of human cells into the Gunn rat liver parenchyma and thanks to IHC we were able to specifically discriminate human cells into the ADHLSC intraportaly injected rat liver. IHC against human albumin and UGT1A1, allows us to determine that injected human cells seem localized in periportal zone. No ADHLSC were identified in the single rat which did not respond to the therapy. This may be due to the loss of cells due to bleeding during the portal vein injection or to an immune rejection in this animal.

Transplantation data confirm our recently published report on ADHLSC and the kinetic of engraftment into liver of immunodeficient mouse as well as their participation in tissue regeneration after 20% of hepatectomy. In this study, analyses were performed only after 2 month post transplantation, and do not allow drawing conclusion on long term engraftment and differentiation [21]. In this experiment rats were injected with a relative low dose of 2.5 millions cells, i.e. 10 to 12,5 million/kg

body weight, without regeneration stimulus and this dose led to a UCB decrease and engraftment demonstrated 6 months later. Moreover UCB decrease obtained in ADHLSC and hepatocytes transplanted Gunn rats is in accordance with results obtained in transplanted rats [32] and in human [24], while animals or patients exhibited a progressive decrease of serum bilirubin 2-4 months after liver cell transplantation.

In our experimental model, we could detect around 1.265 ± 0.288% and 0.973 ± 0.212% for ADHLSC and hepatocytes in transplanted Gunn rats respectively which is still in agreement from what is generally accepted that a repopulation of 1-5% of the hepatic mass is required to restore liver disease in most injury models [31-35] Recently; human clinical hepatocyte transplantation engraftment rates has been documented to range from 0% to a maximum of 12% leading in most cases to a transitory quality of life improvement for metabolic liver disease patients [36].

This repopulation rate is likely due to *in vivo* expansion, as the infused cell mass corresponded to only 0,25% of the total liver mass, assuming that the total supposed liver cell mass is 5 billion per kg body weight [26]. No regeneration stimulus was applied in these animals, and such stimuli using radiotherapy of chemicals might improve the engraftment [37]. In parallel, amelioration of immunosuppression treatment will be interesting (use of microsomal encapsulated clodronate, low liver irradiation,…).

In conclusion, ADHLSC large scale cultured were able to differentiate into hepatocyte-like cells *in vitro*, exhibiting hepatic functions (CYP3A4 activity,

glucuronidation activity,…). *In vivo* these cells were also able to engraft and repopulate the liver parenchyma and led to partially correct a bilirubin conjugation defect in a homologous rodent model of Crigler-Najjar syndrome.

All together, these results make ADHLSC an attractive candidate for cell therapy treatment of Crigler-Najjar type I syndrome.

COMMENTS

Background

Liver cell transplantation using hepatocytes was successfully performed in patients with inborn errors of metabolism. However, the success of such a therapeutic approach remains limited by the quality of transplanted cells. To overcome these problems several approaches to isolate and propagate liver stem or progenitor cells have been developed. The capacity of those cells to restore a liver metabolic function must be demonstrated.

Research frontiers

Crigler-Najjar type I syndrome is characterized by a high unconjugated bilirubin blood level due to UGT1A1 deficiency. Orthotopic liver transplantation remains the only curative treatment but the procedure does not guarantee lifelong complication free survival. Hepatocyte infusion has established that metabolic control is possible, but the procedure remains limited by several organ shortage and transient survival of cells. Stem cells look promising to overcome these problems and adult-derived human liver stem/progenitor cells (ADHLSC) are tested for they ability to engraft and differentiate in a homologous animal model (Gunn rat) of human liver Crigler-Najjar type I metabolic disease.

Innovations and breakthroughs

In this study, authors demonstrate the ability of ADHLSC to engraft in recipient rat livers where they participate in restoration of liver function by a significant reduction of the serum bilirubin levels. Our findings support ADHLSC as a promising candidate for liver cell-based therapy developments.

Applications

In this study, authors demonstrated that large scale culture conditions do not modified adult-derived human liver stem/progenitor cells (ADHLSC) phenotype, ADHLSC were able to specifically conjugate bilirubin when intraportally injected into Gunn rats as demonstrated by blood unconjugated bilirubin measurement at different times post-transplantation; infused-Gunn rats exhibited a metabolic effect 3 months post-transplantation and maintained over a 6 months period. ADHLSC engraftment into Gunn rat's liver was demonstrated by immunohistochemistry. All the results suggest the ADHLSC potential to restore a deficient metabolic function in-situ.

Terminology

Crigler–Najjar syndrome type I and II are characterized by unconjugated bilirubin accumulation in the serum. These syndromes are due to genetic variations in the gene encoding uridine diphosphate glucuronosyltransferase 1A1 (UGT1A1) leading to complete or partial inactivation of the bilirubin glucuronidation. Clinically, Crigler–Najjar syndrome type I is associated with progressive damage of the central nervous system leading to bilirubin encephalopathy (kerincterus)

Gunn rat, derived from Wistar parent strain, has constantly elevated concentrations of serum bilirubin which causes unconjugated hyperbilirubinaemia. Gunn rat inherently lacks all glucuronidation activities catalysed by the UGT1 isoforms and is therefore used as animal model for Crigler–Najjar syndrome type I.

Peer review

This study shows that adult-derived human liver stem/progenitor cells (ADHLSC) were able to specifically conjugate bilirubin when intraportally injected into Gunn rats as demonstrated by blood unconjugated bilirubin measurement at different times post-transplantation; infused-Gunn rats exhibited a metabolic effect 3 months post-transplantation and maintained over a 6 months period. ADHLSC engraftment into Gunn rat's liver was demonstrated by immunohistochemistry. All the results suggest the ADHLSC potential to restore a deficient metabolic function in-situ.

References

1 Chowdhury, J. R., Kondapalli, R. & Chowdhury, N. R. Gunn rat: a model for inherited deficiency of bilirubin glucuronidation. *Advances in veterinary science and comparative medicine* **37**, 149-173 (1993), PMID:8273513

2 Sato, H., Aono, S. & Koiwai, O. [Genetic defect of the hyperbilirubinemic Gunn rat, a model for Crigler-Najjar syndrome type I]. *Nihon rinsho. Japanese journal of clinical medicine* **51**, 501-506 (1993), PMID:8096554

3 Crigler, J. F., Jr. & Najjar, V. A. Congenital familial nonhemolytic jaundice with kernicterus. *Pediatrics* **10**, 169-180 (1952), PMID:12983120

4 Crigler, J. F., Jr. & Najjar, V. A. Congenital familial nonhemolytic jaundice with kernicterus; a new clinical entity. *AMA Am J Dis Child* **83**, 259-260 (1952), PMID:14884759

5 van der Veere, C. N. *et al.* Current therapy for Crigler-Najjar syndrome type 1: report of a world registry. *Hepatology* **24**, 311-315, PMID:8690398, doi: 10.1002/hep.510240205 (1996).

6 Yohannan, M. D., Terry, H. J. & Littlewood, J. M. Long term phototherapy in Crigler-Najjar syndrome. *Arch Dis Child* **58**, 460-462 (1983), PMID:6859942

7 Sokal, E. M. *et al.* Orthotopic liver transplantation for Crigler-Najjar type I disease in six children. *Transplantation* **60**, 1095-1098 (1995), PMID:7482714

8 Schauer, R. *et al.* Treatment of Crigler-Najjar type 1 disease: relevance of early liver transplantation. *J Pediatr Surg* **38**, 1227-1231, PMID:12891498, doi:S0022346803002732

9 Shneider, B. L. Pediatric liver transplantation in metabolic disease: clinical decision making. *Pediatr Transplant* **6**, 25-29, PMID:11906639, doi:ptr1p057.

10 Muraca, M. *et al.* Hepatocyte transplantation as a treatment for glycogen storage disease type 1a. *Lancet* **359**, 317-318, PMID:11830200, doi: 10.1016/S0140-6736(02)07529-3.

11 Najimi, M. & Sokal, E. Update on liver cell transplantation. *J Pediatr Gastroenterol Nutr* **39**, 311-319, PMID:15448415, doi:00005176-200410000-00001.

12 Sokal, E. M. *et al.* Hepatocyte transplantation in a 4-year-old girl with peroxisomal biogenesis disease: technique, safety, and metabolic follow-up. *Transplantation* **76**, 735-738, PMID:12973120, doi:10.1097/01.TP.0000077420.81365.53 (2003).

13 Strom, S. C. *et al.* Hepatocyte transplantation as a bridge to orthotopic liver transplantation in terminal liver failure. *Transplantation* **63**, 559-569 (1997), PMID:9047152

14 Stephenne, X. *et al.* Sustained engraftment and tissue enzyme activity after liver cell transplantation for argininosuccinate lyase deficiency. *Gastroenterology* **130**, 1317-1323, PMID:16618422, doi:S0016-5085(06)00009-6.

15 Stephenne, X. *et al.* Cryopreserved liver cell transplantation controls ornithine transcarbamylase deficient patient while awaiting liver transplantation. *Am J Transplant* **5**, 2058-2061, PMID:15996260, doi: 10.1111/j.1600-6143.2005.00935.x.

16 Dhawan, A. *et al.* Hepatocyte transplantation for inherited factor VII deficiency. *Transplantation* **78**, 1812-1814, PMID:15614156, doi:00007890-200412270-00019.

17 Stephenne, X. *et al.* Cryopreservation of human hepatocytes alters the mitochondrial respiratory chain complex 1. *Cell Transplant* **16**, 409-419 (2007), PMID:17658131

18 Stephenne, X., Najimi, M. & Sokal, E. M. Hepatocyte cryopreservation: is it time to change the strategy? *World J Gastroenterol* **16**, 1-14 (2010), PMID:20039443

19 Najimi, M. *et al.* Adult-derived human liver mesenchymal-like cells as a potential progenitor reservoir of hepatocytes? *Cell Transplant* **16**, 717-728 (2007), PMID:18019361

20 Khuu, D. N. *et al.* In vitro differentiated adult human liver progenitor cells display mature hepatic metabolic functions: a potential tool for in vitro pharmacotoxicological testing. *Cell Transplant* **20**, 287-302, PMID:20719066, doi: 10.3727/096368910X516655

21 Khuu, D. N., Nyabi, O., Maerckx, C., Sokal, E. & Najimi, M. Adult human liver mesenchymal stem/progenitor cells participate to mouse liver regeneration after hepatectomy. *Cell transplantation*, PMID:23211283, doi:10.3727/096368912X659853 (2012).

22 Seglen, P. O. Preparation of isolated rat liver cells. *Methods in cell biology* **13**, 29-83 (1976), PMID:177845

23 Scheers I, M. C., Khuu N, Marcelle M, Decottignies A, Najimi M, Sokal E. Human liver progenitor cells in long term culture maintain appropriate gatekeepers mechanisms against transformation. *Cell Transplant*;21(10):2241-55 (2012), PMID:22525602, doi: 10.3727/096368912X639026.

24 Lysy, P. A. *et al.* Liver cell transplantation for Crigler-Najjar syndrome type I: update and perspectives. *World J Gastroenterol* **14**, 3464-3470 (2008), PMID:18567072.

25 Muraca, M. & Blanckaert, N. Liquid-chromatographic assay and identification of mono- and diester conjugates of bilirubin in normal serum. *Clin Chem* **29**, 1767-1771 (1983), PMID:6616822.

26 Fox, I. J. *et al.* Treatment of the Crigler-Najjar syndrome type I with hepatocyte transplantation. *N Engl J Med* **338**, 1422-1426, PMID:9580649, doi:10.1056/NEJM199805143382004 (1998).
27 Maerckx C., L. C., Tondreau T, Sokal E. Pharmacokinetics, hepatic and renal tolerance of cyclosporine A in Wistar rats. (Submitted).
28 Gunn, C. K. Hereditary Acholuric Jaundice in the Rat. *Can Med Assoc J* **50**, 230-237 (1944), PMID:20323028.
29 Aggarwal, S. & Pittenger, M. F. Human mesenchymal stem cells modulate allogeneic immune cell responses. *Blood* **105**, 1815-1822, PMID:15494428, doi:10.1182/blood-2004-04-1559 (2005).
30 El Haddad, N. *et al.* Mesenchymal stem cells express serine protease inhibitor to evade the host immune response. *Blood* **117**, 1176-1183, PMID:21076046, doi:10.1182/blood-2010-06-287979 (2011).
31 Guha, C. *et al.* Normal hepatocytes correct serum bilirubin after repopulation of Gunn rat liver subjected to irradiation/partial resection. *Hepatology* **36**, 354-362, PMID:12143043, doi:10.1053/jhep.2002.34516 (2002).
32 Fox, I. J. & Roy-Chowdhury, J. Hepatocyte transplantation. *J Hepatol* **40**, 878-886, PMID:15158325, doi:10.1016/j.jhep.2004.04.009S0168827804001552 (2004).
33 Joseph, B. *et al.* Kupffer cells participate in early clearance of syngeneic hepatocytes transplanted in the rat liver. *Gastroenterology* **123**, 1677-1685, PMID:12404242, doi:S0016508502003013 (2002).
34 Grompe, M. Principles of therapeutic liver repopulation. *J Inherit Metab Dis* **29**, 421-425, PMID:16763912, doi:10.1007/s10545-006-0311-2 (2006).
35 Wang, L. J. *et al.* Engraftment assessment in human and mouse liver tissue after sex-mismatched liver cell transplantation by real-time quantitative PCR for Y chromosome sequences. *Liver Transpl* **8**, 822-828, PMID:12200785, doi:10.1053/jlts.2002.34891 (2002).
36 Jorns, C. *et al.* Hepatocyte transplantation for inherited metabolic diseases of the liver. *Journal of internal medicine* **272**, 201-223, PMID:22789058, doi:10.1111/j.1365-2796.2012.02574.x (2012).
37 Bahde, R. *et al.* Directly acting drugs prostacyclin or nitroglycerine and endothelin receptor blocker bosentan improve cell engraftment in rodent liver. *Hepatology* **57**, 320-330, PMID:22899584, doi:10.1002/hep.26005 (2013).

Figures:

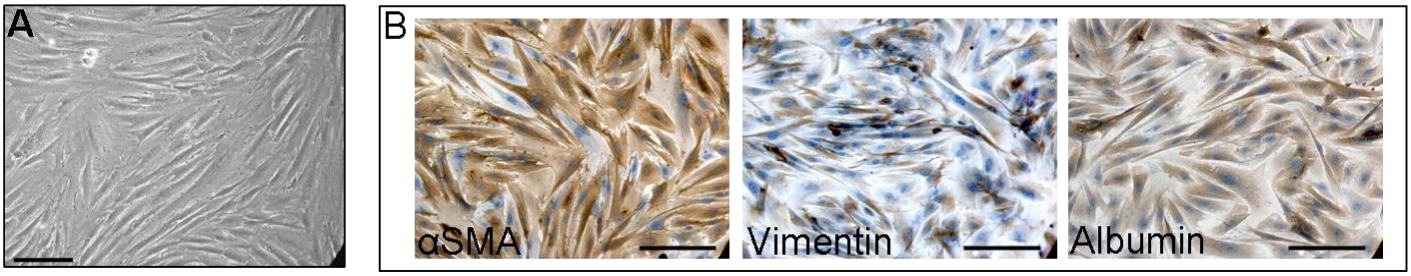

Figure 1: **Adult-derived human liver stem/progenitor cells characterization**

A: Morphology of adult-derived human liver stem/progenitor cells (ADHLSC) in expansion medium. Phase contrast microscopic view of ADHLSC obtained after second passage. Magnification: x100, scale bar: 100µm.

B: Immunocytochemistry characterization (passage 6) analysis: expression of mesenchymal and hepatic markers in ADHLSC. Mesenchymal markers: α-smooth muscle actin (αSMA) and vimentin and hepatic marker albumin immunostaining were analyzed by direct light microscopy. ADHLSC plated on collagen type I-coated coverslips were fixed and incubated with corresponding primary antibodies. Immunoreactivity was visualized using horseradish peroxydase (HRP) Cell nuclei are stained using haematoxylin-eosin (blue). Images are representative of several fields examined. Scale bar: 100µm

A

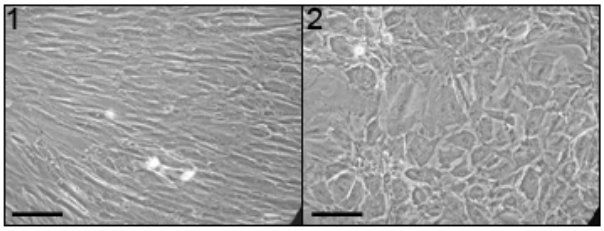

B

Passage	Fold increase (ΔΔCt)
Passage 4	9,31
Passage 9	10,02

C

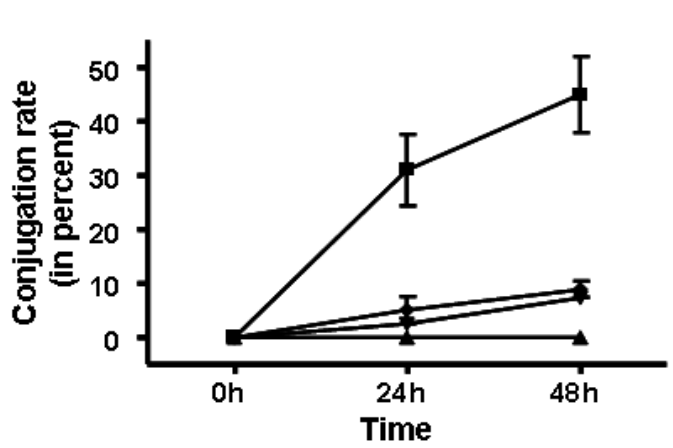

Figure 2: **Hepatogenic differentiation and expression of functional UGT1A1**

A: Evaluation of in vitro ADHLSC hepatic differentiation potential at passage 6. Undifferentiated ADHLSC (1) were able to change their morphology by adopting a polygonal shape with a granular cytoplasm after 4 weeks of treatment with specific growth factors and cytokines. Magnification: x100, scale bar: 100µm.

B: UGT1A mRNA relative expression quantification. Results were obtained after passage 4 and 9. UGT1A mRNA level in differentiated ADHLSC, were normalized to Cyclophilin A and reported to undifferentiated ADHLSC UGT1A mRNA level.

C: In vitro bilirubin conjugation kinetic assessment: squares: wild type hepatocytes (positive control), triangle: Crigler-Najjar patient hepatocytes (negative control), overturned triangle: undifferentiated ADHLSC, rhomb: differentiated ADHLSC. Cells were incubated with 100µM unconjugatred bilirubin,

supernatants were harvested after 24h or 48h. Conjugation rate (CR) was evaluated with HPLC as follow: ((Conjugated bilirubin concentration)/(Total bilirubin concentration)) x100.

Squares: Wild type hepatocytes; Triangles: Crigle Najjar hepatocytes; Inverted triangles: Undifferentiated ADHLSC; Rhombus: Differentiated ADHLSC

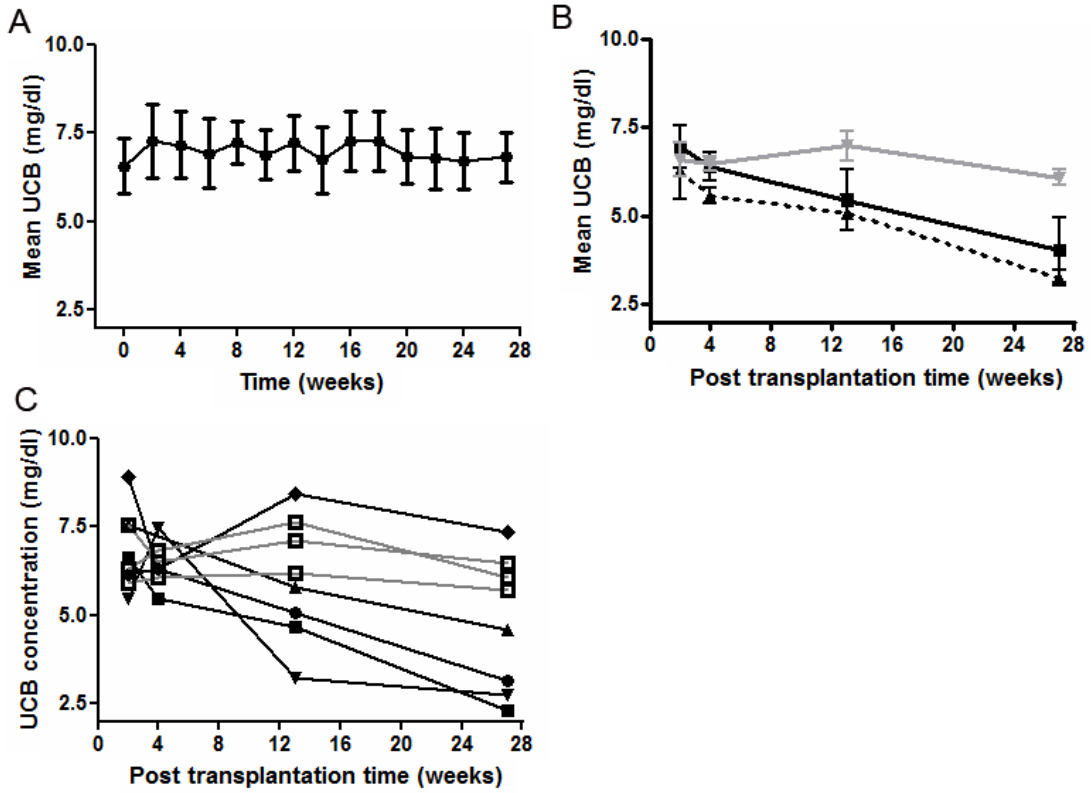

Figure 3: **Injected Gunn rat follow up**

A: Assessment of bilirubin concentration stability in 11 naive rats of the Gunn rat colony followed during 27 weeks. Bilirubin concentration is expressed in mg/dl.

B: Mean of unconjugated bilirubin for ADHLSC injected rats n=4 (black line), human hepatocytes injected rats n=3 and for negative control n=3 (grey line). Difference between 2 weeks and 27 weeks post injection concentration bilirubin was significant for ADHLSC injected rats (p-val=0,0032). Mean of UCB concentration is expressed in mg/dl. Squares: hADHLSC; Triangles: human hepatocytes; Inverted triangles: negative controls.

C: Unconjugated bilirubin evolution with time: black lines: ADHLSC transplanted Gunn rats n=5; red lines: PBS injected rats n=3 (negative control). Bilirubin concentration is expressed in mg/dl. Circles: rat 1; Squares: rat 2; Triangles: rat 3; Inverted triangles: rat 4; Rhombus: rat 5; Empty squares: negative controls

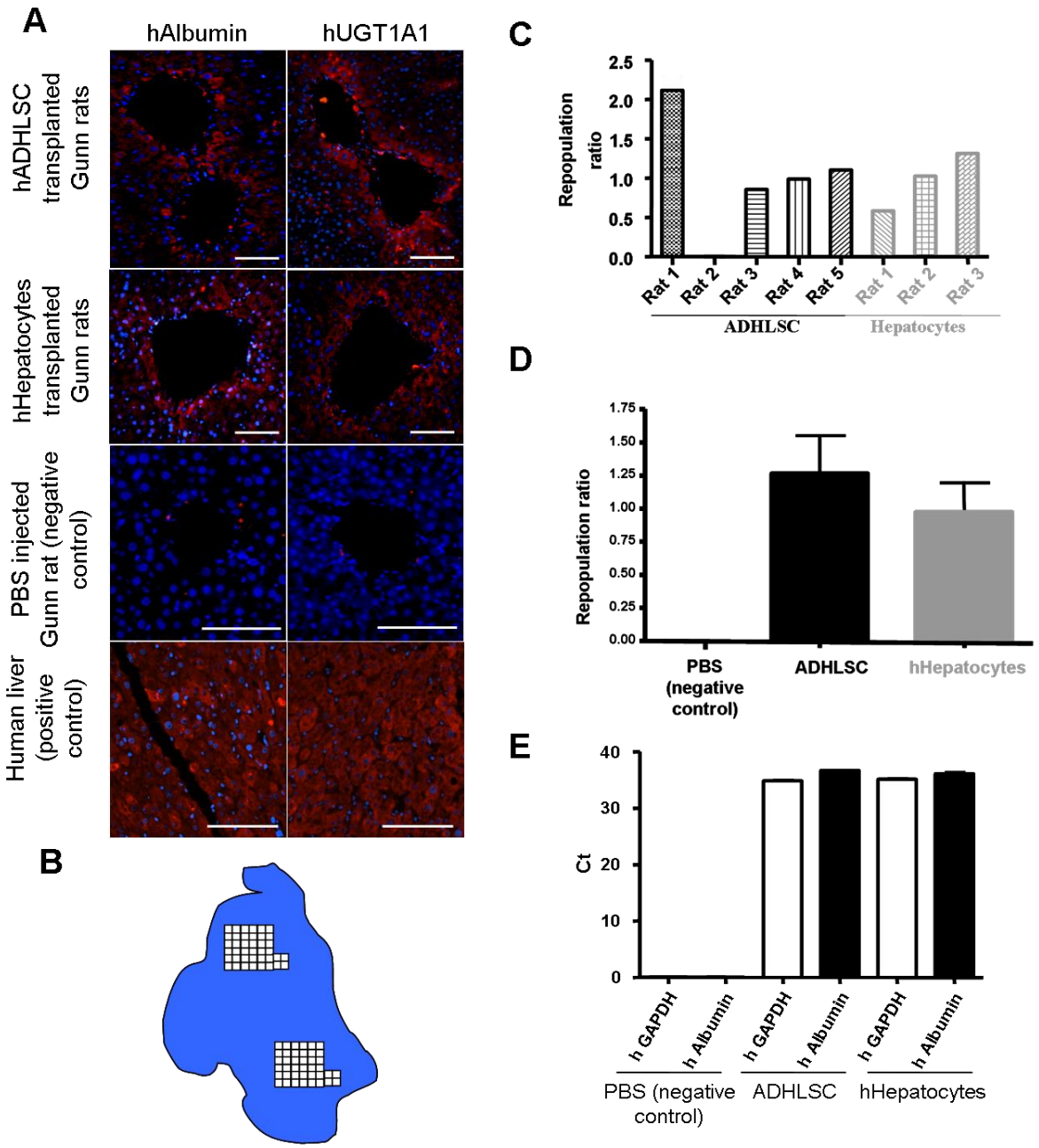

Figure 4: **liver analysis and human cells quantification**

A: Immunohistochemistry against human albumin and human UGT1A1 proteins on serial liver slices in Gunn rats transplanted with ADHLSC and hHepatocytes. Immunostaining were analyzed by fluorescent microscopy. Slices were fixed and incubated with corresponding primary antibodies. Immunoreactivity was visualized using a 1/500 AlexaFluor594 anti-rabbit antibody solution. Human liver was used as positive control for albumin and UGT1A1 staining whereas negative control consisted of Gunn rat liver injected with PBS. Cell nuclei are stained using DAPI (blue). Bar scale: 200µm

B: Schematic representation of an immunostained slide. Human albumin positive cells were counted over two randomly chosen area of the section.

C: Human cells repopulation ration in ADHLSC (black columns) and hHepatocytes (gray columns) transplanted Gunn rats. Measurement was based on human albumin positive cells counted over two randomly chosen area of the section.

D: Mean of human cells repopulation ratio in PBS (negative control), ADHLSC (black column) and hHepatocytes (gray column) transplanted Gunn rats (p-val>0.05). Measurement was based on human albumin positive cells counted over two randomly chosen area of the section.

E: Human GAPDH (white column) and albumin (black column) detection by RTqPCR in negative control (PBS injected), ADHLSC, and human hepatocyte injected rat livers.

Table

Surface marker	Positive cells (%)
CD73	64.1%
CD90	94.1%
CD44	41.6%
CD29	87.4%
CD45	0.1%
CD117	0.7%
CD133	0%
Albumin	61.4%
Pan CK	1%

Table 1: **ADHLSC surface markers expression percentage (passage 6)**

Cell surface markers profile of ADHLSC. Selected cell surface molecules (CD29, CD44, CD45, CD73, CD90, CD117 and CD133) and intracellular markers (albumin and Pan CK) were analyzed using flow cytometry. Their relative expressions are compared to corresponding control isotypes.

3. *In vivo* biodistribution of Adult Human Liver Stem/Progenitor Cells following intraportal transplantation in catheterized rats

Biodistribution of transplanted cells is an important regulatory and safety issue. It allows to understand the risk of ectopic tissue formation and to follow the homing of cells in the target organ. In this study, we evaluated the *in vitro* radio-labeling efficacy of ADHLSC with Indium-111oxine (^{111}In) and subsequently followed the biodistribution of ^{111}In labeled cells after intraportal transplantation in the adult rat. In vitro we determined that the optimal dose to labeled ADHLSC with ^{111}In was 30µCi/1.10^{6} cells for 15 minutes at RT After intraportal infusion of 5.10^{6} labeled cells part of a final cell suspension comprising 5, 10 or 20 millions cells, scintigraphic imaging and quantitative gamma counts demonstrated a specific hepatic biodistribution maintained up to 72h after transplantation without any significant dissemination in other organs. No difference was observed with increased injected cell doses.

In vivo biodistribution of Adult Human Liver Stem/Progenitor Cells following intraportal transplantation in catheterized rats.

Tatiana Tondreau[Ŧ], Cedric Maerckx[Ŧ], Stephan Walrand*, Muriel Helbo*, Nawal Jazouli, Mustapha Najimi , Vinciane Wouters**, Eddy Rommel**, François Jamar*, Etienne Sokal.

Authors[Ŧ] have contributed equally to the work

Université Catholique de Louvain, "Institut de Recherche Clinique et Expérimentale", Laboratory of Pediatric Hepatology and Cell Therapy (PEDI), *Molecular Imaging, Radiotherapy and Oncology (MIRO), Brussels, Belgium

**Promethera Biosciences, Mont-St-Guibert, Belgium

Corresponding author:

Pr Etienne Sokal

UCL-Laboratory of Pediatric Hepatology and Cell Therapy (PEDI)

53 Av Mounier

1200 Bruxelles

Belgium

Etienne.sokal@uclouvain.be

Word count: 4193

This work was supported by Promethera Biosciences

Abstract

Prupose: Biodistribution of stem cells after infusion is an important safety issue in cell based advanced therapies. This study aimed to evaluate the in vitro radiolabeling efficacy of adult human liver stem/progenitor cells (ADHLSC) with Indium-111oxine (In-111) and subsequently to follow the biodistribution of ^{111}In labeled cells after intraportal transplantation in catheterized Sprague-Dawley rats.

Methods: ADHLSC were radiolabeled using different doses of In-111 ranging from 10 to 60µCi/1.10^6 cells. Cellular retention and effects of labeling on the viability were assessed by cell counting and lactate dehydrogenase (LDH) cytotoxicity assay. Biodistribution of In-111-AHDLSC following intraportal infusions of ADHLSC ranging from 5.10^6 to 20.10^6 cells into rats was assessed by means of scintigraphy and organ gamma counting, and compared to rats infused with free In-111 (control group).

Results: In vitro, we demonstrated a time and dose-dependent labeling efficiency with pronounced decrease in population doubling rate at higher In-111 dose. We also demonstrated cytotoxic effect following in In-111 time incubation at dose 30µCi/10^6 cells, as evidenced by increase of LDH release. After intraportal infusion, scintigraphic imaging and quantitative gamma counts demonstrated a specific hepatic biodistribution maintained up to 72h after transplantation without any significant uptake in other organs. No difference was observed with increase injected cell doses.

Conclusion: Labeling of ADHLSC with In-111 at a dose of 30µCi/1.10^6 cells is sufficient to allow cell detection by scintigraphy up to three days post-injection. We also demonstrate that labeling of a small fraction of injected cells is sufficient to explore their biodistribution.

Key words: Indium labeling– Adult Human Liver Stem/Progenitor Cells – Biodistribution – SPECT/CT

Introduction

Cell therapy using stem or progenitor cells to restore deficient metabolic function is an emerging biotechnology approach which may in some situations become an alternative to organ transplantation (1, 2). Biodistribution of infused cells is an important issue, to both understand the risk of ectopic tissue formation and follow the homing of cells in the target organ. Current cell-based therapies using fluorescence labeling, bioluminescence or genetically-modified cells have demonstrated the presence of engrafted cells within tissues, but are limited to animal studies and are not well developed to be used in human. Cell labeling using super magnetic iron oxide (SPIO) nanoparticles, radionuclides or reporter genes have also been well proposed as non-invasive techniques to study the distribution of transplanted cells (3). In the recipient liver, SPIO labeled cells remain detectable for up to three weeks after transplantation. Iron oxide level per cells is diluted during cell proliferation and iron SPIO can be taken up by neighboring cells which leads to false imaging results (4). Furthermore, the low sensitivity of the SPIO labelling requires clusters of more than 10^5cells to be detected (5, 6). Indium-111 oxine (In-111) has been successfully used to label leucocytes for detection of inflammatory sites such as in inflammatory bowel disease, lung infection, neurological infection and fever of unknown origin (7). In-111 has a half-life of 67 hours, which allows the tracking for several days after infusion. Another advantage of this technique is the high sensitivity, since as little as 10^3 In-111 radiolabeled cells can be detected (8). Recent studies have investigated the potential use of ^{111}In to other cell types such as mesenchymal stromal cells from bone marrow, adult or fetal liver stem/progenitor cells and showed neither immediate cytotoxic effect nor change in antigen expression pattern at doses up to 1.1MBq/10^6 cells (30 µCi/10^6 cells) (9-11).

In the present study, we investigated the efficacy of In-111 labeling on adult derived human liver stem/progenitor cells (ADHLSC). These cells isolated from liver parenchymal fraction have demonstrated their ability to be expanded in vitro and display a hepato-mesenchymal profile. Under appropriate culture conditions with specific cytokines and growth factors, ADHLSC acquire a typical polygonal hepatic morphology as well as hepatocyte metabolic hepatic functions such as gluconeogenesis, urea production and xenobiotic detoxifications (12, 13). These cells are considered promising candidates for cell-based advanced therapies of the liver. The aims of this study were to evaluate the ^{111}In labeling on ADHLSC on cell viability, proliferation, phenotype as well as stability of labelling and to monitor their biodistribution following intraportal transplantation in catheterized rats.

Material and methods

ADHLSC cultures

Hepatic stem/progenitor cells (ADHLSC) were isolated from liver parenchymal fraction obtained according to the adapted two-step collagenase perfusion method as previously described by Seglen (14). Production of ADHLSC was performed as previously reported (12) and adapted for large scale GMP production. Briefly, liver cell suspensions were seeded in 175cm^2 CellBind plastic flasks (Corning, Seneffe, Belgium) with Williams'E medium (Invitrogen,Merelbeke, Belgium) added with 150UI/mL insulin (Himulin Regular) and 10^{-7}M dexamethasone (Aacidexam), 10% Fetal Bovine Serum (FBS, AE Scientific, Pisching, Austria), and thereafter in DMEM (Invitrogen) supplemented with 10% FBS (expansion medium). At confluence, cells were trypsinized and replated at 5000 cells/cm^2 in expansion medium and successive cultures were maintained until the five-sixth passage (P5-P6). From this passage, cells were cryopreserved in liquid nitrogen with 90%FBS +10%DMSO (Wak-Chemie, Germany).

Cell procurement, isolation and cell banking of liver stem cells are produced in concordance of the agreement from the Belgian Ministry of Health.

In-111 Oxine Labeling

Cryopreserved cells at P5-P6 (n=3) were first washed in DBPS (Lonza, Verviers, Belgium) for 10 minutes at 260g. Then, cells were resuspended in DPBS (5.10^6 cells/3mL) before incubating with 10, 30 and 60µCi/1.10^6 cells In-111 oxine (GE Healthcare) for 15 - 30 minutes at room temperature in DPBS and gentle shaking. To remove unbound labeling, cells were washed twice with DBPS. After each wash, labeling efficiency was measured with a dose calibrator (Capintec Radioisotope Calibrator CRC12) and calculated as follows: Radioactivity from cells/Radioactivity from (supernatant +Cells) X100. Viability of cells was checked immediately after labeling using the Trypan Blue exclusion method. To evaluate the radioactivity retention (stability of labeling), ^{111}In labeled cells were cultured for 168 hours in expansion medium. Daily, trypsinized cells and their culture medium were centrifuged (260g) and the radioactivity of each fraction was measured with a dose calibrator (Capintec). The percentage of cell retention was calculated as the ratio of radioactivity from cells to the total radioactivity of cells and supernatant (culture medium).

Cell proliferation and cytotoxicity assays

The viability and cell proliferation were assessed on both ^{111}In-labelled cells and non-labelled ADHLSC at 24h, 48h, 72h, 96h and 168 hours with an initial seeding of 1.10^6 cells in T75 cm^2 Flask. For each time point, cell cultures were trypsinized (0,05%Trypsin-EDTA, Invitrogen) for 10 minutes at 37°C. After wash in expansion medium (210g,10min), viability and cell counting were estimated by Trypan Blue exclusion test.

To investigate the cytotoxicity of In-111 on ADHLSC, we first measured the extracellular levels of Lactate Dehydrogenase (LDH) in cell culture supernatant according to manufacturer's instructions (LDH cytotoxicity detection kit, Roche Applied). Secondly, we determined the protein content from 100µL cell lysates in 50mM Tris, 150mM NaCl, 1% NP-40 solution using the Portein Assay Kit (Pierce BCA, ThermoFisher).

Cytotoxicity was calculated as follow: LDH/cell protein content and normalized with the control condition (unlabeled cells).

Imunocytochemistry

The expression of vimentin (monoclonal anti human Vimentin, Progen, Heidelberg, Germany), ASMA (monoclonal mouse anti-smooth muscle actin, Dako, Hervelee, Belgium), CK19 (monoclonal mouse anti-human CK-19, Dako) and Albumin (polyclonal rabbit anti-human Albumin, Calbiochem, Belgium) was also evaluated on unlabeled and radiolabeled cells using immunocytochemistry. Briefly, cells were washed with DPBS (Dulbecco's Phosphate Buffered Saline, Lonza, Verviers, Belgium) and fixed with 3.5% formol for 15 minutes at RT (VWR Heverlee, Belgium) before peroxydase endogene inactivation using 3% Hydrogen Peroxyde (VWR) solution 3 minutes at room temperature (RT). After rinsing with distilled water, cells were permeabilized with 1% Triton (Sigma, Bornem, Belgium) solution for 10 minutes at RT and nonspecific sites were blocked with DPBS-BSA 1% (Sigma) for 1 hour (RT). Then, the primary specific antibody was incubated for 1 hour at room temperature. After washing with DPBS a secondary antibody Envision (Dako) was used for 30 minutes. After washing, immunocytochemistry was evidenced by DAB chromogen (Dako) and counterstained with hematoxilin solution for 10 minutes at room temperature and microscopically checked (Leica- DMIL).

Rat Intra-portal infusion

Catheterized male Sprague Dawley rats were purchased from Charles River laboratories (CD-SIMA250KVP, 6-10 weeks old) and experimented in accordance with the internal Animal Care

program. Catheterized rats received intraportal infusions of either 5.10^6 (group 1) -10.10^6 (group 2) -20.10^6 (groups 3) cells/2mL (150µL/min) containing a single dose of 5.10^6 In-111 labeled cells 15 minutes with a theoretical activity of 30µCi/1.10^6 cells (mean activity infusion: 105.4±12.2 µCi). Three rats in each group were used in this study. The cell suspension was formulated in 5% Human albumin (Hibumine, Baxter) supplemented with glucose (0.025g/L, Stereop), 6.5 mg/mL Sodium Bicarbonate (B52 Braun), 10UI/mL Heparin (LeoPharma) and 0.78% Lysomusyl (Zambon). A control group (n=3) received 105.4±16.5µCi free In-111 oxine in order to evaluate the radioactivity clearance. Three days prior transplantation and until sacrifice, rats were immunosupressed with intraperitoneal injections of 5mg/kg/2days cyclosporin. During infusions and Single-photon emission computed tomography (SPECT) imaging, rats were sedated with Forene 2% (Abbott). Radioactivity in the syringe was measured before and after cell infusion with a dose calibrator (Capintec).

SPECT-CT Imaging and gamma counting

Whole body scintigraphy was performed 1h and 24h (groups 1-2) and after 72h (group 3) following cell infusions, using a small animal SPECT system, with a energy of max to 140keV±10%. The hepatic retention of ^{111}In was calculated as the ratio of regions of interest (liver uptake) to whole body uptake with PMOD analysis program (15). Spatial anatomic imaging was also performed using 120KV CT scan with mAs/mA (200/317). At sacrifice, organs including brain, heart, lungs, sternum, spleen, liver, bladder, kidneys, intestines, pancreas and testis were excised and their radioactivity was measured with the gamma counter (Cobra II Packard). For liver, each lobe was separately counted. Results were expressed as the percentage of injected dose (% ID) by use of an aliquot of the injected syringe as a standard to normalize the In-111 decay correction.

Results

Effect of In-111 labeling on ADHLSC

In order to determine the effect of radiolabeling and the quality of our cells, we first assessed the viability of radiolabeled cells by Trypan blue exclusion assay immediately after labeling, compared to that of unlabeled cells. In comparison with unlabeled cells, no significant impact of In-111 was observed on cell viability regardless of the In-111 dose or incubation times. However, labeling efficiency was increased with high-doses In-111 dosis of 30 and 60µCi independently the incubation time, reaching up to 60% (Table 1).

Analysis of radioactivity retention of cultured In-111 labeled cells showed a rapid leakage of In-111 within the first 24 hours: the percentage of retention decreased from 65.3±1.8% to 25.4±1.9% ($p < 0.0286$, Mann Whitney) with radiolabeling at 30µCi to 60µCi and remained stable until 96 hours, independently the incubation time (Figure 1). At dose 10µCi, no sufficient cellular retention was observed over the investigated time period.

Cell proliferation of radiolabeled ADHLSC in T75 cm^2 flask evaluated after labeling demonstrated an important decrease in time and dose depended manner (Figure 2 A-B).

Based on these results, we explored the ADHLSC integrity after In-111 labeling 30µCi /1.10^6 cells after 15 and 30 incubation time by analyzing the level of LDH present in the extracellular fraction at different times post seeding and up to 168 hours. At this time point, we noted a threefold to six fold increase of extracellular LDH levels with the 30µCi dose, corresponding to 15 and 30 minutes incubation time respectively (Figures 2C).

Phenotypic profile pattern of radiolabeled cells

Finally, the pattern of expression was checked after 7 days of culture by assessing patterns of vimentin, ASMA, Albumin and CK19 expression. Immediately after labeling (1.1MBq/1.10^6 cells, 15minutes), no difference in expression was observed between labeled and unlabeled cell cultures (Figure 3).

Biodistribution of radiolabeled cells

Based on the cell proliferation and cytotoxic results, dose of 30µCi for 15 minutes was used in vivo. To evaluate in vivo the distribution of In-111 labeled ADHLSC after intra-portal infusion, image reconstruction of the whole rat body and pixel-wise modeling (PMOD) analysis was used to detect the infused cells. This analysis confirmed the liver uptake with a detected signal at 1h, 24h and 72 hours. No dissemination to ectopic organs was observed after 24h or 72 hours post transplantation. Fusion imaging of SPECT and CT confirmed that radioactivity localization corresponded to the liver (Figure 4). Semi-quantitative distribution analysis determined by the ratio: liver/ whole body signal, revealed a signal ranging from 54±3.3% - 65±6% -54±4.9% after 1hour, from 35±16.6% - 56±3.8% - 43±2.5% after 24 hours, respectively to 5.10^6 -10.10^6 and 20.10^6 infused cells (Table 2). The mean liver retention of radiotracer in the control group was lower than 8±1% after one hour and 6±2.6% after 24 hours.

At necropsy (24h post infusion), radioactivity was measured by gamma counter in individual organs (brain, sternum, spleen, pancreas, duodenum, jejunum, colon, lung, heart, kidneys, bladder, liver and thymus). Data confirmed the specific distribution within the liver as compared to other organs, in accordance to SPECT count analysis (Figures 5 A-B). Radioactivity was most important in liver including median, left lateral and right lateral superior - caudate lobes and no significant radioactivity was detected in other excised organs, except the kidneys. Urine gamma count at 24h confirmed the natural urinary excretion of In-111 with 19±8.8% of the injected dosis in the control group and 9±1.5% in In-111-labelled cell infusion group.

Discussion

SPECT imaging of radiolabeled cells into catheterized rat proved to be a sensitive method to track transplanted cells. Despite the xenogenic model used, specific hepatic biodistribution was observed and maintained for 72h after transplantation without ectopic hot spots to other organs. Quantitative gamma counts of excised organs confirmed hepatic distribution with a predominance to median, left lateral and right lateral lobes. Gamma counts did not demonstrated ectopic biodistribution to any other organs. In fact, less than 5% of the injected doses were detected in other excised tissues. The percentage of cells retained in the liver varying from 47 to 73% at one hour and 10 to 62% at 24 hours postinfusion. However, it is difficult to extrapolate from these data the percentage of engraftment that would be observed in human in a homologous context. Nevertheless, the present preclinical study gives the experimental basis to address the key safety issue of biodistribution in the emerging field of advanced therapy medicinal products, based on stem cell technology. It shows the feasibility of labeling of human mesenchymal liver progenitor cells with ^{111}In and to track the cells in vivo after intraportal infusion. The lack of extra-hepatic uptake is definitely a strong marker that extrahepatic seeding is unlikely.

The different labeling protocols tested on our ADHLSC demonstrated time-dose-dependent cytotoxic effect, as evidenced by a three to sixfold increase level of LDH in the extracellular fraction at doses 30µCi-15minutes and 30minutes labeling incubation time respectively in comparison with unlabelled cell group after 168h. Similar results were observed in previous studies using In-111 labeling on mesenchymal stromal cells or hematopoietic progenitor cells, in which a decrease in viability of labeling cells after several culture days was demonstrated (11, 16, 17). In contrary, no important decrease of viability neither immediately after labeling nor after 7 culture days was noted in our study.

Indeed cell viability of cultured cells was up to 75% independently the time of labeling (data not shown). Based on phenotypic profile of expression, quality of radiolabeled ADHLSC was not altered in term of ASMA, albumin and vimentin expressions. Radiolabeling at a dose of 30µCi/1.10^6 cells for 15 minutes at room temperature seemed to be the best condition for our ADHLSC, as we did not observe any increase of the of extracellular LDH level. However this dose had a deleterious effect on the cell proliferation rate in a time dependent manner (16).

Other non-invasive imaging technologies have provided sensitive methods to track the fate of transplanted cells. Different protocols have been described in animal studies using bioluminescence, fluorescence as well as reporter gene and SPIO. However these methods, except for SPIO labeling are precluded in human (6, 18, 19). SPIO labeling, although feasible in clinical practice, has demonstrated a low sensitivity and potential biased results due to iron particles release and subsequent macrophage uptake. Unfortunately, both SPIO and In-111 labeling cannot truly differentiate viable from dead cells

In-111 labeling of leucocytes is a method widely used in clinical practice to detect inflammation sites in patients. The Indium-111 oxine complex is neutral and lipid-soluble, which enables to penetrate across the cell membrane and become strongly attached to cytoplasmic components such as lactoferrin. The complex In-oxine further dissociates and the oxine is released by the cells. The relatively low retention rate observed in our study may be aggravated by early immune cell mediated damage in xenotransplantation leading to an even more important radioactive leakage during the first 24h. Loss of labeling is a well-known phenomenon observed with various cell types. Rapid leakage of In-111 to 35 to 45% after 24 and 48h was demonstrated on both hematopoietic progenitor cells and mesenchymal stromal cells (16, 20, 21).

SPECT imaging of radiolabeled cells into catheterized rat proved to be a sensitive method to track transplanted cells. Specific hepatic biodistribution was observed and maintained for more than 72h after transplantation without ectopic hot spots to other organs as demonstrated in the kidney of control group receiving the radiotracer alone. Quantitative gamma counts of excised organs confirmed hepatic distribution with a predominance to median, left lateral and right lateral lobes. Gamma counts did not demonstrate ectopic biodistribution to any other organs. In fact, less than 5% of the injected doses were detected in other excised tissues.

Conclusion

In conclusion, intraportal infusion of a small fraction of radio labeled ADHLSC with In-111 at dose 30µCi/1.10^6 cells for 15 minutes at RT was sufficient to detect biodistribution by scintigraphy images up to three days. Neither ectopic hot spots nor signals were evidenced outside of the liver, demonstrating the engraftment and the homing of cells preferentially within the liver parenchyma. Previous in vivo studies in immunocompromized mice, RT-PCR analysis and immunohistochemistry revealed the presence of ADHLSC more than 10 weeks after intrasplenic transplantation (12, 13).

Acknowledgments

The authors declare that they have no conflict of interest.

This work was supported by Promethera Biosciences.

References

1. Smets F, Najimi M, Sokal EM. Cell transplantation in the treatment of liver diseases. Pediatr Transplant. 2008; 12:6-13.

2. Sokal EM. From hepatocytes to stem and progenitor cells for liver regenerative medicine: advances and clinical perspectives. Cell Prolif. 2011; Suppl 1:39-43.

3. Ransohoff KJ, Wu JC. Advances in cardiovascular molecular imaging for tracking stem cell therapy. Thromb Haemost. 2010 ;104:13-22.

4. Leconte I, Pallu S, Abarca-Quinones J, Michoux N, Peeters F, Radermacher K, et al. MRI of iron-oxide labelled transplanted hepatocytes in mice: effect of treatment with cyclophosphamide. J Magn Reson Imaging. 2010; 32:367-375.

5. Beeres SL, Bengel FM, Bartunek J, Atsma DE, Hill JM, Vanderheyden M, et al. Role of imaging in cardiac stem cell therapy. J Am Coll Cardiol. 2007; 49:1137-1148

6. Puppi J, Mitry RR, Modo M, Dhawan A, Raja K, Hughes RD. Use of a clinically approved iron oxide MRI contrast agent to label human hepatocytes. Cell Transplant. 2011;20:963-975

7. Roca M, de Vries EF, Jamar F, Israel O, Signore A. Guidelines for the labelling of leucocytes with (111)In-oxine. Inflammation/Infection Taskgroup of the European Association of Nuclear Medicine. Eur J Nucl Med Mol Imaging. 2010; 37:835-841. Erratum in: Eur J Nucl Med Mol Imaging. 2010;37:1234.

8. Jin Y, Kong H, Stodilka RZ, Wells RG, Zabel P, Merrifield PA, et al. Determining the minimum number of detectable cardiac-transplanted 111In-tropolone-labelled bone-marrow-derived mesenchymal stem cells by SPECT. Phys Med Biol. 2005; 50:4445-4455

9. Lyngbaek S, Ripa RS, Haack-Sørensen M, Cortsen A, Kragh L, Andersen CB, et al. Serial in vivo imaging of the porcine heart after percutaneous, intramyocardially injected 111In-labeled human mesenchymal stromal cells. Int J Cardiovasc Imaging. 2010; 26(3):273-384.

10. Cheng K, Benten D, Bhargava K, Inada M, Joseph B, Palestro C, et al. Hepatic targeting and biodistribution of human fetal liver stem/progenitor cells and adult hepatocytes in mice. Hepatology. 2009; 50:1194-1203.

11. Kraitchman DL, Tatsumi M, Gilson WD, et al. Dynamic imaging of allogeneic mesenchymal stem cells trafficking to myocardial infarction. Circulation. 2005; 112:1451-1461.

12. Najimi M, Khuu DN, Lysy PA, et al. Adult-derived human liver mesenchymal-like cells as a potential progenitor reservoir of hepatocytes? Cell Transplant. 2007;16:717-28.

13. Khuu DN, Scheers I, Ehnert S, Ishimori T, Kedziorek D, Walczak P, et al. In vitro differentiated adult human liver progenitor cells display mature hepatic metabolic functions: A potential tool for in vitro pharmacotoxicological testing. Cell Transplant. 2011; 20:287-302.

14. Seglen PO . Preparation of isolated rat liver cells. Methods. Cell Biol 1976;13:29–83

15. Walrand S, Jamar F, de Jong M, Pauwels S. Evaluation of novel whole-body high-resolution rodent SPECT (Linoview) based on direct acquisition of linogram projections.J Nucl Med. 2005; 46:1872-1880.

16. Nowak B, Weber C, Schober A, Zeiffer U, Liehn EA, von Hundelshausen P, et al. Indium-111 oxine labelling affects the cellular integrity of haematopoietic progenitor cells. Eur J Nucl Med Mol Imaging. 2007; 34:715-721.

17. Bindslev L, Haack-Sørensen M, Bisgaard K, Kragh L, Mortensen S, Hesse B, et al. Labelling of human mesenchymal stem cells with indium-111 for SPECT imaging: effect on cell proliferation and differentiation. Eur J Nucl Med Mol Imaging. 2006; 33:1171-1177.

18. Fontanellas A, Hervas-Stubbs S, Sampedro A, Collantes M, Azpilicueta A, Mauleón I, et al. PET imaging of thymidine kinase gene expression in the liver of non-human primates following systemic delivery of an adenoviral vector. Gene Ther. 2009; 16:136-141

19. Love Z, Wang F, Dennis J, Awadallah A, Salem N, Lin Y, Weisenberger A, et al. Imaging of mesenchymal stem cell transplant by bioluminescence and PET. J Nucl Med. 2007; 48:2011-2020.

20. Gholamrezanezhad A, Mirpoura S, Ardekanie MJ, Bagherib M, Alimoghadamc K, YarmandaS, et al. Cytotoxicity of 111In-oxine on mesenchymal stem cells: a time-dependent adverse effect. Nuclear Medicine Communications 2009; 30:210–216

21. Aicher A, Brenner W, Zuhayra M, Badorff C, Massoudi S, Assmus B, et al. Assessment of the tissue distribution of transplanted human endothelial progenitor cells by radioactive labeling. Circulation 2003; 107:2134-2139.

Figures – Tables

Figure 1:

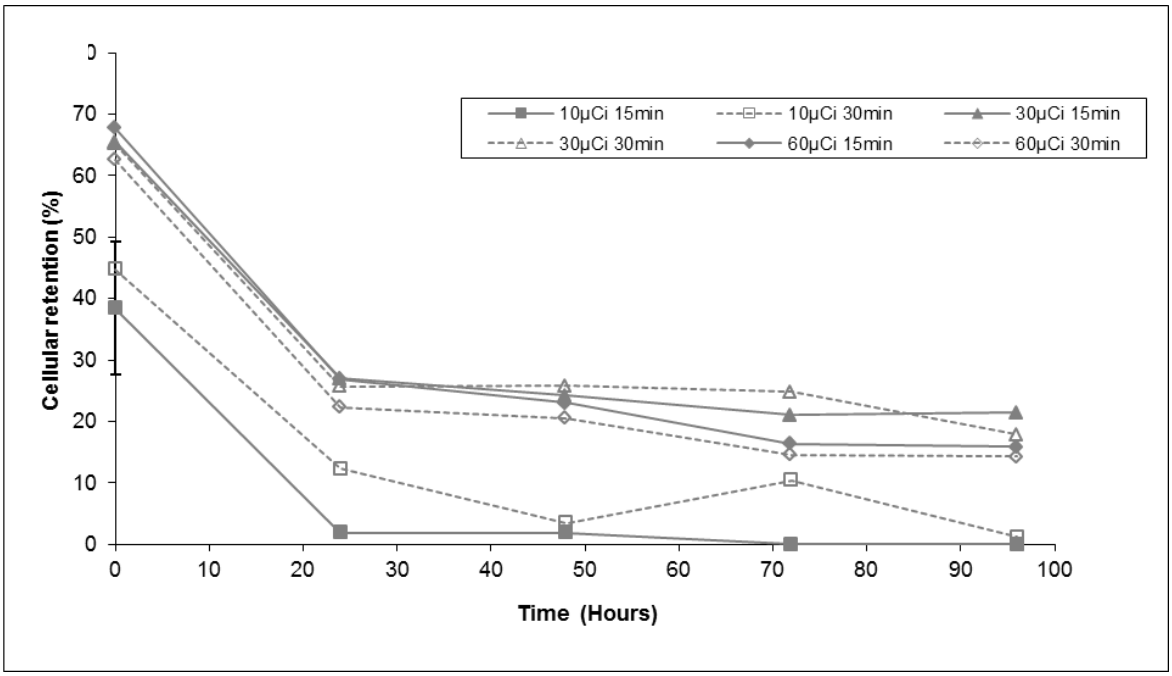

Figure 1: Cellular retention percentage of In-111 cultured cells following decay correction demonstrated an important leakage within the first 24h after labeling from 65.3±1.8% to 25.4±1.9% at doses 30µCi and 60µCi, independently the incubation time with radiotracer. After 24h retention rate remained stable over time until 96h and no more detectable after 168h. At dose 10µCi, no sufficient cellular retention was observed.

Figure 2

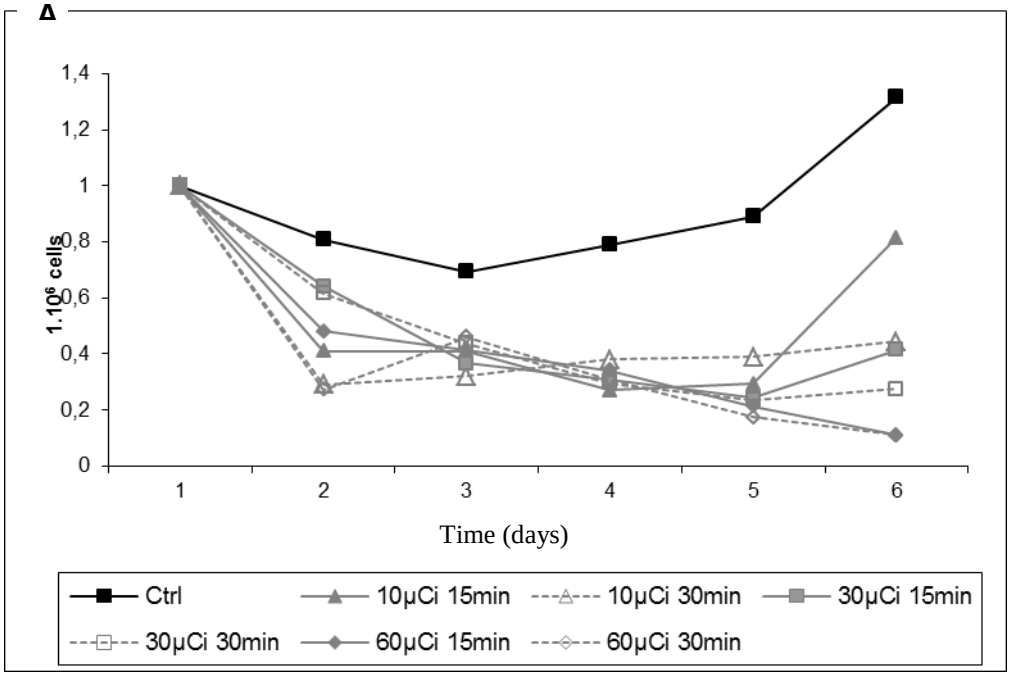
A
1,4
1,2
1
0,8
0,6
0,4
0,2
0
1.10⁶ cells
1
2
3
4
5
6
Time (days)
Ctrl
10µCi 15min
10µCi 30min
30µCi 15min
30µCi 30min
60µCi 15min
60µCi 30min

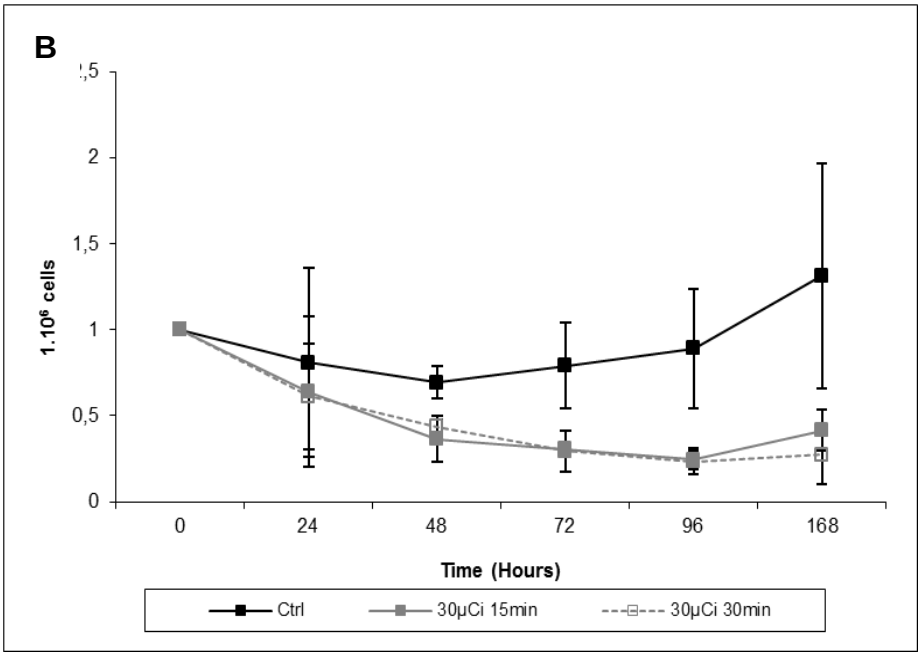
B
2
1,5
1
0,5
0
1.10⁶ cells
0
24
48
72
96
168
Time (Hours)
Ctrl
30µCi 15min
30µCi 30min

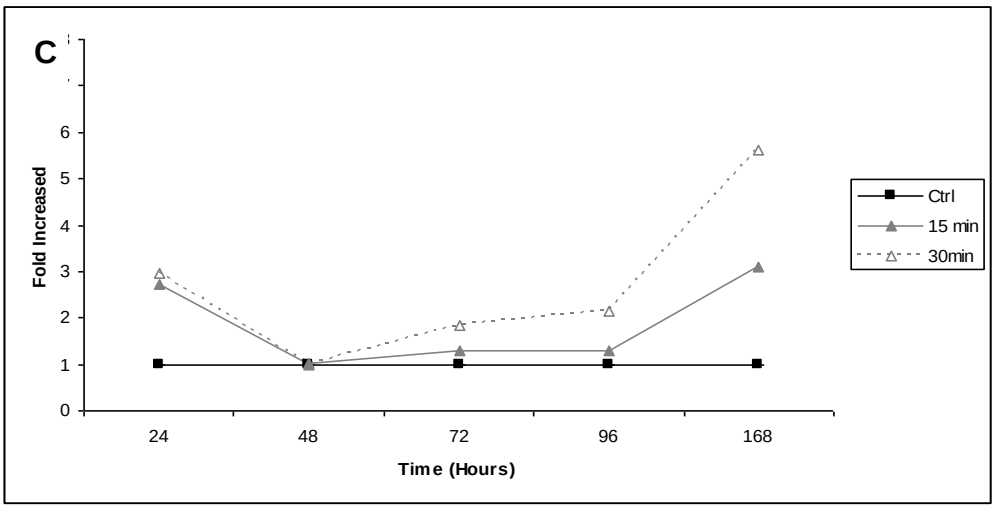

Figure 2: **A**. Cell proliferation curves over 168 hours cultures after In-111-cell labeling and compared with unlabelled cells demonstrated an important decrease of proliferation at high In-111-dose 60µCi. **B**. At dose 30µCi, higher impact on cell proliferation is observed with In-111-30 minutes than In-111-15 minutes incubation time. **C**. Cytotoxic effect of In-111 30µCi demonstrated a three to six fold increased level of extracellular LDH compared to unlabelled cells, after 15 to 30 minutes incubation time respectively. Results are expressed as LDH/protein content and normalized with the control group for each time point

.**Figure 3:** Immunocytochemical staining

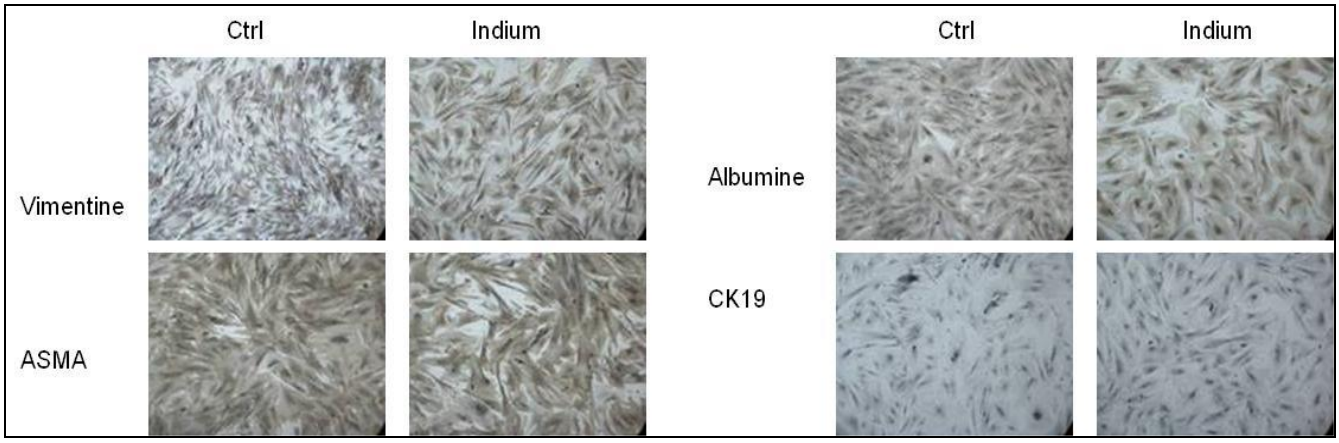

Figure 3: Phenotypic profile of radiolabeled cells did not demonstrate differences in vimentine, Albumine, ASMA (anti-smooth muscle actin) expression in comparison with the control group.

Figure 4 :

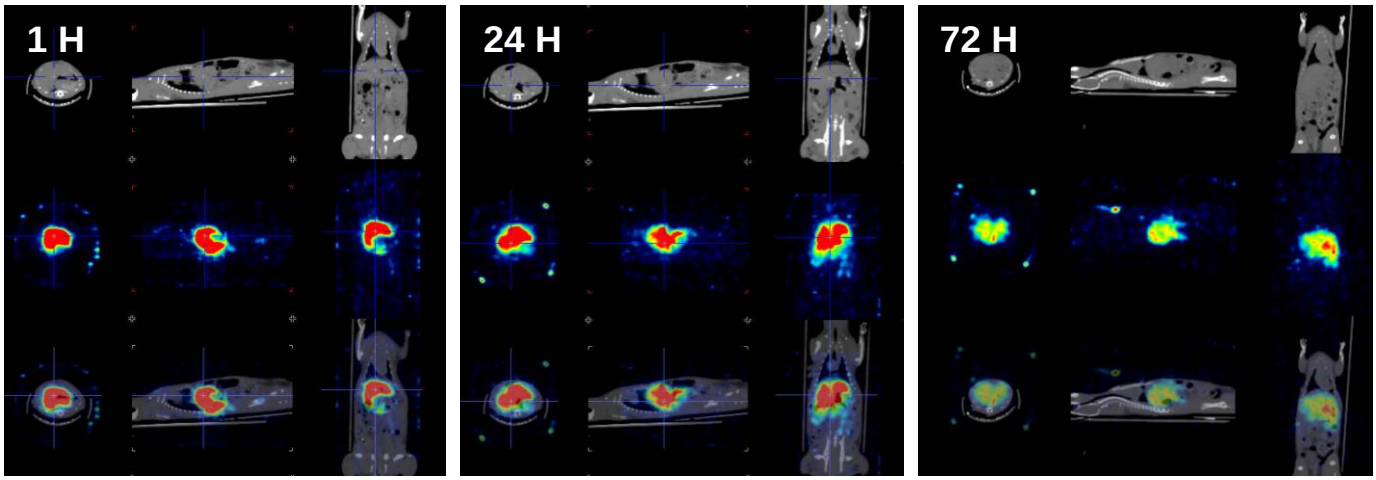

Figure 4: SPECT images of in vivo biodistribution of radioctracer in the whole rat body during the first 72hours post In-111-labeling receiving a total of 20.10^6 cells which contained in all case In-111-5.10^6 cells.

Figure 5 :

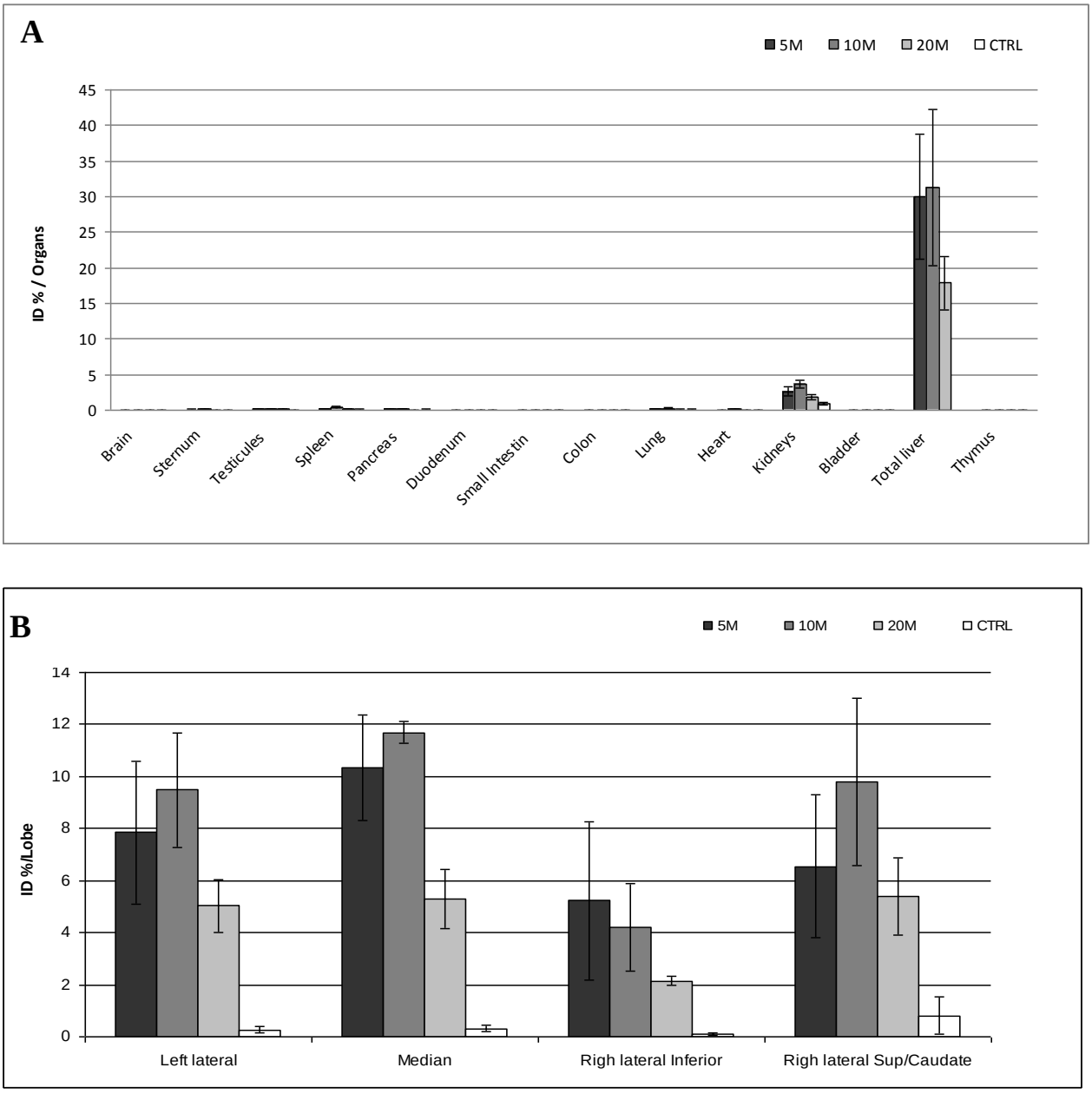

Figure 5: Organ biodistribution of labeled cells 24 hour after intraportal cell infusions assessed by the gamma counter demonstrated the specific signal localization in the liver (**A**) an specially into the left lateral, median and right lateral/caudal lobes (**B**). Data are normalized to the radioactivity count measured in the syringe before and after cell infusion (injected dose) and following decay correction.

Table 1: Cell viability and In-111 cell retention after labeling

	Viability (%)				In-111 Retention (%)		
	Ctrl	**10µCi**	**30µCi**	**60µCi**	**10µCi**	**30µCi**	**60µCi**
15 min	74.3±6.2	63.5±17.5	68.7±15.1	60.5±11.5	38.4±10.8	65.5±16.1	67.7±10.8
30 min	Not done	68.7±12.4	70.9±9.3	64.7±16.4	44.7±1.3	65.1±13.3	62.6±5.3

Table 2: Radiolabeled cells distribution in the liver expressed as a percentage of the whole body activity

	Ctrl		**5.10^6 cells**		**10.10^6 cells**		**20.10^6 cells**		
	1h	**24h**	**1h**	**24h**	**1h**	**24h**	**1h**	**24h**	**72h**
Rat 1	9%	10%	50%	53%	66%	62%	59%	45%	31%
Rat 2	8%	5%	59%	43%	56%	52%	57%	ND	ND
Rat 3	6%	4%	53%	10%	73%	55%	47%	40%	27%
Mean	**8%**	**6%**	**54%**	**35%**	**65%**	**56%**	**54%**	**43%**	**29%**
SEM	**1.1**	**2.5**	**3.3**	**16.9**	**6**	**3.8**	**4.9**		

ND: Non Determined

Conclusions and perspectives

1. Isolation of homologous ADHLSC in rat

The first part of this work was dedicated to the isolation and characterization of homologous ADHLSC in rat. Isolation of such cell would be useful to test the efficiency of such cells in a syngenic model of liver metabolic diseases.

Like ADHLSC, rat fibroblastic-like liver derived cells (rFLDC) emerged *in vitro* after primary culture of liver cells obtained after enzymatic desegregation (two-step collagenase perfusion) of the adult rat liver. Both cells exhibit common features like a fibroblastic like morphology; they displayed a mesenchymal profile as evidenced by the expression of CD44, CD73, and CD90 proteins (Table 5) and the absence of hematopoietic CD45 marker expression. However, rFLDC exhibit several original among which a higher proliferative potential and with a senescence not reached before at least 50 passages in contrast to human cells that stop proliferating after 10-12 passages.

RT-PCR analyses also revealed expression of cytokeratin (CK) 8, UDP-glucuronosyltransferase 1A1 (UGT1A1) and glucose-6-phosphatase (G6P) underlining the hepatic origin and the hepatic like profile of rFLDC. Undifferentiated rFLDCs have the capacity to store glycogen and show G6Pase activity as mature hepatocytes.

At the differentiation level, rFLDCs were able, at early passages, to differentiate into adipocytes, on the contrary to ADHLSCs (Table 5). Under hepatogenic differentiation medium, low number of rFLDCs displays the polygonal morphology of mature hepatocytes as compared to ADHLSC. Differentiated rFLDCs express both albumin (Alb) and tryptophan 2,3-dioxygenase (TDO). However, we do not observe the expression of more specific hepatic markers such as hepatic nuclear factor 4 (HNF4) or tyrosine aminotransferase (TAT). Despite

the expression of UGT1A1 mRNA, rFLDCs were not able to specifically conjugate bilirubin even after differentiation.

	rFLDC	ADHLSC
Proliferation	>50 passages	<12 passages
Genotype/phenotype		
- Mesenchymal markers	vimentin, fibronectin, ASMA, CD44, CD73, CD90, CD105	vimentin, fibronectin, ASMA, CD44, CD73, CD90, CD105
- Hepatic markers	CK8, UGT1A1, G6P	Alb, G6P, HNF4
- Biliary markers	CK19	-
Plasticity:		
- Osteocytic	-	-
- Adipocytic	<P2	-
- Hepatic	Alb and TDO expression	TDO and TAT expression
Functionality (undifferentiated state):		
- Glycogen storage	+	-
- Glucose-6-phosphatase activity	+	-
- Bilirubin conjugation	-	+

Table 5: common features and differences between rat fibroblastic like liver derived cells (rFLDC) and human adult liver progenitor cells (ADHLSC)
ASMA: α-smooth muscle actin, CK: cytokeratin, UGT1A1: UDP-glucuronosyl transferase 1A1, G6P: glucose-6-phosphatase, Alb: albumin, HNF4: hepatic nuclear factor 4, TDO: Tryptophan 2,3-dioxygenase, TAT: tyrosine aminotransferase

Despite the same liver cell isolation protocol applied, notably differences exist between human and rat cell types which make rFLDC not suitable for their use in syngenic models of liver metabolic diseases. According to literature data, majority of liver rat progenitor cells was only obtained after submitting animals to carcinogenic agents or toxic injuries. Yin et *al*. [107] described liver progenitor cells (LPC) in allyl alcohol treated rats livers. These cells were also characterized

by their immuno-positivity for albumin, αFP and CD90 expression, a high proliferative potential (100 population doublings). In rats subjected to 2-acetylaminofluorene treatment followed by partial hepatectomy, Yovchev [108] and Qin [109] described oval cells expressing mesenchymal (CD24, CD44, CD90), hepatocytic (albumin) and biliary marker (CK19).

Few groups obtained liver progenitor cells from healthy rat livers. In 1996, Tateno established small hepatocytes cell line but from the non parenchymal liver fraction [110]. Such small hepatocytes expressed hepatocytic marker proteins such as albumin, CK8, and CK18 in the early proliferation phase of culture. However, Cx32, a differentiated hepatocyte marker, and bile duct epithelial markers such as BD1, CK7, and CK19 were not expressed in this stage of the culture but appeared after 7-10 days of culture. Nagai et *al*. [111] characterized hepatic stem like cells (HSL) by expression of αFP, and GST and non-expression of albumin and CK19. Using a co-cultured with stellate cells protocol, HSL acquired albumin expression after 2-3 days. Recently, Behnan Sahin et *al*. [112], using a 2-step collagenase protocol, reported a cell population derived from adult rat liver and called LDPCs (Liver-derived progenitor cells). Regarding their oval morphology and expression of HNF3beta, CD90 and hematopoietic markers CD45, CD34, these cells seem to be closely related to oval cells despite the absence of CK7, CK8 and CK19 expression. All together, these data suggest that rFLDC was an original cell type that, to our knowledge, was never described in the literature.

2. Metabolic correction in the Gunn rat

The second part of this work was to prove the efficiency of ADHLSC in a model of Crigler-Najjar liver metabolic disease rat (Gunn rat). Several laboratories are using this animal model for the evaluation of gene and cell therapy efficacy to recover the disease (Table 6).

In 1990 Dixit et *al*. demonstrated a 34.8% serum bilirubin level reduction after 10 days in rats injected with 50 millions encapsulated wild type (WT) rat hepatocytes [113]. Microcapsules were studied by light and electron microscopy 1 month after transplantation indicating the presence of donor cells. Two years later, Zhang et *al*. [114] injected 10 millions WT rat hepatocytes directly into the liver of 75% hepatectomized Gunn rats. One month after the injection, they observed a significant decrease in total serum bilirubin levels and the presence of mono- and diglucuronides into the bile. Kokudo et *al*. [115] in 1995 injected, through the spleen, 10 millions adult or fetal WT rat hepatocytes in recipients Gunn rats. Two months post-transplantation, serum bilirubin level decrease from 7.16 +/- 0.25 mg/dl to 4.38 +/- 0.60 mg/dl and from 7.22 +/- 0.24 mg/dl to 4.92 +/- 0.24mg/dl in rats injected with adult and fetal hepatocytes respectively. Ilan et *al*. [116] were the first ones to inject two millions cells into the portal vein of right portal vein ligation Gunn rats. They observed a dramatically decrease of serum bilirubin concentration from 6.9+/-1.2 mg/dl to 1.7+/-0.45 mg/d after 1 month. In 2002, Guha et *al*. [117] injected 5 millions hepatocytes of congenic Wistar rat into the splenic pulp. Recipient rats were prior irradiated (50Gy) and submitted to a 68% hepatectomy. Twelve weeks after hepatocyte transplantation, serum bilirubin dramatically decrease from 10.4mg/dl to 0.64mg/dl, this effect was preserved

during at least 14 weeks. Immunohistochemistry liver analysis revealed in transplanted rats clusters of UGT1A1 positive cells, undetected in non injected rats. In 2005, Cubero et *al*. [118] injected into the spleen 10 millions adult and fetal WT rat hepatocytes in retrorsine-Triiodothyronine pretreated Gunn rats. Ninety days post transplantation adult and fetal hepatocytes transplanted rats exhibit a serum bilirubin decrease and bilirubin conjugates into the bile and a proliferating cell nuclear antigen positive immunostaining. In 2007, Muraca et *al*. [119] injected 10 millions Lewis rat GFP bone marrow derived cells through the portal vein through the portal vein. Gunn rat liver was, before injection, subjected to ischemia/reperfusion damages. Three days post injection, GFP positive cells were found into the recipient liver parenchyma. Thirty days post-transplantation, transplanted rats showed a 35% decrease in plasma bilirubin associated with the appearance of monoconjugated bilirubin in bile and expression of UGT1A1 mRNA as assayed by RT-PCR.

	Injected cell type	Number of cells	Injection route	Hepatic injury	Results	Study duration	Cell tracking
Dixit (1990)	Encapsulated rat hepatocytes	50 millions	Intraperitoneal	None	34,8% total bilirubin decrease	1 month	Light and electron microscopy
Zhang (1992)	Rat hepatocytes	10 millions	Portal vein	75% hepatectomy	36.2% total bilirubin decrease, glucuronides in bile	1 month	ND
Kakudo (1995)	Rat hepatocytes	10 millions	Spleen	None	55% total bilirubin decrease, glucuronides in bile	12 months	ND
Kakudo (1995)	Fetal rat hepatocytes	10 millions	Spleen	None	58% total bilirubin decrease, glucuronides in bile	12 months	ND
Ilan (1997)	Rat hepatocytes	2 millions	Portal vein	Right portal vein ligation	76% total bilirubin decrease, glucuronides in bile	1 month	UGT1A1 activity, *UGT1* PCR,
Guha (2002)	Rat hepatocytes	5 millions	Spleen	50Gy irradiation and 68% hepatectomy	94% total bilirubin decrease, glucuronides in bile	6 months	UGT1A1 activity, WB, IHC
Cubero (2005)	Adult and fetal rat hepatocytes	40 millions	Spleen	Retrorsine-Triiodothyronine treatment	43% total bilirubin decrease, glucuronides in bile	3 months	PCNA
Muraca (2007)	Rat bone marrow derived cells	10 millions	Portal vein	Ischemia/ reperfusion	35% total bilirubin decrease, glucuronides in bile	1 month	IHC, GFP fluorescence

Table 6: Representative liver cell transplantation experiments in the Gunn rat model
ND: not done, UGT1A1: UDP-glucuronosyltransferase 1A1, PCR: polymerase chain reaction, WB: western blot, IHC: immunohistochemistry, PCNA: proliferating cell nuclear antigen, GFP: green fluorescent protein

In this study, our aim was to assay directly ADHLSC in an animal model of liver deficient metabolic activity (Gunn rat presenting a UGT1A1 deficiency). We injected 2.5 millions ADHLSC through the portal vein of 5 Gunn rats. Cryopreserved human hepatocytes, used as positive controls, were infused into 3 Gunn rats. No hepatic injury was applied to transplanted rats which were followed during 27 weeks and plasma unconjugated bilirubin (UCB) was measured after 2, 4, 13 and 27 weeks. At the end of the experiment, UCB levels revealed a 50% decrease in comparison with levels measured 2 weeks post-transplantation in rats transplanted with ADHLSC or hHepatocytes (hHep).

Immunohistochemistry analysis demonstrated that in transplanted rats showing a metabolic recovery, human cells mainly localized near the portal vein, corresponding to a limited proportion of the liver mass (1.3 ± 0.3% and 1.0 ± 0.2% for ADHLSC and hHep respectively), which is expected in view of the small quantity of cell infused. These data are in agreement with what is generally accepted that a replacement of 1-5% of the hepatic mass is required to restore liver disease in most injury models [61, 117]. Recently in his review; Jorns argues that in human clinical hepatocyte transplantation engraftment rates range from 0% to a maximum of 12% leading in most cases to a transitory quality of life improvement for metabolic liver disease patients[120].

These preclinical data are also in agreement which those obtained after ADHLSC transplantation into liver of immunodeficient mouse [106] which demonstrated that the number of human transplanted cells decrease from transplantation day to one month post transplantation and increases after 8 weeks. Moreover the ADHLSC *in situ* differentiation near the portal vein was established by the co-

expression of albumin and ornithine transcarbamylase[106]. Recently, Ichinohe proposed that survival of donor cells may have a close relation to not only early integration into hepatic plates but also the differentiated state of the cells at the time of transplantation [121]. Moreover, Haridass demonstrated that an increase in transplanted cell number does not allow higher repopulation [122].

Replacement of native liver by infused cells is one of the major hurdles encountered in cell therapy. A lot of progresses were accomplished to decrease cell rejection but, in rats, guidelines were not clear yet. Indeed, CsA has been shown to result in nephrotoxicity due to overproduction of ROS and lipid peroxidation [123]. In addition, CsA treatment has been associated with hepatotoxicity characterized by cholestasis, hyperbilirubinemia, increased alkaline phosphatase, elevated transaminases in the blood, inhibition of protein synthesis and disturbed lipid secretion in both humans and experimental animals [123, 124]. In order to avoid these side effects, several experiments were carried out to determine the appropriate dosage. These researches lead us to establish the optimal dose at 5mg/kg/2days during all the experiment [125].

One of the 5 ADHLSC transplanted rat did not exhibit a UCB decrease and the lack of effect was correlated with the absence of human cells into the liver parenchyma. The low repopulation rate must also be due to limited number of infused cells ($2.5\ 10^6$ cells/rat), it will be interesting to establish a correlation between amount of injected cells and decrease in unconjugated bilirubin blood concentration; it will also be useful to test the infusion of hepatogenic *in vitro* (pre) differentiated ADHLSC. The absence of regeneration stimulus can also explain the low repopulation rate; most of experiment carried out in animal liver diseases used physical (partial hepatectomy or high dose irradiation) or chemical (CCl_4

injection) stimuli. In parallel, amelioration of immunosuppression treatment will be interesting (use of microsomal encapsulated clodronate, low liver irradiation,…).

3. *In vivo* biodistribution of Adult Human Liver Stem/Progenitor Cells

In vivo biodistribution of ADHLSC was assayed using ^{111}Indium-oxine (^{111}In). ^{111}In is an inert metal that is not normally encountered in biological life systems, although complexing with oxine renders it neutral and lipid-soluble, permitting transfer across the cell membrane, followed by binding to cytosolic proteins. This characteristic may account for its successful incorporation in adult hepatocytes and fetal liver stem/progenitor cells, including their epithelial and non-epithelial cell fractions. ^{111}In has a half-life of 67 hours, which allows the tracking for several days after infusion. Another advantage of this technique is the high sensitivity, since little as 10^3 ^{111}In-radiolabeled cells can be detected.

Working on human fetal liver stem/progenitor cells and adult hepatocytes Cheng et al established that ^{111}In labeling did not alter cell viability or function, as indicated by the urea synthesis assay [126]. This finding was similar to those of studies in rodent hepatocytes, which additionally showed by autoradiography that the incorporated ^{111}In was inside cells in the cytoplasm [127]. Our data based on cell proliferation and cytotoxic results (measure of extracellular levels of Lactate Dehydrogenase) indicated that the dose of 30µCi for 15 minutes incubation gave the best results.

In the ADHLSC biodistribution study, catheterized rats received intraportal infusions of either 5.10^6 (group 1) -10.10^6 (group 2) - 20.10^6 (groups 3)

ADHLSC/2mL (injection speed: 150µL/min) containing a single dose of 5.10^6 ^{111}In labeled cells (15 minutes with a theoretical activity of 30µCi/1.10^6 cells). Three rats in each group were used in this study. Whole body scintigraphy was performed 1h and 24h (groups 1-2) and after 72h (group 3) following cell infusions and confirmed the liver uptake with a detected signal at 1h, 24h and 72 hours. No dissemination to ectopic organs was observed after 24h or 72 hours post transplantation. Semi-quantitative distribution analysis determined by the ratio: liver/ whole body signal, revealed a signal ranging from 54±3.3% - 65±6% - 54±4.9% after 1hour, from 35±16.6% - 56±3.8% - 43±2.5% after 24 hours, respectively to 5.10^6 -10.10^6 and 20.10^6 infused cells. At necropsy (24h post infusion), radioactivity was measured by gamma counter, in individual organs. Radioactivity was most important in liver including median, left lateral and right lateral superior - caudate lobes and no significant radioactivity was detected in other analyzed organs, except kidneys. In fact, less than 5% of the injected doses were detected in other excised tissues. These results are in accordance with Cheng et *al*. data. Indeed, working with fetal and adult human liver cells, they demonstrated by imaging studies that biodistribution analysis of organs verified restriction of transplanted cells to the liver. Moreover, those data showed good correlation with molecular assays, including PCR and in situ hybridization studies [126].

Therefore, radiolabeling of cells will not only permit noninvasive imaging for assessing biodistribution of transplanted cells, it will be far more sensitive than genetic probes requiring tissue sampling and will be helpful in demonstrating deleterious distributions of cells. Also, it should be noteworthy that not all transplanted cells need to be radiolabeled, because a mixture of radiolabeled and

non-radiolabeled cells should be equally effective. The radiolabelling hepatocytes technique was successfully applied for tracking transplanted adult hepatocytes in a child [128].

A wide number of animal models are utilized to test the efficacy of isolated hepatocytes or stem/progenitor cells to repopulate the liver (Table 7). Some models are preferentially used depending on the investigated endpoint: we can differentiate (i) animal models presenting a liver disease where the cell transplantation effect can be quantified by specific assays and compared to accurate positive and negative controls (ii) models where the measured parameters are the in situ engraftment and hepatocytic differentiation of injected cells (iii) models where the important criteria is the model size. In the first group, several differences are highlighted regarding natural endogenous/exogenous liver damages supporting the engraftment (like toxic milk mouse and Long Evans cinnamon rat (model of Wilson disease), Mdr2 mouse (model of progressive familial intrahepatic cholestasis type 3) Fas ligand-mediated damage, acetaminophen injury, carbon tetrachloride administration or partial hepatectomy), affecting the cell proliferation (combination of acute liver failure and choline-deficient ethionine-supplemented diet , carrefully dosed acetaminophen toxicity, 3,5-diethoxycarbonyl-1,4-dihydrocollidine or D-galactosamine), leading to chronic liver failure (by bile duct ligation, chronic hepatitis by administration of toxins, use of diphteria toxin receptors under the control of an albumin promoter or HSV-tk transgenic mouse) or conferring a selective advantage of grafted cells (FAH mouse a model of tyrosimenia type I, uPA model: mouse presenting the hepatocyte-specific expression of the uroplasminogen activator under the control of the albumin promoter.

Most of these animal models are not well standardized for cell therapy purposes whereas their predictive value for an optimal repopulation efficacy in the human liver is unknown.

• Proof that a given cell population can be used to ameliorate liver disease	Animal models without liver parenchyma degradation and no space and no selective advantage of grafted cells	• Gunn rat (model of Crigler-Najjar syndrome type I) [129, 130]
		• Sph-ash mouse (model of ornithine transcarbamylase deficiency) [131]
		• Factor VIII-deficient mice (haemophilia) [132]
	Animal models with endogenous/exogenous liver parenchyma degradation but not selective advantage of grafted cells	• Toxic milk mouse (Wilson disease) [133]
		• Long Evans cinnamon rat (model of Wilson disease) [134]
		• Mdr2 mouse (model of progressive familial intrahepatic cholestasis type 3) [135]
		• Fas ligand-mediated damage [136, 137]
		• Acetaminophen injury [138]
		• Carbon tetrachloride administration [139]
		• Partial hepatectomy
	Animal models with with endogenous liver parenchyma degradation and selective advantage of grafted cells	• FAH mouse (model of tyrosimenia type I) [140]
		• uPA model (hepatocyte-specific expression of the uroplasminogen activator under the control of the albumin promoter [141, 142]
	Illustration of liver progenitor cell proliferation: combination of acute liver failure and	• Choline-deficient ethionine-supplemented diet [143]
		• Carrefully dosed acetaminophen toxicity [144]
		• 3,5-diethoxycarbonyl-1,4-dihydrocollidine
		• D-galactosamine [145]
		• Use of hepatocyte injury combined with retrorsine to inhibit mature hepatocyte replication [146]
	Chronic liver failure	• Bile duct ligation [147, 148]
		• Chronic hepatitis by administration of toxins [149-151]
		• Diphteria toxin receptors under the control of an albumin promoter [152]
		• HSV-tk transgenic mouse[153]
Proof that a given human cell population can differentiate into a parenchymal liver cell in vivo		• NOD/SCID or the Rag2-/- and/or IL2Rγ-/- mice [154-156]
		• FAH-/- Rag2-/- IL2Rγ-/- mice [157]
		• uPA-Rag2-/- IL2Rγ-/- mice [157]
When size matters		• Swine [158]
		• Hyperuricaemic Dalmatian dog [159]
		• Watanabe rabbit (hypercholesterolaemia caused by a low-density lipoprotein receptor defect) [160-162]

Table 7: The different animal models and their suitability for testing the efficacy of cells to repopulate the liver with hepatocytes or stem/progenitor cells (Adapted from [163])

In this work we focused on the immuno-competent Gunn rat model (model of Crigler-Najjar type I syndrome). This model provides neither space nor a proliferative advantage of transplanted cells. Nevertheless it mimics the clinical situation of the disease where life-threatening genetic defect may not be associated with significant liver damage. However, Gunn rat is useful to provide the proof of concept that ADHLSC can restore bilirubin conjugation deficiency underling their potential clinical application in the treatment of Crigler-Najjar type 1 syndrome.

4. General conclusions

Animal models are essential tools to study cell distribution, engraftment, metabolic efficacy and safety issues in early research development stages. Translational studies involving ADHLSC for treating liver metabolic disease are still in progress. Despite the results illustrating that rodent progenitor cell homologous to ADHLSC cannot be easily obtained even when the same isolation and culture protocol were applied. The protocol used in the current study allowed the isolation of a novel type of liver progenitor cell population with both hepatic and biliary phenotype with no plain hepatogenic differentiation potential, stressing again the difficulty to generate homologous models.

We demonstrated the stable ADHLSC characteristics when cultured in large scale conditions: expression of mesenchymal markers (CD73, CD90, CD29, CD44, vimentin and ASMA) and hepatic markers expression (albumin). Cells exhibit the ability to specifically conjugate bilirubin and revealed an increase in UGT1A mRNA (mRNA constituted of the 4 first common exons of UGT1A family).

Moreover, as demonstrated by HPLC and immunohistochemistry (IHC) our study provides long-term activity and engraftment of ADHLSC integrate in an

immunocompetent rodent liver parenchyma used as model for Crigler-Najjar metabolic liver disorder. HPLC results indicate that 27 weeks after transplantation the four responsive injected Gunn rat, exhibit a high decrease in UCB blood level. RTqPCR and IHC results indicated the presence of human cells into the Gunn rat liver parenchyma; IHC allows us to determine that injected human cells seem localized in periportal zone.

Finally, using intraportal infusion of a small fraction of radio labeled ADHLSC we were able to detect biodistribution by scintigraphy images up to three days. Neither ectopic hot spots nor signals were evidenced outside of the liver, demonstrating the homing and the subsequent engraftment of ADHLSC preferentially within the liver parenchyma.

5. Perspectives: from bench to clinic or pharmaceutical application

Stem cells have great potential to serve medicine: from treating diseases, to pharmacological drug testing and to a better understanding of developmental biology. In all cases, the production of large amount of cells needed for clinical or commercial use imposes to evaluate the stability of the cells over time. The precise evaluation of stem cells in terms of safety and stability must be relied on a rigorous characterization of the initial phenotype under standardized procedures of isolation and culture techniques. This standardization can lead to obtaining a highly purified cell suspension excluding the possible contamination with other cell types. Moreover, it will help to guarantee a lot-to-lot reliability.

The efficiency of stem cells regenerative medicine depends on long-term metabolic effects of stem cells in the diseased organ. It is therefore important to ensure that stem cells are efficient enough when injected to engraft, repopulate and

differentiate. The amelioration of stem cell culture conditions, adapted to the differential requirements of stem and progenitor cells, will be beneficial to enhance culture yield. In this context, several researcher teams have tested the impact of antioxidant drugs, specific supplemented culture media, different serums or platelet lysates and 3D matrix to ameliorate cell quality. In addition to *in vitro* investigation, the impact of the development of culture conditions should also be assessed in terms of improved cell engraftment and metabolic activity *in vivo*. In the context of liver cell therapy, the hepatocytic differentiation ability of stem/progenitor cells has been extensively described *in vitro*. Results underlined that their hepatic commitment remains incomplete with a persistent chimerical phenotype. Nevertheless these results would further benefit from being completed by *in vivo* proof of concept data. Indeed, stem/progenitor cell transplantation in animal models mimicking human metabolic diseases provides the needed information on their ability to differentiate within the diseased hepatic environment and to correct impaired functionality. The metabolic activity *in vivo* should be quantified by specific assays and compared to accurate positive and negative controls. It should be kept in mind that none of the existing transplantation models is entirely representative of the human situation

Cell therapy also faces safety challenges. The tumorigenic potential is an important question in the development of safe cell therapies. Tumors can arise from contaminating cells or from primary cells that may differentiate or transform. Cytogenetic provides powerful complementary techniques (G-banding, FISH, SNP) to identify cells carrying specific abnormalities. Moreover, *in vivo* tumorogenic studies should also be performing in accurate immunodeficient animal model [164]. The potential of convey infectious diseases caused by microbes needs to be carefully assessed to provide a high quality pathogen free

final product. Therefore, cells should be manufactured in a GMP environment using well establish and standardized protocols to assess sterility during the whole production cycle. Stem cells possess the ability to reduce immune reaction in hosts [165] and some authors reported the capacity of bone marrow stem cells to sustain cancer growth by favoring the proliferation of tumor cells that would otherwise have been rejected by immunocompetent patients [166]. Finally, the injection of highly concentrated cell suspensions may favor stem cell aggregation and formation of cell emboli and also the procoagulant activity mediated by the production of tissue factor from the part of the transplanted cells [167, 168].

As research goes forward, our understanding of stem cell biology will improve and new questions will arise. All these new questions may need careful attention and analysis before moving from bench to clinical/commercial applications.

References

1. Berk, P.D., et al., *Studies of bilirubin kinetics in normal adults.* J Clin Invest, 1969. **48**(11): p. 2176-90.
2. London, I.M., et al., *On the origin of bile pigment in normal man.* J Biol Chem, 1950. **184**(1): p. 351-8.
3. Hayes, J.D. and D.J. Pulford, *The glutathione S-transferase supergene family: regulation of GST and the contribution of the isoenzymes to cancer chemoprotection and drug resistance.* Crit Rev Biochem Mol Biol, 1995. **30**(6): p. 445-600.
4. Rowe, J.D., E. Nieves, and I. Listowsky, *Subunit diversity and tissue distribution of human glutathione S-transferases: interpretations based on electrospray ionization-MS and peptide sequence-specific antisera.* Biochem J, 1997. **325 (Pt 2)**: p. 481-6.
5. Bernstein, L.H., et al., *Hepatic intracellular distribution of tritium-labeled unconjugated and conjugated bilirubin in normal and Gunn rats.* J Clin Invest, 1966. **45**(7): p. 1194-201.
6. Chowdhury, J.R., et al., *Distribution of UDPglucuronosyltransferase in rat tissue.* Proc Natl Acad Sci U S A, 1985. **82**(9): p. 2990-4.
7. Jansen, P.L. and I.M. Arias, *Delipidation and reactivation of UDPglucuronosyltransferase from rat liver.* Biochim Biophys Acta, 1975. **391**(1): p. 23-38.
8. Zakim, D. and H. Eibl, *The influence of charge and the distribution of charge in the polar region of phospholipids on the activity of UDP-glucuronosyltransferase.* J Biol Chem, 1992. **267**(19): p. 13166-70.
9. Upson, D.W., R.R. Gronwall, and C.E. Cornelius, *Maximal hepatic excretion of bilirubin in sheep.* Proc Soc Exp Biol Med, 1970. **134**(1): p. 9-12.
10. Lester, R. and R. Schmid, *Intestinal absorption of bile pigments. II. Bilirubin absorption in man.* N Engl J Med, 1963. **269**: p. 178-82.
11. Chowdhury, J.R.W., A. W.; Chowdhury, N. R.; Arias, I. M, *Hereditary jaundice and disorders of bilirubin metabolism*, in *The Metabolic and Molecular Bases of Inherited Disease*, C.R.B. Scriver, A. L.; Sly, W. S.; Valle, D., Editor. 2001, McGraw-Hill: New York. p. 3063–3101.
12. Labrune, P., *Crigler-Najjar Syndrome.* www.orpha.net/data/patho/Pro/en/CriglerNajjar-FRenPro242.pdf, 2004.
13. Crigler, J.F., Jr. and V.A. Najjar, *Congenital familial nonhemolytic jaundice with kernicterus.* Pediatrics, 1952. **10**(2): p. 169-80.
14. Childs, B., J.B. Sidbury, and C.J. Migeon, *Glucuronic acid conjugation by patients with familial nonhemolytic jaundice and their relatives.* Pediatrics, 1959. **23**(5): p. 903-13.
15. Berk, P.D., et al., *Unconjugated hyperbilirubinemia. Physiologic evaluation and experimental approaches to therapy.* Ann Intern Med, 1975. **82**(4): p. 552-70.
16. Sleisenger, M.H., *Nonhemolytic unconjugated hyperbilirubinemia with hepatic glucuronyl transferase deficiency: a genetic study in four generations.* Trans Assoc Am Physicians, 1967. **80**: p. 259-66.
17. Szabo, L. and P. Ebrey, *Studies on the Inheritance of Crigler--Najjar's Syndrome by the Menthol Test.* Acta Paediatr Acad Sci Hung, 1963. **4**: p. 153-8.
18. Wolkoff, A.W., et al., *Clinical conference. Crigler-Najjar syndrome (type I) in an adult male.* Gastroenterology, 1979. **76**(4): p. 840-8.
19. Arias, I.M., *Chronic familial nonhemolytic jaundice with conjugated bilirubin in the serum.* Gastroenterology, 1962. **43**: p. 588-90.

20. Gollan, J.L., et al., *Prolonged survival in three brothers with severe type 2 Crigler-Najjar syndrome. Ultrastructural and metabolic studies.* Gastroenterology, 1975. **68**(6): p. 1543-55.
21. Gordon, E.R., E.A. Shaffer, and A. Sass-Kortsak, *Bilirubin secretion and conjugation in the Crigler-Najjar syndrome type II.* Gastroenterology, 1976. **70**(5 PT.1): p. 761-5.
22. Drake, R.R., et al., *Application of 5-azido-UDP-glucose and 5-azido-UDP-glucuronic acid photoaffinity probes for the determination of the active site orientation of microsomal UDP-glucosyltransferases and UDP-glucuronosyltransferases.* J Biol Chem, 1992. **267**(16): p. 11360-5.
23. Bosma, P.J., et al., *Bilirubin UDP-glucuronosyltransferase 1 is the only relevant bilirubin glucuronidating isoform in man.* J Biol Chem, 1994. **269**(27): p. 17960-4.
24. Bosma, P.J., et al., *Mechanisms of inherited deficiencies of multiple UDP-glucuronosyltransferase isoforms in two patients with Crigler-Najjar syndrome, type I.* FASEB J, 1992. **6**(10): p. 2859-63.
25. Bosma, P.J., et al., *Sequence of exons and the flanking regions of human bilirubin-UDP-glucuronosyltransferase gene complex and identification of a genetic mutation in a patient with Crigler-Najjar syndrome, type I.* Hepatology, 1992. **15**(5): p. 941-7.
26. Kadakol, A., et al., *Genetic lesions of bilirubin uridine-diphosphoglucuronate glucuronosyltransferase (UGT1A1) causing Crigler-Najjar and Gilbert syndromes: correlation of genotype to phenotype.* Hum Mutat, 2000. **16**(4): p. 297-306.
27. Ritter, J.K., et al., *Identification of a genetic alteration in the code for bilirubin UDP-glucuronosyltransferase in the UGT1 gene complex of a Crigler-Najjar type I patient.* J Clin Invest, 1992. **90**(1): p. 150-5.
28. Seppen, J., et al., *Discrimination between Crigler-Najjar type I and II by expression of mutant bilirubin uridine diphosphate-glucuronosyltransferase.* J Clin Invest, 1994. **94**(6): p. 2385-91.
29. Gunn, C.K., *Hereditary Acholuric Jaundice in the Rat.* Can Med Assoc J, 1944. **50**(3): p. 230-7.
30. Chowdhury, J.R., R. Kondapalli, and N.R. Chowdhury, *Gunn rat: a model for inherited deficiency of bilirubin glucuronidation.* Adv Vet Sci Comp Med, 1993. **37**: p. 149-73.
31. Schmid, R., et al., *Congenital jaundice in rats, due to a defect in glucuronide formation.* J Clin Invest, 1958. **37**(8): p. 1123-30.
32. Iyanagi, T., *Molecular basis of multiple UDP-glucuronosyltransferase isoenzyme deficiencies in the hyperbilirubinemic rat (Gunn rat).* J Biol Chem, 1991. **266**(35): p. 24048-52.
33. Sato, H., et al., *Genetic defect of bilirubin UDP-glucuronosyltransferase in the hyperbilirubinemic Gunn rat.* Biochem Biophys Res Commun, 1991. **177**(3): p. 1161-4.
34. elAwady, M., et al., *Mechanism of the lack of induction of UDP-glucuronosyltransferase activity in Gunn rats by 3-methylcholanthrene. Identification of a truncated enzyme.* J Biol Chem, 1990. **265**(18): p. 10752-8.
35. Greenfield, S. and A.P. Majumdar, *Bilirubin encephalopathy: effect on protein synthesis in the brain of the Gunn rat.* J Neurol Sci, 1974. **22**(1): p. 83-9.
36. Diamond, I. and R. Schmid, *Oxidative phosphorylation in experimental bilirubin encephalopathy.* Science, 1967. **155**(767): p. 1288-9.
37. Constantopoulos, A. and N. Matsaniotis, *Bilirubin inhibition of protein kinase: its prevention by cyclic AMP.* Cytobios, 1976. **17**(65): p. 17-20.
38. Morphis, L., et al., *Bilirubin-induced modulation of cerebral protein phosphorylation in neonate rabbits in vivo.* Science, 1982. **218**(4568): p. 156-8.

39. Call, N.B. and C.C. Tisher, *The urinary concentrating defect in the Gunn strain of rat. Role of bilirubin.* J Clin Invest, 1975. **55**(2): p. 319-29.
40. Axelsen, R.A., *Spontaneous renal papillary necrosis in the Gunn rat.* Pathology, 1973. **5**(1): p. 43-50.
41. Nguyen, N., et al., *Disruption of the ugt1 locus in mice resembles human Crigler-Najjar type I disease.* J Biol Chem, 2008. **283**(12): p. 7901-11.
42. Fujiwara, R., et al., *Developmental hyperbilirubinemia and CNS toxicity in mice humanized with the UDP glucuronosyltransferase 1 (UGT1) locus.* Proc Natl Acad Sci U S A, 2010. **107**(11): p. 5024-9.
43. Bortolussi, G., et al., *Rescue of bilirubin-induced neonatal lethality in a mouse model of Crigler-Najjar syndrome type I by AAV9-mediated gene transfer.* FASEB J, 2012. **26**(3): p. 1052-63.
44. Lund, H.T. and J. Jacobsen, *Influence of phototherapy on the biliary bilirubin excretion pattern in newborn infants with hyperbilirubinemia.* J Pediatr, 1974. **85**(2): p. 262-7.
45. van der Veere, C.N., et al., *Current therapy for Crigler-Najjar syndrome type 1: report of a world registry.* Hepatology, 1996. **24**(2): p. 311-5.
46. Blaschke, T.F., et al., *Crigler-Najjar syndrome: an unusual course with development of neurologic damage at age eighteen.* Pediatr Res, 1974. **8**(5): p. 573-90.
47. Sellier, A.L., et al., *Successful plasmapheresis for acute and severe unconjugated hyperbilirubinemia in a child with crigler najjar type I syndrome.* JIMD Rep, 2012. **2**: p. 33-6.
48. Sugatani, J., et al., *The phenobarbital response enhancer module in the human bilirubin UDP-glucuronosyltransferase UGT1A1 gene and regulation by the nuclear receptor CAR.* Hepatology, 2001. **33**(5): p. 1232-8.
49. Kaufman, S.S., et al., *Orthotopic liver transplantation for type I Crigler-Najjar syndrome.* Hepatology, 1986. **6**(6): p. 1259-62.
50. Sokal, E.M., et al., *Orthotopic liver transplantation for Crigler-Najjar type I disease in six children.* Transplantation, 1995. **60**(10): p. 1095-8.
51. Evans, H.M., et al., *Progressive histological damage in liver allografts following pediatric liver transplantation.* Hepatology, 2006. **43**(5): p. 1109-17.
52. Heaton, N., *Small-for-size liver syndrome after auxiliary and split liver transplantation: donor selection.* Liver Transpl, 2003. **9**(9): p. S26-8.
53. Najimi, M. and E. Sokal, *Liver cell transplantation.* Minerva Pediatr, 2005. **57**(5): p. 243-57.
54. Stephenne, X., et al., *Liver allograft radiotherapy to treat rejection in children: efficacy in orthotopic liver transplantation and long-term safety.* Liver Int, 2005. **25**(6): p. 1108-13.
55. Muraca, M., et al., *Hepatocyte transplantation as a treatment for glycogen storage disease type 1a.* Lancet, 2002. **359**(9303): p. 317-8.
56. Dhawan, A., et al., *Hepatocyte transplantation for inherited factor VII deficiency.* Transplantation, 2004. **78**(12): p. 1812-4.
57. Fox, I.J., et al., *Treatment of the Crigler-Najjar syndrome type I with hepatocyte transplantation.* N Engl J Med, 1998. **338**(20): p. 1422-6.
58. Ambrosino, G., et al., *Isolated hepatocyte transplantation for Crigler-Najjar syndrome type 1.* Cell Transplant, 2005. **14**(2-3): p. 151-7.
59. Darwish, A.A., et al., *Permanent access to the portal system for cellular transplantation using an implantable port device.* Liver Transpl, 2004. **10**(9): p. 1213-5.

60. Dhawan, A., R.R. Mitry, and R.D. Hughes, *Hepatocyte transplantation for liver-based metabolic disorders.* J Inherit Metab Dis, 2006. **29**(2-3): p. 431-5.
61. Fox, I.J. and J. Roy-Chowdhury, *Hepatocyte transplantation.* J Hepatol, 2004. **40**(6): p. 878-86.
62. Lysy, P.A., et al., *Liver cell transplantation for Crigler-Najjar syndrome type I: update and perspectives.* World J Gastroenterol, 2008. **14**(22): p. 3464-70.
63. Ribes-Koninckx, C., et al., *Clinical outcome of hepatocyte transplantation in four pediatric patients with inherited metabolic diseases.* Cell Transplant, 2012. **21**(10): p. 2267-82.
64. Smets, F., M. Najimi, and E.M. Sokal, *Cell transplantation in the treatment of liver diseases.* Pediatr Transplant, 2008. **12**(1): p. 6-13.
65. Stephenne, X., et al., *Cryopreservation of human hepatocytes alters the mitochondrial respiratory chain complex 1.* Cell Transplant, 2007. **16**(4): p. 409-19.
66. Bartholomew, A., et al., *Mesenchymal stem cells suppress lymphocyte proliferation in vitro and prolong skin graft survival in vivo.* Exp Hematol, 2002. **30**(1): p. 42-8.
67. Aggarwal, S. and M.F. Pittenger, *Human mesenchymal stem cells modulate allogeneic immune cell responses.* Blood, 2005. **105**(4): p. 1815-22.
68. Haack-Sorensen, M., et al., *The influence of freezing and storage on the characteristics and functions of human mesenchymal stromal cells isolated for clinical use.* Cytotherapy, 2007. **9**(4): p. 328-37.
69. Ichikawa, H., et al., *Cryopreservation of mouse embryoid bodies.* Cryobiology, 2007. **54**(3): p. 290-3.
70. Lee, M.W., et al., *Neural differentiation of novel multipotent progenitor cells from cryopreserved human umbilical cord blood.* Biochem Biophys Res Commun, 2007. **358**(2): p. 637-43.
71. Xiang, Y., et al., *Ex vivo expansion and pluripotential differentiation of cryopreserved human bone marrow mesenchymal stem cells.* J Zhejiang Univ Sci B, 2007. **8**(2): p. 136-46.
72. Martin-Rendon, E. and S.M. Watt, *Stem cell plasticity.* Br J Haematol, 2003. **122**(6): p. 877-91.
73. Verfaillie, C.M., M.F. Pera, and P.M. Lansdorp, *Stem cells: hype and reality.* Hematology Am Soc Hematol Educ Program, 2002: p. 369-91.
74. Liedtke, C. and K.L. Streetz, *Hepatocytes from embryonic stem cells: Prometheus revisited?* Hepatology, 2007. **45**(3): p. 829-30.
75. Tsuchiya, H., et al., *Evaluation of human embryonic stem cell-derived hepatocyte-like cells for detection of CYP1A inducers.* Drug Metab Pharmacokinet, 2012. **27**(6): p. 598-604.
76. Frankel, M.S., *In search of stem cell policy.* Science, 2000. **287**(5457): p. 1397.
77. Wainwright, S.P., et al., *Ethical boundary-work in the embryonic stem cell laboratory.* Sociol Health Illn, 2006. **28**(6): p. 732-48.
78. Erdo, F., et al., *Host-dependent tumorigenesis of embryonic stem cell transplantation in experimental stroke.* J Cereb Blood Flow Metab, 2003. **23**(7): p. 780-5.
79. Scheers, I., *Characterization of human derived liver progenitor cells and mesenchymal stem cells for their risk of malignant transformation*, in *Institut de recherche expérimentale et clinique*. 2012, Université Catholique de Louvain: Laboratory of pediatric hepatology and cell therapy. p. 236.
80. Wognum, A.W., A.C. Eaves, and T.E. Thomas, *Identification and isolation of hematopoietic stem cells.* Arch Med Res, 2003. **34**(6): p. 461-75.
81. Dao, M.A. and J.A. Nolta, *CD34: to select or not to select? That is the question.* Leukemia, 2000. **14**(5): p. 773-6.

82. Cantz, T., et al., *Reevaluation of bone marrow-derived cells as a source for hepatocyte regeneration.* Cell Transplant, 2004. **13**(6): p. 659-66.
83. Di Campli, C., et al., *No evidence of hematopoietic stem cell mobilization in patients submitted to hepatectomy or in patients with acute on chronic liver failure.* Transplant Proc, 2005. **37**(6): p. 2563-6.
84. Lian, G., et al., *Failure of hepatocyte marker-expressing hematopoietic progenitor cells to efficiently convert into hepatocytes in vitro.* Exp Hematol, 2006. **34**(3): p. 348-58.
85. Stadtfeld, M. and T. Graf, *Assessing the role of hematopoietic plasticity for endothelial and hepatocyte development by non-invasive lineage tracing.* Development, 2005. **132**(1): p. 203-13.
86. Yamaguchi, K., et al., *In vivo selection of transduced hematopoietic stem cells and little evidence of their conversion into hepatocytes in vivo.* J Hepatol, 2006. **45**(5): p. 681-7.
87. Masson, S., et al., *Potential of hematopoietic stem cell therapy in hepatology: a critical review.* Stem Cells, 2004. **22**(6): p. 897-907.
88. Thorgeirsson, S.S. and J.W. Grisham, *Hematopoietic cells as hepatocyte stem cells: a critical review of the evidence.* Hepatology, 2006. **43**(1): p. 2-8.
89. da Silva Meirelles, L., P.C. Chagastelles, and N.B. Nardi, *Mesenchymal stem cells reside in virtually all post-natal organs and tissues.* J Cell Sci, 2006. **119**(Pt 11): p. 2204-13.
90. Kuroda, Y., et al., *Bone marrow mesenchymal cells: how do they contribute to tissue repair and are they really stem cells?* Arch Immunol Ther Exp (Warsz), 2011. **59**(5): p. 369-78.
91. Lee, K.D., et al., *In vitro hepatic differentiation of human mesenchymal stem cells.* Hepatology, 2004. **40**(6): p. 1275-84.
92. Banas, A., et al., *Adipose tissue-derived mesenchymal stem cells as a source of human hepatocytes.* Hepatology, 2007. **46**(1): p. 219-28.
93. Aurich, I., et al., *Functional integration of hepatocytes derived from human mesenchymal stem cells into mouse livers.* Gut, 2007. **56**(3): p. 405-15.
94. Campard, D., et al., *Native umbilical cord matrix stem cells express hepatic markers and differentiate into hepatocyte-like cells.* Gastroenterology, 2008. **134**(3): p. 833-48.
95. Tao, X.R., et al., *Clonal mesenchymal stem cells derived from human bone marrow can differentiate into hepatocyte-like cells in injured livers of SCID mice.* J Cell Biochem, 2009. **108**(3): p. 693-704.
96. Sato, Y., et al., *Human mesenchymal stem cells xenografted directly to rat liver are differentiated into human hepatocytes without fusion.* Blood, 2005. **106**(2): p. 756-63.
97. Aurich, H., et al., *Hepatocyte differentiation of mesenchymal stem cells from human adipose tissue in vitro promotes hepatic integration in vivo.* Gut, 2009. **58**(4): p. 570-81.
98. Farber, E., *Similarities in the sequence of early histological changes induced in the liver of the rat by ethionine, 2-acetylamino-fluorene, and 3'-methyl-4-dimethylaminoazobenzene.* Cancer Res, 1956. **16**(2): p. 142-8.
99. Knight, B., et al., *Jekyll and Hyde: evolving perspectives on the function and potential of the adult liver progenitor (oval) cell.* Bioessays, 2005. **27**(11): p. 1192-202.
100. Lowes, K.N., et al., *Oval cell numbers in human chronic liver diseases are directly related to disease severity.* Am J Pathol, 1999. **154**(2): p. 537-41.
101. Zhou, H., et al., *Identification of hepatocytic and bile ductular cell lineages and candidate stem cells in bipolar ductular reactions in cirrhotic human liver.* Hepatology, 2007. **45**(3): p. 716-24.

102. Duncan, A.W., C. Dorrell, and M. Grompe, *Stem cells and liver regeneration.* Gastroenterology, 2009. **137**(2): p. 466-81.
103. Herrera, M.B., et al., *Isolation and characterization of a stem cell population from adult human liver.* Stem Cells, 2006. **24**(12): p. 2840-50.
104. Najimi, M., et al., *Adult-derived human liver mesenchymal-like cells as a potential progenitor reservoir of hepatocytes?* Cell Transplant, 2007. **16**(7): p. 717-28.
105. Khuu, D.N., et al., *In vitro differentiated adult human liver progenitor cells display mature hepatic metabolic functions: a potential tool for in vitro pharmacotoxicological testing.* Cell Transplant, 2011. **20**(2): p. 287-302.
106. Khuu, D.N., et al., *Adult human liver mesenchymal stem/progenitor cells participate to mouse liver regeneration after hepatectomy.* Cell Transplant, 2012.
107. Yin, L., et al., *Derivation, characterization, and phenotypic variation of hepatic progenitor cell lines isolated from adult rats.* Hepatology, 2002. **35**(2): p. 315-24.
108. Yovchev, M.I., et al., *Novel hepatic progenitor cell surface markers in the adult rat liver.* Hepatology, 2007. **45**(1): p. 139-49.
109. Qin, A.L., et al., *Characterization and enrichment of hepatic progenitor cells in adult rat liver.* World J Gastroenterol, 2004. **10**(10): p. 1480-6.
110. Tateno, C. and K. Yoshizato, *Growth and differentiation in culture of clonogenic hepatocytes that express both phenotypes of hepatocytes and biliary epithelial cells.* Am J Pathol, 1996. **149**(5): p. 1593-605.
111. Nagai, H., et al., *Differentiation of liver epithelial (stem-like) cells into hepatocytes induced by coculture with hepatic stellate cells.* Biochem Biophys Res Commun, 2002. **293**(5): p. 1420-5.
112. Sahin, M.B., et al., *Isolation and characterization of a novel population of progenitor cells from unmanipulated rat liver.* Liver Transpl, 2008. **14**(3): p. 333-45.
113. Dixit, V., et al., *Restoration of liver function in Gunn rats without immunosuppression using transplanted microencapsulated hepatocytes.* Hepatology, 1990. **12**(6): p. 1342-9.
114. Zhang, H., et al., *Intrahepatic hepatocyte transplantation following subtotal hepatectomy in the recipient: a possible model in the treatment of hepatic enzyme deficiency.* J Pediatr Surg, 1992. **27**(3): p. 312-5; discussion 315-6.
115. Kokudo, N., et al., *Long-term effects of intrasplenically transplanted adult hepatocytes and fetal liver in hyperbilirubinemic Gunn rats.* Transpl Int, 1995. **8**(4): p. 262-7.
116. Ilan, Y., et al., *Massive repopulation of rat liver by transplantation of hepatocytes into specific lobes of the liver and ligation of portal vein branches to other lobes.* Transplantation, 1997. **64**(1): p. 8-13.
117. Guha, C., et al., *Normal hepatocytes correct serum bilirubin after repopulation of Gunn rat liver subjected to irradiation/partial resection.* Hepatology, 2002. **36**(2): p. 354-62.
118. Cubero, F.J., et al., *Hepatic proliferation in Gunn rats transplanted with hepatocytes: effect of retrorsine and tri-iodothyronine.* Cell Prolif, 2005. **38**(3): p. 137-46.
119. Muraca, M., et al., *Liver repopulation with bone marrow derived cells improves the metabolic disorder in the Gunn rat.* Gut, 2007. **56**(12): p. 1725-35.
120. Jorns, C., et al., *Hepatocyte transplantation for inherited metabolic diseases of the liver.* J Intern Med, 2012. **272**(3): p. 201-23.
121. Ichinohe, N., et al., *Growth ability and repopulation efficiency of transplanted hepatic stem cells, progenitor cells, and mature hepatocytes in retrorsine-treated rat livers.* Cell Transplant, 2012. **21**(1): p. 11-22.

122. Haridass, D., et al., *Repopulation efficiencies of adult hepatocytes, fetal liver progenitor cells, and embryonic stem cell-derived hepatic cells in albumin-promoter-enhancer urokinase-type plasminogen activator mice.* Am J Pathol, 2009. **175**(4): p. 1483-92.
123. Rezzani, R., *Exploring cyclosporine A-side effects and the protective role-played by antioxidants: the morphological and immunohistochemical studies.* Histol Histopathol, 2006. **21**(3): p. 301-16.
124. Calne, R., *Cyclosporine as a milestone in immunosuppression.* Transplant Proc, 2004. **36**(2 Suppl): p. 13S-15S.
125. Maerckx C., L.C., Tondreau T, Sokal E, *Pharmacokinetics, hepatic and renal tolerance of cyclosporine A in Wistar rats.* Submitted.
126. Cheng, K., et al., *Hepatic targeting and biodistribution of human fetal liver stem/progenitor cells and adult hepatocytes in mice.* Hepatology, 2009. **50**(4): p. 1194-203.
127. Gupta, S., et al., *111Indium labeling of hepatocytes for analysis of short-term biodistribution of transplanted cells.* Hepatology, 1994. **19**(3): p. 750-7.
128. Bohnen, N.I., et al., *Use of indium-111-labeled hepatocytes to determine the biodistribution of transplanted hepatocytes through portal vein infusion.* Clin Nucl Med, 2000. **25**(6): p. 447-50.
129. Holzman, M.D., et al., *Selective intraportal hepatocyte transplantation in analbuminemic and Gunn rats.* Transplantation, 1993. **55**(6): p. 1213-9.
130. Matas, A.J., et al., *Hepatocellular transplantation for metabolic deficiencies: decrease of plasms bilirubin in Gunn rats.* Science, 1976. **192**(4242): p. 892-4.
131. Michel, J.L., et al., *[Intrasplenic transplantation of hepatocytes in spf-ash mice with congenital ornithine transcarbamylase deficiency]*. Chirurgie, 1993. **119**(10): p. 666-71.
132. Kumaran, V., et al., *Transplantation of endothelial cells corrects the phenotype in hemophilia A mice.* J Thromb Haemost, 2005. **3**(9): p. 2022-31.
133. Biempica, L., et al., *Morphologic and chemical studies on a murine mutation (toxic milk mice) resulting in hepatic copper toxicosis.* Lab Invest, 1988. **59**(4): p. 500-8.
134. Yoshida, Y., et al., *Intrahepatic transplantation of normal hepatocytes prevents Wilson's disease in Long-Evans cinnamon rats.* Gastroenterology, 1996. **111**(6): p. 1654-60.
135. De Vree, J.M., et al., *Correction of liver disease by hepatocyte transplantation in a mouse model of progressive familial intrahepatic cholestasis.* Gastroenterology, 2000. **119**(6): p. 1720-30.
136. Nonome, K., et al., *Human umbilical cord blood-derived cells differentiate into hepatocyte-like cells in the Fas-mediated liver injury model.* Am J Physiol Gastrointest Liver Physiol, 2005. **289**(6): p. G1091-9.
137. Mignon, A., et al., *Selective repopulation of normal mouse liver by Fas/CD95-resistant hepatocytes.* Nat Med, 1998. **4**(10): p. 1185-8.
138. Newsome, P.N., et al., *Animal models of fulminant hepatic failure: a critical evaluation.* Liver Transpl, 2000. **6**(1): p. 21-31.
139. Cai, J., et al., *Directed differentiation of human embryonic stem cells into functional hepatic cells.* Hepatology, 2007. **45**(5): p. 1229-39.
140. Grompe, M., et al., *Loss of fumarylacetoacetate hydrolase is responsible for the neonatal hepatic dysfunction phenotype of lethal albino mice.* Genes Dev, 1993. **7**(12A): p. 2298-307.
141. Sandgren, E.P., et al., *Complete hepatic regeneration after somatic deletion of an albumin-plasminogen activator transgene.* Cell, 1991. **66**(2): p. 245-56.

142. Rhim, J.A., et al., *Complete reconstitution of mouse liver with xenogeneic hepatocytes.* Proc Natl Acad Sci U S A, 1995. **92**(11): p. 4942-6.
143. Akhurst, B., et al., *A modified choline-deficient, ethionine-supplemented diet protocol effectively induces oval cells in mouse liver.* Hepatology, 2001. **34**(3): p. 519-22.
144. Kofman, A.V., et al., *Dose- and time-dependent oval cell reaction in acetaminophen-induced murine liver injury.* Hepatology, 2005. **41**(6): p. 1252-61.
145. Dabeva, M.D. and D.A. Shafritz, *Activation, proliferation, and differentiation of progenitor cells into hepatocytes in the D-galactosamine model of liver regeneration.* Am J Pathol, 1993. **143**(6): p. 1606-20.
146. Vig, P., et al., *The sources of parenchymal regeneration after chronic hepatocellular liver injury in mice.* Hepatology, 2006. **43**(2): p. 316-24.
147. Sandbichler, P., et al., *Hepatocellular transplantation into the lung for temporary support of acute liver failure in the rat.* Gastroenterology, 1992. **102**(2): p. 605-9.
148. Kountouras, J., B.H. Billing, and P.J. Scheuer, *Prolonged bile duct obstruction: a new experimental model for cirrhosis in the rat.* Br J Exp Pathol, 1984. **65**(3): p. 305-11.
149. Petersen, B.E., V.F. Zajac, and G.K. Michalopoulos, *Hepatic oval cell activation in response to injury following chemically induced periportal or pericentral damage in rats.* Hepatology, 1998. **27**(4): p. 1030-8.
150. Oyagi, S., et al., *Therapeutic effect of transplanting HGF-treated bone marrow mesenchymal cells into CCl4-injured rats.* J Hepatol, 2006. **44**(4): p. 742-8.
151. Kobayashi, N., et al., *Hepatocyte transplantation in rats with decompensated cirrhosis.* Hepatology, 2000. **31**(4): p. 851-7.
152. Ishii, T., et al., *Transplantation of embryonic stem cell-derived endodermal cells into mice with induced lethal liver damage.* Stem Cells, 2007. **25**(12): p. 3252-60.
153. Zhang, Y., et al., *Development of an HSV-tk transgenic mouse model for study of liver damage.* FEBS J, 2005. **272**(9): p. 2207-15.
154. Ohbo, K., et al., *Modulation of hematopoiesis in mice with a truncated mutant of the interleukin-2 receptor gamma chain.* Blood, 1996. **87**(3): p. 956-67.
155. Shinkai, Y., et al., *RAG-2-deficient mice lack mature lymphocytes owing to inability to initiate V(D)J rearrangement.* Cell, 1992. **68**(5): p. 855-67.
156. Yahata, T., et al., *Functional human T lymphocyte development from cord blood CD34+ cells in nonobese diabetic/Shi-scid, IL-2 receptor gamma null mice.* J Immunol, 2002. **169**(1): p. 204-9.
157. Azuma, H., et al., *Robust expansion of human hepatocytes in Fah-/-/Rag2-/-/Il2rg-/- mice.* Nat Biotechnol, 2007. **25**(8): p. 903-10.
158. Muraca, M., et al., *Intraportal hepatocyte transplantation in the pig: hemodynamic and histopathological study.* Transplantation, 2002. **73**(6): p. 890-6.
159. Kocken, J.M., et al., *Correction of an inborn error of metabolism by intraportal hepatocyte transplantation in a dog model.* Transplantation, 1996. **62**(3): p. 358-64.
160. Attaran, M., et al., *Regional and transient ischemia/reperfusion injury in the liver improves therapeutic efficacy of allogeneic intraportal hepatocyte transplantation in low-density lipoprotein receptor deficient Watanabe rabbits.* J Hepatol, 2004. **41**(5): p. 837-44.
161. Wiederkehr, J.C., G.T. Kondos, and R. Pollak, *Hepatocyte transplantation for the low-density lipoprotein receptor-deficient state. A study in the Watanabe rabbit.* Transplantation, 1990. **50**(3): p. 466-71.
162. Wilson, J.M., et al., *Temporary amelioration of hyperlipidemia in low density lipoprotein receptor-deficient rabbits transplanted with genetically modified hepatocytes.* Proc Natl Acad Sci U S A, 1990. **87**(21): p. 8437-41.

163. Sancho-Bru, P., et al., *Stem and progenitor cells for liver repopulation: can we standardise the process from bench to bedside?* Gut, 2009. **58**(4): p. 594-603.
164. Knoepfler, P.S., *Deconstructing stem cell tumorigenicity: a roadmap to safe regenerative medicine.* Stem Cells, 2009. **27**(5): p. 1050-6.
165. Di Nicola, M., et al., *Human bone marrow stromal cells suppress T-lymphocyte proliferation induced by cellular or nonspecific mitogenic stimuli.* Blood, 2002. **99**(10): p. 3838-43.
166. Djouad, F., et al., *Immunosuppressive effect of mesenchymal stem cells favors tumor growth in allogeneic animals.* Blood, 2003. **102**(10): p. 3837-44.
167. Stephenne, X., et al., *Tissue factor-dependent procoagulant activity of isolated human hepatocytes: relevance to liver cell transplantation.* Liver Transpl, 2007. **13**(4): p. 599-606.
168. Stephenne, X., et al., *Bivalirudin in combination with heparin to control mesenchymal cell procoagulant activity.* PLoS One, 2012. **7**(8): p. e42819.

Summary:

In the last decade, stem cell therapy has raised much hope to treat patients presenting a variety of illnesses. Liver progenitor cells offer a promising alternative for the treatment of hepatic diseases. Despite the enthusiasm, cell efficiency need to be assessed on the route to clinic. This study is part of a larger medical translational research project that aims to treat inherited metabolic liver diseases with stem cell therapy.

In the present study we evaluate the presence of progenitor cells in healthy adult rat liver which would display the same advanced hepatogenic profile as that decribed in human adult liver derived progenitor cells (ADHLSC). We observed that rat progenitor cells homologous to ADHLSC cannot be easily obtained even when the same isolation and culture protocol was applied. However, we isolated a novel type of rat liver progenitor cell population: fibroblastic-like liver derived cells (rFLDC) which expressed hepatic and biliary markers.

Then we focused on the ability of transplanted ADHLSC to correct a UGT1A1 activity deficiency in the Gunn rat model homologous to the human hyperbilirubinemic Crigler-Najjar syndrome type I. We demonstrated that ADHLSCs were able to integrate into the Gunn rat liver parenchyma and these rats exhibit a metabolic effect 3 months post-transplantation and maintained over a 6 months period.

Finally, using ^{111}Indium-oxine labeled ADHLSC, we demonstrate the engraftment and the homing of cells preferentially within the liver parenchyma.

All together, these results make ADHLSC an attractive candidate for cell therapy treatment of Crigler-Najjar type I syndrome.

Résumé :

Ces dix dernières années, la thérapie cellulaire a suscité beaucoup d'espoirs pour le traitement de diverses maladies. Les cellules souches/progénitrices hépatiques offrent une alternative de choix pour le traitement de maladies hépatiques. Malgré cet enthousiasme, l'efficacité de ce traitement doit être prouvée avant son utilisation clinique. Cette étude fait partie d'un large projet de recherche médicale translationnel visant à traiter les maladies métaboliques hépatiques au moyen de cellules souches/progénitrices.

Dans cette étude, nous évaluons la présence, dans le foie de rats sains, de progéniteurs hépatiques possédant le même profil hépatogénique que celui décrit pour les cellules souches/progénitrices obtenues à partir de foie humain adulte (ADHLSC). Malgré l'utilisation du même protocole d'obtention pour les deux types cellulaires, de nombreuses différences existent. Les cellules obtenues chez le rat constituent une nouvelle population de progéniteurs hépatiques : fibroblastic-like liver derived cells (rFLDC) ; ces cellules se caractérisent notamment par l'expression de marqueurs hépatiques et biliaires.

La suite de ce travail a été axée sur la capacité des ADHLSC à corriger une déficience de l'activité de l'UGT1A1 dans le modèle du rat Gunn, modèle homologue au syndrome de Crigler-Najjar de type I décrit chez l'homme et conduisant à une hyper bilirubinémie.

Finalement, grâce à l'utilisation d'ADHLSC marquées à l'^{111}Indium-oxine, il a été démontré la capacité d'implantation et de cantonnement des cellules au parenchyme hépatique.

Ces résultats font des ADHLSC un candidat attrayant pour le traitement du syndrome de Crigler-Najjar de type I par la thérapie cellulaire.

Annexes

1. Optimization of the immunosuppression regimen

a. *Use of cyclosporine: Cyclosporine A disposition, hepatic and renal tolerance in Wistar rat.*

Cyclosporine A disposition, hepatic and renal tolerance in Wistar rat.

Running title: Guidelines for cyclosporine A use in rats

Authors: C. Maerckx*, C. Lombard*, T. Tondreau*, M. Najimi*, P. Wallemacq[+], E. Sokal*
*Université Catholique de Louvain, Institut de Recherche Clinique et Expérimentale (IREC), Laboratory of Pediatric Hepatology and Cell Therapy, Brussels 1200, Belgium
[+]Université Catholique de Louvain, Louvain Centre for Toxicology and Applied Pharmacology, Brussels 1200, Belgium

Key Words: cyclosporine A, hepatic and renal enzymes, intraperitoneal and per os administration, kinetic, Wistar rat

To whom correspondence should be addressed:

Etienne Sokal MD. PhD

Laboratory of Pediatric Hepatology and Cell Therapy

Avenue Hippocrate 10/11

1200, Brussels

Belgium

E-mail: etienne.sokal@uclouvain.be

This work was financially supported by Fonds pour la formation à la recherche dans l'industrie et dans l'agriculture (FRIA)

Abstract

Cyclosporine A, a potent calcineurin inhibitor, has been widely used in organ transplantation and in the treatment of autoimmune diseases. It has however been shown to induce serious renal and hepatic side effects. The drug is also used in preclinical studies, but with little published information on the optimal dose and route of administration in rodents.

Objectives of this study were to identify efficient and safe doses of cyclosporine A in rodent and to assess its effects on hepatic and renal functions. For this purpose, we tested the effects of different doses and administration routes of cyclosporine A (5, 2.5 and 1 mg/kg) administered during 28 days intraperitoneally, or by gastric feeding on Wistar rats.

Our data indicate that rats injected intraperitoneally with 5 mg/kg/2d exhibited trough cyclosporine A levels within known therapeutic range in human, but were subject to blood cyclosporine A accumulation, whereas the 5 mg/kg/d gavage resulted in only a mild cyclosporine A accumulation over time. In both cases this accumulation was not deleterious to renal and hepatic functions, as shown by transaminase, urea, creatinine and bilirubin measurements.

Introduction

Advances in immunosuppression therapy have led to successful transplantation of allogeneic tissues and organs, and have improved the management of autoimmune disorders (Calne et al., 1979). In preclinical setting, immunosuppression has allowed the development of various animal graft models, including xenogeneic transplantation of human cells for safety and efficacy studies.

Since its discovery in 1976 by Borel and colleagues, cyclosporine A (CsA), a potent immunosuppressive cyclic peptide, has been commonly used in transplantation. CsA binds to the cytosolic protein cyclophilin of immunocompetent lymphocytes (Borel et al., 1976). The resulting drug-receptor complex in turn inhibits calcineurin, which, under normal circumstances, is responsible for inducing the transcription of interleukin 2 and the subsequent activation of T cells (Hamawy et al., 2003). In addition to inhibiting immune reactions *in vitro*, CsA has been shown to prolong skin graft survival in a rat model. Similarly, a two-week CsA-treatment of rats with heart allografts was shown to result in subsequent prolonged graft acceptance without the need for any further drug treatment (White et al., 1980).

Despite its therapeutic benefits, the use of CsA has been somewhat limited by its adverse effects. Indeed, CsA has been shown to result in nephrotoxicity due to overproduction of ROS and lipid peroxidation (Rezzani, 2006). In addition, CsA treatment has been associated with hepatotoxicity characterized by cholestasis, hyperbilirubinemia, increased alkaline phosphatase, elevated transaminases in the blood, inhibition of protein synthesis and disturbed lipid secretion in both humans and experimental animals (Calne, 2004; Rezzani, 2006).

In rat, the CsA doses used for maintenance immunosuppressive therapy differ in various studies, ranging from 50 mg/kg/d to 0.625 mg/kg/d. In addition, several routes of administration are described, making more difficult any comparison in terms of efficacy and

safety (Chen et al.,2010; Fiedel et al, 2009; Gao et al., 2005; Rijkelijkhuizen et al., 2010; Sun et al, 2009; Unadkat et al., 2009; Wee et al., 2010; Yang et al, 2003; Zijlstra et al., 2009).

We therefore attempted to determine, in rats, the optimal dosage regimen. We compared two administration routes (intraperitoneal and per os) and 3 different doses. The rats were followed for 28 days. CsA elimination, long-term accumulation, and associated hepatic and renal side effects were assessed.

Materials and methods

Animals: Wild type Wistar rats aged from 8 to 12 weeks were purchased from UCL *Animalerie Centrale* (Brussels, Belgium) and treated in accordance to internal Animal Ethic and Welfare Committees (UCL/MD/2009/003). Rats were anesthetized for blood sampling.

Cyclosporine A solution and administration: CsA (5 mg/ml) (Sandimmun, Novartis, Vilvoorde, Belgium) was diluted 1:10 (5 mg/kg), 1:20 (2.5 mg/kg) and 1:50 (1 mg/kg) with sterile sodium chloride 0,9% (Braun, Diegem, Belgium). Three groups of 3 rats were injected intraperitoneally every two days with 5 mg/kg, 2.5 mg/kg and 1 mg/kg CsA.

CsA oral solution (100 mg/mL) (Neoral, Novartis) was diluted 1:100 (5 mg/kg) and 1:200 (2.5 mg/kg) with sterile water. Two groups of 5 rats were given daily 5 mg/kg or 2.5 mg/kg CsA by gastric feeding.

Five naïve rats were used as negative control.

Cyclosporine A quantification: CsA concentration was measured in 600 µL of whole blood collected on EDTA monovette (Sarstedt, Essen, Belgium) through the retro orbital plexus. Measurements were obtained on a Dimension Xpand (Siemens, Brussels, Belgium) using Flex reagent cartridges (Siemens) according to the manufacturer's instructions. In order to determine its elimination profile, CsA blood concentrations were determined 0, 2, 4, 6, 8, 24 and 48 h, and 0, 2, 5 and 24h following intraperitoneal and oral administration, respectively.

CsA blood levels were again determined after 8 days (192 h) and after 28 days (672 h) to detect CsA accumulation.

Renal and hepatic function: After 28 days of CsA administration 900 µL blood samples were collected on lithium heparin monovette (Sarstedt) and centrifuged at 340 g during 5 minutes at 4°C in order to obtain plasma for the liver enzymes aspartate aminotransferase, alanine aminotransferase and gamma-glutamyl transpeptidase. Measurements were performed using an automate Unicel DxC800 (Beckman Coulter, Villepinte, France) according to the manufacturer's instructions.

Statistical analysis: Kruskall-Wallis analyses were performed with the GraphPad Prism software program (San Diego, California, USA). Statistical analyses are detailed on Annexe 2.

Results

Cyclosporine A profiles

Both intraperitoneal and oral administration of CsA resulted in substantial systemic blood levels (Figure 1).

Intraperitoneal injection of 5 mg/kg CsA (figure 1A) resulted to a rapid increase of its blood levels, with a peak appearing two hours after injection (3805 ± 439 ng/mL; n=3) and a progressive decrease characterized by a concentration of 1059 ± 162 ng/mL 24 hours later. Lower profiles were observed after 1 and 2.5 mg/kg ip injection: 325 ± 33 and 702 ± 66 ng/mL at 2 hours, and 95 ± 2 and 117 ± 12 ng/mL at 24 hours, respectively.

Forty-eight hours post ip injection, CsA was almost entirely cleared in rats injected with 1 and 2.5 mg/kg, while the third group still showed moderate CsA blood levels (493 ± 74 ng/mL).

In contrast to intraperitoneal injection, oro gastric tube administration led to lower CsA blood levels (Figure 1B); CsA reached a 2 hours peak in both groups (282 ± 124 and 995 ± 249 ng/mL for rats given orally 2.5 and 5 mg/kg of CsA, respectively). At 24 hours, CsA was

totally cleared in the 2.5 mg/kg group (46 ± 8 ng/mL) whereas the 5 mg/kg group showed low but still detectable CsA blood levels (137 ± 19 ng/mL).

Cyclosporine A accumulation

In order to evaluate the potential CsA accumulation, rats were treated with CsA intraperitoneally or orally (gastric tube) and CsA blood levels were quantified after 8 and 28 days of treatment, as shown in figure 1C.

After 8 days, rats injected with 5 mg/kg of CsA intraperitoneally showed a peak reaching 2735 ± 332 ng/mL two hours after the last injection. CsA was partially cleared 48 hours after the injection (517 ± 4 ng/mL). After 28 days, rats exhibited a higher CsA trough level (1920 ± 331 ng/mL) and the peak reached 5568 ± 220 ng/mL, as shown in figure 1C.

In contrast, after 8 days, oral fed rats only exhibited moderate CsA trough levels (73 and 286 ng/mL for the 2.5 and 5 mg/kg group, respectively.) No difference in CsA trough levels was observed between the 8^{th} day and the 28^{th} day of treatment.

Renal and hepatic function

At the end of the experiment, renal and hepatic function was evaluated, for each group (table 1).

No significant difference ($p > 0.05$) in urea and creatinine levels was found between controls (38 ± 5.77 – 0.245 ± 0.021; n=5), 2.5 mg/kg/d PO (35.8 ± 1.92 – 0.34 ± 0.06; n=5), 5mg/kg/d PO (48.75±2.87 – 0.423±0.055; n=5) and 5mg/kg/2d IP(46.5±4.98 – 0.44±0.082 n=3), as shown in table 1A.

Similarly, no significant difference ($p > 0.05$) was found in aspartate aminotransferase level (between 67.4 and 104 IU/mL), alanine aminotransferase (between 37.8 and 45.4 IU/mL) and gamma glutamyl transpeptidase (between 2 and 3.2 IU/mL), (table 1B). Rats injected with 5 mg/kg/2d intraperitoneally exhibited higher bilirubin levels (0.355±0.05) than the other groups but this difference was not statistically significant ($p > 0.05$).

Discussion

Research teams have used a broad range of CsA doses and routes of administration to avoid graft rejection in preclinical studies, with various degrees of success. Chen et al. used a 50 mg/kg/d PO in the context of renal allograft and reported no obvious sign of toxicity (Chen et al., 2010). Wee et al. injected 5 mg/kg/d and 15 mg/kg/d in rats transplanted with allograft of porcine pancreatic islets (Wee et al., 2010). None of these doses seemed to induce side effects, but only the 15 mg/kg/d treatment effectively allowed graft survival. Rijkelijkhuizen et al injected 15 or 25 mg/kg 3 times a week in a porcine islet transplantation model in the rat (Rijkelijkhuizen et al, 2010). In this case, rats subjected to injections of 25 mg/kg died after 11 weeks for CsA toxicity. Fiedel was reported heart allograft rejection after 24 days in rats injected with 0.625 mg/kg/d (Fiedel et al, 2009). Similarly, Zijlstra demonstrated lung rejection in rats treated with CsA inhalation for 8 days (Zijlstra, 2009).

In such variable practice, it seemed relevant to determine the drug disposition profile of CsA, compatible with pre-clinical studies and tolerance in animals. In previous experiments, we observed that intraperitoneal treatment of rats with 10 mg/kg of CsA every other day resulted in renal damage, as indicated by the presence of hematuria (unpublished observation). Therefore, in this work, we treated rats with 5 mg/kg, 2.5 mg/kg, and 1 mg/kg of CsA and compared two administration routes: oro gastric tube feeding and intraperitoneal injection.

Rats orally fed with 2.5 mg/kg/d exhibited a moderate CsA peak 2 hours after treatment with complete clearance in less than 24 hours. This dose was thus deemed inappropriate as it could lead to infra therapeutic levels in transplantation. In contrast, rats orally fed with 5 mg/kg/d showed a higher CsA peak and an acceptable trough level. The CsA blood levels never dropped below 100 ng/mL, which is considered as the cutoff for appropriate immunosuppression in human transplantation (Miller, 1996). Finally, we found that under these treatment conditions, rats presented a low CsA accumulation over time.

Similarly, rats injected with low CsA doses (1 and 2.5 mg/kg/2d) completely cleared cyclosporine A within 48 hours. These doses may therefore not appear suitable for appropriate immunosuppression.

Rats injected with 5 mg/kg/2d exhibited trough CsA levels within therapeutic range, but were subject to blood CsA accumulation. However, this accumulation was not deleterious to renal and hepatic functions, as shown by transaminase, urea, creatinine and bilirubin measurements.

In conclusion, in Wistar rats, we recommend a daily gavage with 5 mg/kg of CsA or an intraperitoneal injection of 5 mg/kg/2d CsA in order to maintain therapeutic immunosuppression. A regular monitoring of blood CsA, hepatic and renal function tests are recommended in order to assess CsA accumulation and adapt the dose accordingly.

References

Borel, J. F., C. Feurer, H. U. Gubler, and H. Stahelin. 1976. Biological effects of cyclosporin A: a new antilymphocytic agent. Agents and actions 6: 468-475.

Calne, R. 2004. Cyclosporine as a milestone in immunosuppression. Transplantation proceedings 36: 13S-15S.

Calne, R. Y. et al. 1979. Cyclosporin A initially as the only immunosuppressant in 34 recipients of cadaveric organs: 32 kidneys, 2 pancreases, and 2 livers. Lancet 2: 1033-1036.

Calne, R. Y., D. J. White, K. Rolles, D. P. Smith, and B. M. Herbertson. 1978. Prolonged survival of pig orthotopic heart grafts treated with cyclosporin A. Lancet 1: 1183-1185.

Chen, B. et al. 2010. The changes of aquaporin 2 in the graft of acute rejection rat renal transplantation model. Transplantation proceedings 42: 1884-1887.

Fiedel, S. et al. 2009. The influence of antigen-dependent and antigen-independent factors on the development of graft vasculopathy in a fully allogeneic cardiac allograft model in the rat. Transplantation proceedings 41: 2625-2627.

Gao, L. H. et al. 2005. A rat model of chronic allograft liver rejection. Transplantation proceedings 37: 2327-2332.

Hamawy, M. M. 2003. Molecular actions of calcineurin inhibitors. Drug news & perspectives 16: 277-282.

Miller, L. W. 1996. Cyclosporine-associated neurotoxicity. The need for a better guide for immunosuppressive therapy. Circulation 94: 1209-1211.

Rezzani, R. 2006. Exploring cyclosporine A-side effects and the protective role-played by antioxidants: the morphological and immunohistochemical studies. Histology and histopathology 21: 301-316.

Rijkelijkhuizen, J. K., A. Tons, O. T. Terpstra, and E. Bouwman. 2010. Transplantation of long-term cultured porcine islets in the rat: prolonged graft survival and recipient growth on reduced immunosuppression. Cell transplantation 19: 387-398.

Sun, Z. et al. 2009. Recruitment of host progenitor cells in rat liver transplants. Hepatology 49: 587-597.

Unadkat, J. V. et al. 2009. Investigation of antibody-mediated rejection in composite tissue allotransplantation in a rat limb transplant model. Transplantation proceedings 41: 542-545.

Wee, Y. M. et al. 2010. The synergistic effect of Tautomycetin on Cyclosporine A-mediated immunosuppression in a rodent islet allograft model. Mol Med 16: 298-306.

White, D. J., K. Rolles, T. Ottawa, and O. Turell. 1980. Cyclosporin-A-induced long-term survival of fully incompatible skin and heart grafts in rats. Transplantation proceedings 12: 261-265.

Yang, Y. L., J. P. Li, K. F. Dou, and K. Z. Li. 2003. Influence of liver nonparenchymal cell infusion combined with cyclosporin A on rejection of rat small bowel transplantation. World journal of gastroenterology : WJG 9: 2859-2862.

Zijlstra, G. S. et al. 2009. Efficacy of a new pulmonary cyclosporine a powder formulation for prevention of transplant rejection in rats. The Journal of heart and lung transplantation : the official publication of the International Society for Heart Transplantation 28: 486-492.

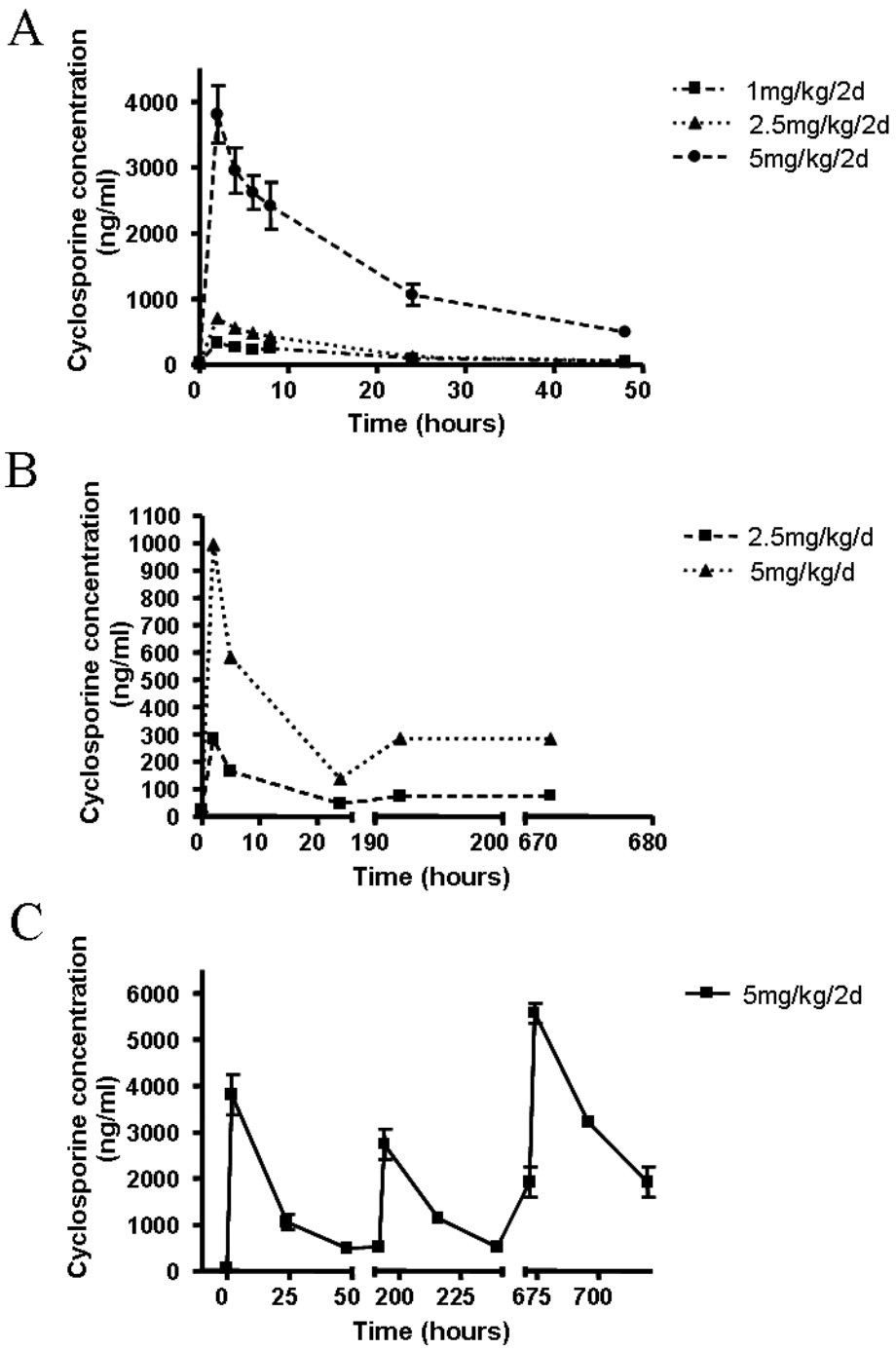

Figure 1 Cyclosporine A concentration (ng/ml) kinetics.
A: 48h Cyclosporine A concentration kinetics in rats injected intraperitoneally with 1mg/kg/2d (squares), 2.5mg/kg/2d (triangles), or 5mg/kg/2d (circles) cyclosporine A. n=3 for each dose
B: Cyclosporine A concentration kinetics and accumulation measure in rats gavaged with 2.5mg/kg/d (squares) and 5 mg/kg/d (triangles) cyclosporine A. n=5 for each dose
C: Cyclosporine A kinetic in rats injected intraperitoneally with 5mg/kg/2d cyclosporine A after 48 hours, 8 days (192h) and 28 days (672h). n=3
Data are expressed as means, error bars = standard deviation.

A

	2.5mg/kg/d PO	5mg/kg/d PO	5mg/kg/2d IP	Negative control
Urea	35.8 ± 1.9 mg/dl	48.75 ± 2.9 mg/dl	46.5± 5 mg/dl	38 ±0.6 mg/dl
Creatinine	0.345 ± 0.059 mg/dl	0.423 ± 0.55 mg/dl	0.44 ± 0.082 mg/dl	0.245 ± 0.021 mg/dl
Total bilirubine	0.172 ±0.048 mg/dl	0.208 ± 0.069 mg/dl	0.355 ± 0.046 mg/dl	0.280 ± 0.012 mg/dl
Direct bilirubin	0.063 ± 0.025 mg/dl	0.074 ± 0.021 mg/dl	0.075 ± 0.023 mg/dl	0.055 ± 0.01 mg/dl

B

	2.5mg/kg/d PO	5mg/kg/d PO	5mg/kg/2d IP	Negative control
Aspartate transaminase	67.4 ± 5.8 IU/l	67.8 ± 12.3 IU/l	82 ±16.7 IU/l	104 ± 30 IU/l
Alanine transaminase	37.8 ± 4.1 IU/l	45.4 ± 8.4 IU/l	43 ± 4.6 IU/l	40.5 ± 4.5 IU/l
Gamma-glutamyl transferase	3 ± 0.7 IU/l	3.2 ± 1.1 IU/l	2 ± 1.2 IU/l	2.5 ± 2.1 IU/l

Table 1: blood measurement of renal and hepatic parameters in control and in cyclosporine A-treated rats.
A: evaluation of renal (urea, creatinine) and hepatic (total and direct bilirubin) parameters in rats treated with 2.5mg/kg/d per os (PO) (n=5), 5mg/kg/d per os (n=5), 5mg/kg/2d intraperitonealy (IP) (n=3) cyclosporine A or negative control (n=5).
B: evaluation of hepatic enzymes (aspartate transaminase, alanine transaminase and gamma-glutamyl transferase) in rats treated with 2.5mg/kg/d per os (n=5), 5mg/kg/d per os (n=5), 5mg/kg/2d intraperitonealy (n=3) cyclosporine A or negative control (n=5).
Data are expressed as mean ± standard deviation.

b. Use of clodronate

Clodronate is a biphosphonate molecule used as anti-osteoporotic drug. In the context of immunosuppression, chlodronate is encapsulated into liposomes because free clodronate will not easily pass phospholipid bilayers of cell membranes. The clodronate liposome complexe will come into contact with macrophages and other phagocytic cells. The phagocyte immediately recognizes liposomes as foreign particles and proceeds with destroying it. The first step in this destruction is phagocytosis in which the liposomes are engulfed by the cell into

phagosome. Lysosomes, which contain phospholipases, fuse with the phagosome forming a phagolysosome. The lysosomal membrane also contains proton pumps which will lower the internal pH of the phagolysosome. The low pH, phospholipases and other macromolecular interactions all contribute to compromising the liposomal membrane thus releasing the encapsulated clodronate. The low internal pH of the phagolysosome may contribute to the ability of the clodronate to cross the phagolysosomal membrane into the macrophage's cytosol.

Once in the cytosolic medium, clodronate is mistakenly recognized as cellular pyrophosphate and used by several Class II aminoacyl-tRNA synthetases to produce a non-hydrolyzable ATP analog, adenosine 5'-(*β, γ*-dichloromethylene) triphosphate ($AppCCl_2p$) [1-3]. The exact mechanism by which $AppCCl_2p$ causes cell death was described by Lehenkari et *al*. Basically, their hypothesis involves cytosolic $AppCCl_2p$ crossing the mitochondrial outer membrane and irreversibly binding to the ATP/ADP translocase which transverses the mitochondrial inner membrane. Inhibiting this enzyme initiates pore openings in the mitochondrial inner membrane. Loss of mitochondrial inner membrane integrity, in turn, results in depolarization and allows molecular signals to be released from the mitochondria which initiate cell death via apoptosis [4].

We evaluated the combination of cyclosporine and clodronate on the efficiency of immunosuppression. To do so, different doses of clodronate (4 and 40 mg/kg) were concomitantly used in association with 5mg/kg cyclosporine. The cocktail was intramuscularly injected in rats in addition with five millions human hepatocytes. The cells were suspended with PBS or with the infusion solution (used in the clinic and containing human albumin). In order to precisely localize

the injection site after sacrifice, blue Evans colorant was added to the injection solution. Rats were sacrificed 24h post-injection and immunohistochemistry against rodent macrophage markers (CD68 positive cells) and human HLA-ABC was performed on the injection site. To determine the optimal clodronate dose we generated 6 conditions. One rat was allocated to every condition (Table 8).

Rat identification	Cyclosporine	Clodronate	Evans blue 1%	Injected cells	Vehicle solution
1	J-3, J-1	No	Yes	**0 (negative control)**	PBS
2	**No**	No	Yes	5 millions (rejection positive control)	PBS
3	J-3, J-1	No	Yes	5 millions	**PBS**
4	J-3, J-1	**4mg/kg**	Yes	5 millions	PBS
5	J-3, J-1	**40mg/kg**	Yes	5 millions	PBS
6	J-3, J-1	No	Yes	5 millions	**Injection solution**

Table 8: summary of experimental conditions to determine the optimal clodronate dose for effective immunosuppression in Gunn rats.

As illustrated in Figure 7D, Figure 8 A and C, Figure 9 A and C, human HLA-ABC positive cells were detected 24h post-injection in 5 millions hepatocytes injected rats. Both rats injected with 5 millions human hepatocytes suspended in PBS or injection solution (containing human albumin) exhibited CD68 positive cells infiltrate (Figure 8 B and D). As illustrated in figure 10 D absence of macrophagic infiltrates was obtained with a 40mg/kg clodronate injection in association with 5mg/kg cyclosporine whereas rat injected with cells and 4mg/kg clodronate reveal macrophagic infiltrates (Figure 9 B)

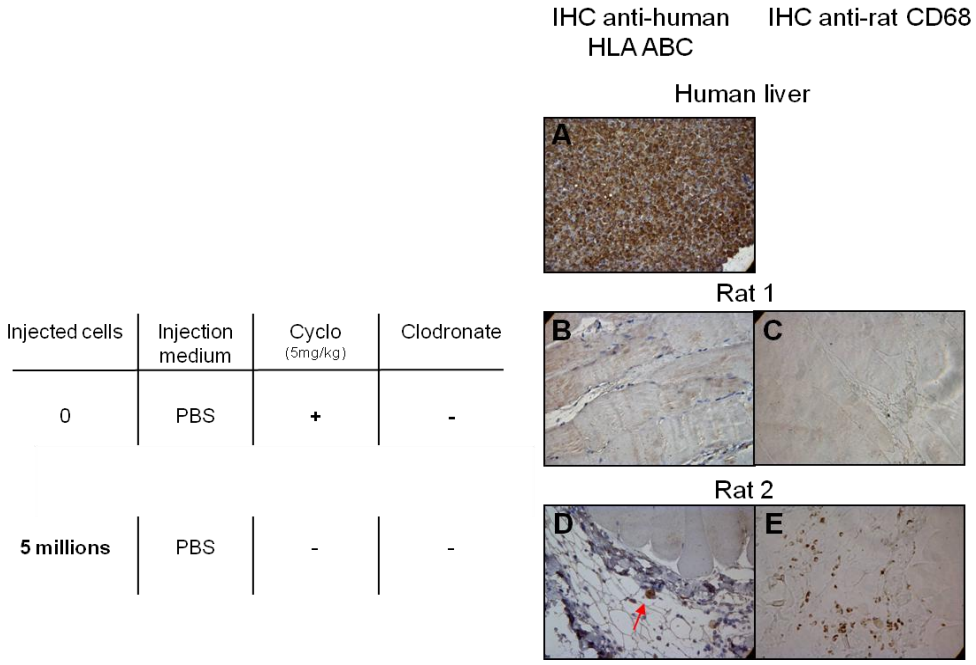

Injected cells	Injection medium	Cyclo (5mg/kg)	Clodronate
0	PBS	+	-
5 millions	PBS	-	-

Figure 7: Immunohistochemistry against human HLA-ABC and rat CD68 proteins (controls)

Immunohistochemistry against human HLA-ABC (pictures A, B, D) and rat CD68 (C, E) proteins on serial liver slices. Human liver (A) was used as positive control for HLA-ABC. Rat 1 negative control (pictures B and C) rat injected with PBS. Rat 2 positive CD68 control (pictures D and E). hHLA-ABC positive cells are indicated by arrow. Immunostaining were analyzed by light microscopy. Immunoreactivity was visualized using horseradish peroxydase solution. Magnification: x400

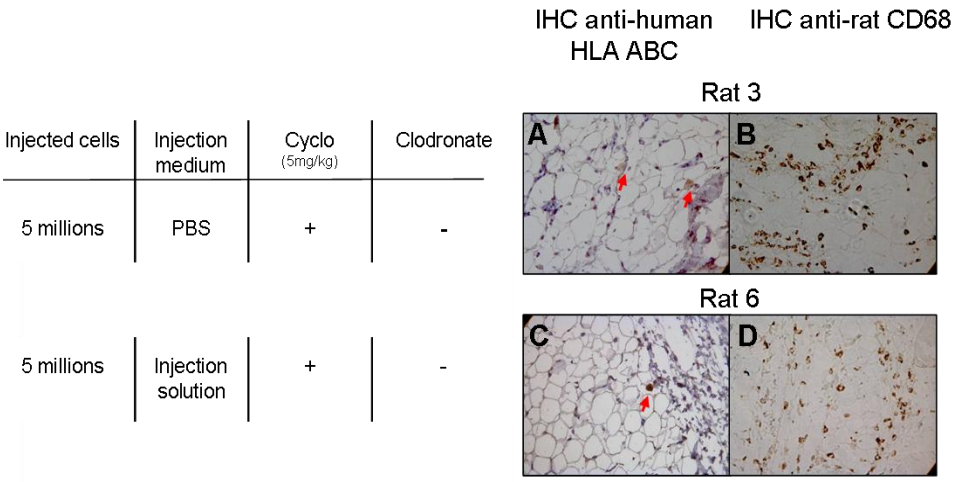

Injected cells	Injection medium	Cyclo (5mg/kg)	Clodronate
5 millions	PBS	+	-
5 millions	Injection solution	+	-

Figure 8: Immunohistochemistry against human HLA-ABC and rat CD68 proteins (injection medium influence)

Immunohistochemistry against human HLA-ABC (pictures A, C) and rat CD68 (B, D) proteins on serial liver slices in wistar rats injected with human hepatocytes. Rat 3 (pictures A and B) rat injected cyclosporine at D-3 and D-1 and with 5 millions hepatocytes suspended in PBS. Rat 6 (pictures C and D) rat injected cyclosporine at D-3 and D-1 and with 5 millions hepatocytes suspended in infusion solution. hHLA-ABC positive cells are indicated by arrow. Immunostaining were analyzed by light microscopy. Immunoreactivity was visualized using horseradish peroxydase solution. Magnification: x400

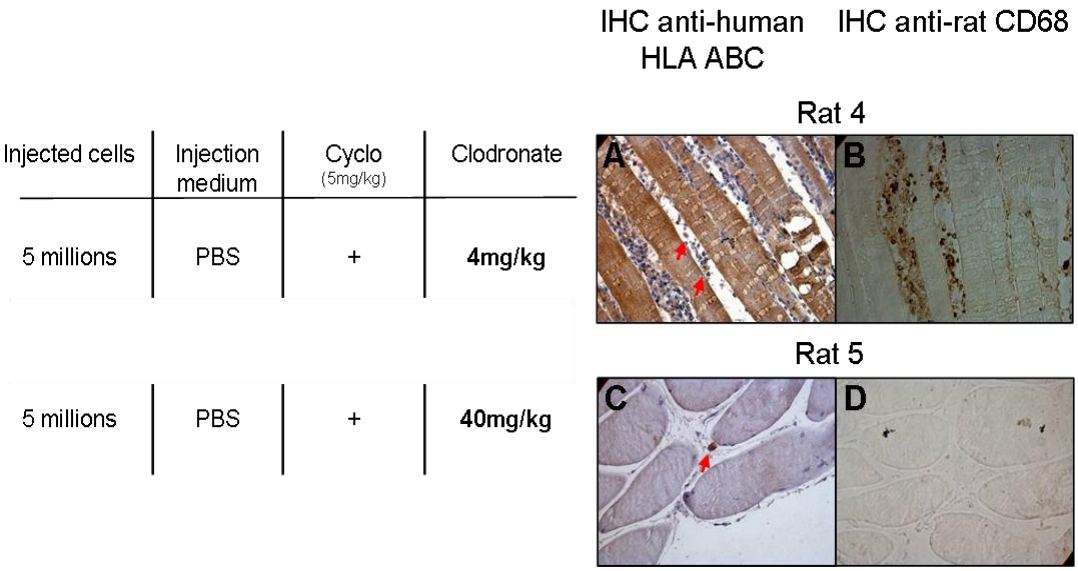

Figure 9: Immunohistochemistry against human HLA-ABC and rat CD68 proteins (clodronate concentration influence)
Immunohistochemistry against human HLA-ABC (pictures A, C) and rat CD68 (B, D) proteins on serial liver slices in wistar rats injected with human hepatocytes. Rat 4 (pictures A and B) rat injected cyclosporine at D-3 and D-1, chlodronate 4 mg/kg at D-1 and with 5 millions hepatocytes suspended in PBS. Rat 5 (pictures C and D) rat injected cyclosporine at D-3 and D-1, chlodronate 40 mg/kg at D-1 and with 5 millions hepatocytes suspended in PBS. hHLA-ABC positive cells are indicated by arrow. Immunostaining were analyzed by light microscopy. Immunoreactivity was visualized using horseradish peroxydase solution. Magnification: x400

Injection medium (PBS or injection solution) in rats injected at D-3 and D-1 with 5mg/kg cyclosporine seems not have an influence on macrophagic infiltrates. On the other hand absence of macrophagic (CD68+) infiltrates was obtained with a 40mg/kg clodronate injection in association with 5mg/kg cyclosporine prior to cell injection.

In order to support these conclusions, experiments will be repeated and CD68 infiltrates must be quantified.

References

1. Rogers, M.J., et al., *Metabolism of halogenated bisphosphonates by the cellular slime mould Dictyostelium discoideum.* Biochem Biophys Res Commun, 1992. **189**(1): p. 414-23.
2. Rogers, M.J., et al., *Inhibitory effects of bisphosphonates on growth of amoebae of the cellular slime mold Dictyostelium discoideum.* J Bone Miner Res, 1994. **9**(7): p. 1029-39.
3. Frith, J.C., et al., *Clodronate and liposome-encapsulated clodronate are metabolized to a toxic ATP analog, adenosine 5'-(beta, gamma-dichloromethylene) triphosphate, by mammalian cells in vitro.* J Bone Miner Res, 1997. **12**(9): p. 1358-67.
4. Lehenkari, P.P., et al., *Further insight into mechanism of action of clodronate: inhibition of mitochondrial ADP/ATP translocase by a nonhydrolyzable, adenine-containing metabolite.* Mol Pharmacol, 2002. **61**(5): p. 1255-62.

2. Statistical analysis (row data)

a. *Human Liver stem/progenitor cells decrease serum bilirubin in hyperbilirubinemic Gunn rat*

The aim of this study was to demosntarte that human adult-derived liver progenitor cells (ADHLSC) transplantation can reverse hyperbilirubinemic symptoms in a relevant animal model of Crigler-Najjar disease. Unconjugated bilirubin decrease effect from injected ADHLSC rats was compared to transplanted human hepatocytes rats and negative controls (rats injected with PBS and 4%NAC).

We assume that all results follow a normal distribution. This hypothesis must further be confirmed increasing the number of rats in each experimental group.

i. Evolution of bilirubin concentration with time: comparison of bilirubin levels 2 weeks and 27 weeks after cell injection.

1. Mann-Whitney test (non parametric test).

- Human adult-derived liver progenitor cells (ADHLSC) transplanted rats:

Table Analyzed	ADHLSC
Column A	2
vs	vs
Column D	27
Mann Whitney test	
P value	0.0286
Exact or approximate P value?	Exact
P value summary	*
Are medians signif. different? (P < 0.05)	Yes
One- or two-tailed P value?	Two-tailed
Sum of ranks in column A,D	26 , 10
Mann-Whitney U	0.0000

Unconjugated bilirubin (UCB) concentration exhibits a significant decrease 27 weeks after ADHLSC transplantation in comparison with UCB level after 2 weeks (p-val<0.05).

- Human hepatocytes transplanted rats:

Table Analyzed	hHep
Column A	2
vs	vs
Column D	27
Mann Whitney test	
P value	0.1000
Exact or approximate P value?	Exact
P value summary	ns
Are medians signif. different? (P < 0.05)	No
One- or two-tailed P value?	Two-tailed
Sum of ranks in column A,D	15 , 6
Mann-Whitney U	0.0000

Unconjugated bilirubin (UCB) concentration does not exhibit a significant decrease 27 weeks after human hepatocytes transplantation in comparison with UCB level after 2 weeks (p-val>0.05). The obtained p-value lets supposed that increasing the rat involved in this assay we can demonstrate a significant effect.

- Negative controls

Table Analyzed	SHAM
Column A	2
vs	vs
Column D	27
Mann Whitney test	
P value	0.7000
Exact or approximate P value?	Exact
P value summary	ns
Are medians signif. different? (P < 0.05)	No
One- or two-tailed P value?	Two-tailed
Sum of ranks in column A,D	12 , 9
Mann-Whitney U	3.000

Negative controls (rats injected with PBS, 4% NAC) do not exhibit a significant decrease in UCB concentration after 27 weeks (p-val>0.05)

2. Human paired student's t-test (parametric test).

We assume that all results follow a normal distribution. This hypothesis must further be confirmed increasing the number of rats in each experimental group.

Comparison of bilirubin levels 2 weeks and 27 weeks after cell injection.

- Human adult-derived liver progenitor cells (ADHLSC) transplanted rats:

Table Analyzed	ADHLSC
Column A	2
vs	vs
Column D	27
Paired t test	
P value	0.0030
P value summary	**
Are means signif. different? (P < 0.05)	Yes
One- or two-tailed P value?	Two-tailed
t, df	t=8.844 df=3
Number of pairs	4
How big is the difference?	
Mean of differences	3.248
95% confidence interval	2.079 to 4.416
R squared	0.9631

Unconjugated bilirubin (UCB) concentration exhibits a significant decrease 27 weeks after ADHLSC transplantation in comparison with UCB level after 2 weeks (p-val<0.05).

-

Human hepatocytes transplanted rats:

Table Analyzed	hHep
Column A	2
vs	vs
Column D	27
Paired t test	
P value	0.0658
P value summary	ns
Are means signif. different? (P < 0.05)	No
One- or two-tailed P value?	Two-tailed
t, df	t=3.705 df=2
Number of pairs	3
How big is the difference?	
Mean of differences	3.027
95% confidence interval	-0.4887 to 6.542
R squared	0.8728

Unconjugated bilirubin (UCB) concentration does not exhibit a significant decrease 27 weeks after human hepatocytes transplantation in comparison with UCB level after 2 weeks (p-val>0.05). The obtained p-value lets supposed that increasing the rat involved in this assay we can demonstrate a significant effect.

- Negative controls

Table Analyzed	SHAM
Column A	2
vs	vs
Column D	27
Paired t test	
P value	0.2139
P value summary	ns
Are means signif. different? (P < 0.05)	No
One- or two-tailed P value?	Two-tailed
t, df	t=1.799 df=2
Number of pairs	3
How big is the difference?	
Mean of differences	0.5067
95% confidence interval	-0.7054 to 1.719
R squared	0.6180

Negative controls (rats injected with PBS, 4% NAC) do not exhibit a significant decrease in UCB concentration after 27 weeks (p-val>0.05).

ii. Evolution of bilirubin concentration with time; comparison between treatment groups with repeated measures: 2 way ANOVA

Table Analyzed	Copy of Recap			
Two-way RM ANOVA	Matching by cols			
Source of Variation	% of total variation	P value		
Interaction	14.09	0.0205		
Time	36.11	P<0.0001		
Treatment	21.01	0.0155		
Subjects (matching)	9.1661	0.1385		
Source of Variation	P value summary	Significant?		
Interaction	*	Yes		
Time	***	Yes		
Treatment	*	Yes		
Subjects (matching)	ns	No		
Source of Variation	Df	Sum-of-squares	Mean square	F
Interaction	6	11.47	1.912	3.243
Time	3	29.40	9.801	16.62
Treatment	2	17.11	8.553	8.021
Subjects (matching)	7	7.464	1.066	1.808
Residual	21	12.38	0.5896	
Number of missing values	0			
Bonferroni posttests				
Negative controls vs ADHLSC				
Treatment	Negative controls	ADHLSC	Difference	95% CI of diff.
2.000	6.583	6.445	-0.1383	-2.040 to 1.763
4.000	6.470	6.303	-0.1675	-2.069 to 1.734
13.00	6.980	4.680	-2.300	-4.201 to -0.3988
27.00	6.077	3.198	-2.879	-4.780 to -0.9780
Treatment	Difference	t	P value	Summary
2.000	-0.1383	0.2151	P > 0.05	ns
4.000	-0.1675	0.2605	P > 0.05	ns
13.00	-2.300	3.577	P<0.01	**
27.00	-2.879	4.478	P<0.001	***
Negative controls vs hHepatocyte				
Treatment	Negative controls	hHepatocyte	Difference	95% CI of diff.
2.000	6.583	6.263	-0.3200	-2.352 to 1.712
4.000	6.470	5.567	-0.9033	-2.936 to 1.129
13.00	6.980	5.077	-1.903	-3.936 to 0.1291
27.00	6.077	3.237	-2.840	-4.872 to -0.8076
Treatment	Difference	t	P value	Summary
2.000	-0.3200	0.4655	P > 0.05	ns
4.000	-0.9033	1.314	P > 0.05	ns
13.00	-1.903	2.769	P < 0.05	*
27.00	-2.840	4.132	P<0.01	**

Source of Variation	DF	Sum of Squares	Mean Square
Interaction	6.0	11.47	1.912
Time	3.0	29.40	9.801
Treatment	2.0	17.11	8.553
Subjects (matching)	7.0	7.464	1.066
Residual (Error)	21.0	12.38	0.5896
Total	39.0	81.43	

Does Time have the same effect at all values of Treatment?

Interaction accounts for 14.09% of the total variance.
F = 3.24. DFn=6 DFd=21
The P value = 0.0205
If there is no interaction overall, there is a 2% chance of randomly observing so much interaction in an experiment of this size. The interaction is considered significant.

Since the interaction is statistically significant, the P values that follow for the row and column effects are difficult to interpret.

Does Treatment affect the result? (Are the curves different?)

Treatment accounts for 21.01% of the total variance (after adjusting for matching).
F = 8.02. DFn=2 DFd=21
The P value = 0.0155
If Treatment has no effect overall, there is a 1.5% chance of randomly observing an effect this big (or bigger) in an experiment of this size. The effect is considered significant.

Does Time affect the result? (Are the curves horizontal?)

Time accounts for 36.11% of the total variance (after adjusting for matching).
F = 16.62. DFn=3 DFd=21
The P value is <0.0001
If Time has no effect overall, there is a less than 0.01% chance of randomly observing an effect this big (or bigger) in an experiment of this size. The effect is considered extremely significant.

The 2 way ANOVA results indicate that UCB levels after 13 weeks and 27 weeks or 27 weeks are significantly different in comparison with negative controls for ADHLSC and human hepatocytes treatment respectively. Time, treatments and the interaction time-treatments explain the significant differences.

b. *Cyclosporine A disposition, hepatic and renal tolerance in Wistar rat.*

Objectives of this study were to identify efficient and safe doses of cyclosporine A in rodent and to assess its effects on hepatic and renal functions. For this purpose, we tested the effects of different doses and administration routes of cyclosporine A (5, 2.5 and 1 mg/kg) administered during 28 days intraperitoneally, or by gastric feeding on Wistar rats.

i. Evaluation of renal and hepatic parameters and hepatic enzymes:

Kruskall-Wallis test (nonparametric test)

- Urea

Table Analyzed	Urea		
Kruskal-Wallis test			
P value	0.3916		
Exact or approximate P value?	Gaussian Approximation		
P value summary	ns		
Do the medians vary signif. (P < 0.05)	No		
Number of groups	4		
Kruskal-Wallis statistic	3.000		
Dunn's Multiple Comparison Test	Difference in rank sum	Significant? P < 0.05?	Summary
Negative controls vs 2,5mg/kg/j PO	1.000	No	ns
Negative controls vs 5mg/kg/j PO	-2.000	No	ns
Negative controls vs 5mg/kg/2j IP	-1.000	No	ns

- Creatinine

Table Analyzed	Creatinine		
Kruskal-Wallis test			
P value	0.3916		
Exact or approximate P value?	Gaussian Approximation		
P value summary	ns		
Do the medians vary signif. (P < 0.05)	No		
Number of groups	4		
Kruskal-Wallis statistic	3.000		
Dunn's Multiple Comparison Test	Difference in rank sum	Significant? P < 0.05?	Summary
Negative controls vs 2,5mg/kg/j PO	-1.000	No	ns
Negative controls vs 5mg/kg/j PO	-3.000	No	ns
Negative controls vs 5mg/kg/2j IP	-2.000	No	ns

- Total bilirubin

Table Analyzed	Tbil		
Kruskal-Wallis test			
P value	0.3916		
Exact or approximate P value?	Gaussian Approximation		
P value summary	ns		
Do the medians vary signif. (P < 0.05)	No		
Number of groups	4		
Kruskal-Wallis statistic	3.000		
Dunn's Multiple Comparison Test	Difference in rank sum	Significant? P < 0.05?	Summary
Negative controls vs 2,5mg/kg/j PO	2.000	No	ns
Negative controls vs 5mg/kg/j PO	1.000	No	ns
Negative controls vs 5mg/kg/2j IP	-1.000	No	ns

- Direct bilirubin

Table Analyzed	Dbil		
Kruskal-Wallis test			
P value	0.3916		
Exact or approximate P value?	Gaussian Approximation		
P value summary	ns		
Do the medians vary signif. (P < 0.05)	No		
Number of groups	4		
Kruskal-Wallis statistic	3.000		
Dunn's Multiple Comparison Test	Difference in rank sum	Significant? P < 0.05?	Summary
Negative controls vs 2,5mg/kg/j PO	-1.000	No	ns
Negative controls vs 5mg/kg/j PO	-3.000	No	ns
Negative controls vs 5mg/kg/2j IP	-2.000	No	ns

- Aspartate transaminase

Table Analyzed	AST		
Kruskal-Wallis test			
P value	0.3916		
Exact or approximate P value?	Gaussian Approximation		
P value summary	ns		
Do the medians vary signif. (P < 0.05)	No		
Number of groups	4		
Kruskal-Wallis statistic	3.000		
Dunn's Multiple Comparison Test	Difference in rank sum	Significant? P < 0.05?	Summary
Negative controls vs 2,5mg/kg/j PO	3.000	No	ns
Negative controls vs 5mg/kg/j PO	2.000	No	ns
Negative controls vs 5mg/kg/2j IP	1.000	No	ns

- Alanine transaminase

Table Analyzed	ALT		
Kruskal-Wallis test			
P value	0.3916		
Exact or approximate P value?	Gaussian Approximation		
P value summary	ns		
Do the medians vary signif. (P < 0.05)	No		
Number of groups	4		
Kruskal-Wallis statistic	3.000		
Dunn's Multiple Comparison Test	Difference in rank sum	Significant? P < 0.05?	Summary
Negative controls vs 2,5mg/kg/j PO	1.000	No	ns
Negative controls vs 5mg/kg/j PO	-1.000	No	ns
Negative controls vs 5mg/kg/2j IP	-2.000	No	ns

- Gamma-glutamyl transferase

Table Analyzed	GGT		
Kruskal-Wallis test			
P value	0.3916		
Exact or approximate P value?	Gaussian Approximation		
P value summary	ns		
Do the medians vary signif. (P < 0.05)	No		
Number of groups	4		
Kruskal-Wallis statistic	3.000		
Dunn's Multiple Comparison Test	Difference in rank sum	Significant? P < 0.05?	Summary
Negative controls vs 2,5mg/kg/j PO	-1.000	No	ns
Negative controls vs 5mg/kg/j PO	-2.000	No	ns
Negative controls vs 5mg/kg/2j IP	1.000	No	ns

No significant differences were obtained in term of renal (urea, creatinine), hepatic (total and direct bilirubin) parameters and hepatic enzymes (aspartate transaminase, alanine transaminase and gamma-glutamyl transferase) level in rats treated with 2.5mg/kg/d per os (n=5), 5mg/kg/d per os (n=5), 5mg/kg/2d intraperitonealy (n=3) cyclosporine A in comparison with negative control (n=5).

ii. Evaluation of renal and hepatic parameters and hepatic enzymes:

ANOVA (parametric test)

In this case, we assume that all results follow a normal distribution. This hypothesis must further be confirmed increasing the number of rats in each experimental group.

- Urea

Table Analyzed	Copy of Urea				
One-way analysis of variance					
P value	0.2320				
P value summary	ns				
Are means signif. different? (P < 0.05)	No				
Number of groups	4				
F	1.624				
R squared	0.2726				
ANOVA Table	SS	df	MS		
Treatment (between columns)	17.86	3	5.954		
Residual (within columns)	47.67	13	3.667		
Total	65.53	16			
Dunnett's Multiple Comparison Test	Mean Diff.	q	Significant? P < 0.05?	Summary	95% CI of diff
Negative controls vs 2,5mg/kg/j PO	1.867	1.335	No	ns	-1.845 to 5.579
Negative controls vs 5mg/kg/j PO	0.1667	0.1140	No	ns	-3.716 to 4.049
Negative controls vs 5mg/kg/2j IP	-0.7333	0.5244	No	ns	-4.445 to 2.979

- Creatinine

Table Analyzed	Copy of Creatinine				
One-way analysis of variance					
P value	0.1042				
P value summary	ns				
Are means signif. different? (P < 0.05)	No				
Number of groups	4				
F	2.608				
R squared	0.4157				
ANOVA Table	SS	df	MS		
Treatment (between columns)	0.03266	3	0.01089		
Residual (within columns)	0.04591	11	0.004174		
Total	0.07857	14			
Dunnett's Multiple Comparison Test	Mean Diff.	q	Significant? P < 0.05?	Summary	95% CI of diff
Negative controls vs 2,5mg/kg/j PO	-0.08833	1.790	No	ns	-0.2224 to 0.04574
Negative controls vs 5mg/kg/j PO	-0.1167	2.212	No	ns	-0.2600 to 0.02666
Negative controls vs 5mg/kg/2j IP	-0.1253	2.656	No	ns	-0.2535 to 0.002864

- Total bilirubin

Table Analyzed	Copy of Tbil				
One-way analysis of variance					
P value	0.0020				
P value summary	**				
Are means signif. different? (P < 0.05)	Yes				
Number of groups	4				
F	8.310				
R squared	0.6404				
ANOVA Table	SS	df	MS		
Treatment (between columns)	0.06365	3	0.02122		
Residual (within columns)	0.03575	14	0.002553		
Total	0.09940	17			
Dunnett's Multiple Comparison Test	Mean Diff.	q	Significant? P < 0.05?	Summary	95% CI of diff
Negative controls vs 2,5mg/kg/j PO	0.07133	1.933	No	ns	-0.02574 to 0.1684
Negative controls vs 5mg/kg/j PO	0.07533	2.041	No	ns	-0.02174 to 0.1724
Negative controls vs 5mg/kg/2j IP	-0.06267	1.698	No	ns	-0.1597 to 0.03441

- Direct bilirubin

Table Analyzed	Dbil				
One-way analysis of variance					
P value	0.8203				
P value summary	ns				
Are means signif. different? (P < 0.05)	No				
Number of groups	4				
F	0.3064				
R squared	0.07114				
ANOVA Table	SS	df	MS		
Treatment (between columns)	0.0004371	3	0.0001457		
Residual (within columns)	0.005707	12	0.0004756		
Total	0.006144	15			
Dunnett's Multiple Comparison Test	Mean Diff.	q	Significant? P < 0.05?	Summary	95% CI of diff
Negative controls vs 2,5mg/kg/j PO	-0.003333	0.1872	No	ns	-0.05110 to 0.04444
Negative controls vs 5mg/kg/j PO	-0.0140	0.8791	No	ns	-0.05673 to 0.02873
Negative controls vs 5mg/kg/2j IP	-0.006000	0.3767	No	ns	-0.04873 to 0.03673

- Aspartate transaminase

Table Analyzed	AST				
One-way analysis of variance					
P value	0.1975				
P value summary	ns				
Are means signif. different? (P < 0.05)	No				
Number of groups	4				
F	1.778				
R squared	0.2759				
ANOVA Table	SS	df	MS		
Treatment (between columns)	1127	3	375.8		
Residual (within columns)	2959	14	211.4		
Total	4087	17			
Dunnett's Multiple Comparison Test	Mean Diff.	q	Significant? P < 0.05?	Summary	95% CI of diff
Negative controls vs 2,5mg/kg/j PO	21.27	2.003	No	ns	-6.665 to 49.20
Negative controls vs 5mg/kg/j PO	20.87	1.965	No	ns	-7.065 to 48.80
Negative controls vs 5mg/kg/2j IP	10.87	1.023	No	ns	-17.07 to 38.80

- Alanine transaminase

Table Analyzed	ALT				
One-way analysis of variance					
P value	0.1437				
P value summary	ns				
Are means signif. different? (P < 0.05)	No				
Number of groups	4				
F	2.119				
R squared	0.3123				
ANOVA Table	SS	df	MS		
Treatment (between columns)	216.8	3	72.27		
Residual (within columns)	477.5	14	34.10		
Total	694.3	17			
Dunnett's Multiple Comparison Test	Mean Diff.	q	Significant? P < 0.05?	Summary	95% CI of diff
Negative controls vs 2,5mg/kg/j PO	2.867	0.6722	No	ns	-8.353 to 14.09
Negative controls vs 5mg/kg/j PO	-4.733	1.110	No	ns	-15.95 to 6.486
Negative controls vs 5mg/kg/2j IP	-5.133	1.204	No	ns	-16.35 to 6.086

- Gamma-glutamyl transferase

Table Analyzed	GGT				
One-way analysis of variance					
P value	0.3068				
P value summary	ns				
Are means signif. different? (P < 0.05)	No				
Number of groups	4				
F	1.343				
R squared	0.2513				
ANOVA Table	SS	df	MS		
Treatment (between columns)	5.388	3	1.796		
Residual (within columns)	16.05	12	1.338		
Total	21.44	15			
Dunnett's Multiple Comparison Test	Mean Diff.	q	Significant? P < 0.05?	Summary	95% CI of diff
Negative controls vs 2,5mg/kg/j PO	-0.5000	0.5167	No	ns	-3.096 to 2.096
Negative controls vs 5mg/kg/j PO	-0.7000	0.7234	No	ns	-3.296 to 1.896
Negative controls vs 5mg/kg/2j IP	0.7500	0.7488	No	ns	-1.937 to 3.437

No significant differences were obtained regarding renal (urea, creatinine), hepatic (total and direct bilirubin) parameters and hepatic enzymes (aspartate transaminase, alanine transaminase and gamma-glutamyl transferase) in rats treated with 2.5mg/kg/d per os (n=5), 5mg/kg/d per os (n=5), 5mg/kg/2d intraperitonealy (n=3) cyclosporine A in comparison with negative control (n=5). Absence of significant differences must be due to the small number of rats in each experimental group.

In the last decade, stem cell therapy has raised much hope to treat patients presenting a variety of illnesses. Liver progenitor cells offer a promising alternative for the treatment of hepatic diseases. Despite the enthusiasm, cell efficiency need to be assessed on the route to clinic. This study is part of a larger medical translational research project that aims to treat inherited metabolic liver diseases with stem cell therapy.

In the present study we evaluate the presence of progenitor cells in healthy adult rat liver which would display the same advanced hepatogenic profile as that decribed in human adult liver derived progenitor cells (ADHLSC). We observed that rat progenitor cells homologous to ADHLSC cannot be easily obtained even when the same isolation and culture protocol was applied. However, we isolated a novel type of rat liver progenitor cell population: fibroblastic-like liver derived cells (rFLDC) which expressed hepatic and biliary markers.

Then we focused on the ability of transplanted ADHLSC to correct a UGT1A1 activity deficiency in the Gunn rat model homologous to the human hyperbilirubinemic Crigler-Najjar syndrome type I. We demonstrated that ADHLSCs were able to integrate into the Gunn rat liver parenchyma and these rats exhibit a metabolic effect 3 months post-transplantation and maintained over a 6 months period.

Finally, using ^{111}Indium-oxine labeled ADHLSC, we demonstrate the engraftment and the homing of cells preferentially within the liver parenchyma.

All together, these results make ADHLSC an attractive candidate for cell therapy treatment of Crigler-Najjar type I syndrome.